

REDUCING OCCUPANT INJURY IN REAR-END COLLISIONS THROUGH THE
IMPLEMENTATION OF ENERGY-ABSORBING FOAM TO THE SEAT BASE

by

Rami Mansour

B.A.Sc., University of Waterloo, 2008

A THESIS SUBMITTED IN PARTIAL FULFILLMENT OF THE REQUIREMENTS FOR THE
DEGREE OF

MASTERS OF APPLIED SCIENCE

in

THE FACULTY OF GRADUATE STUDIES

(Biomedical Engineering)

THE UNIVERSITY OF BRITISH COLUMBIA
(Vancouver)

December 2010

© Rami Mansour, 2010

Abstract

Rear-end collisions account for approximately \$9 billion in medical and damaged property costs annually in the United States alone. These types of collisions account for nearly 30% of all vehicle impacts, making them the most common collision type. Soft tissue injury to the neck (i.e., “whiplash”) is typically associated with this type of collision. The vehicle seating system is the predominant safety device employed to protect the occupant during a rear-end collision. Currently, designers focus predominantly on seat base strength, seat back stiffness/compliance, and head restraint size and position as a means of mitigating injury. While all of these aspects are important and have increased the crashworthiness of the seat, the concept of utilizing the seat base as a component to further assist in whiplash protection has remained relatively unexamined. The addition of a supplemental safety system to the seat base may offer the potential for reducing injuries in higher severity collisions.

This thesis examines the potential for deformable materials, (in this study energy-absorbing foam), to absorb transmitted energy to the vehicle seat in order to reduce the dynamic loading experienced by the occupant. The relationships between the type and geometry of the foam and occupant dynamics, and how they affect potential occupant injury (as assessed using selected neck injury criteria) are assessed and reported. Several energy-absorbing foams currently available have been investigated in order to determine the best foam type and geometry for a range of collision speeds. The results indicate that the time to completely crush the foam, dictated by foam relative density, stress vs. strain behavior, foam geometry, and acceleration pulse, can affect the degree to which injury potential is reduced for a large range of collision speeds. Further discussions of design considerations for implementation of such a supplemental system are also provided in this thesis. Reducing rear-end collision severity with the implementation of this device can potentially lead to a decrease in rear-end collision induced injury and fatality.

Table of Contents

Abstract	ii
Table of Contents	iii
List of Tables	vi
List of Figures	vii
Abbreviations and Acronyms	x
Acknowledgments	xii
1 Introduction	1
1.1 Overview	1
1.2 Incidence of Rear-End Collision Induced Injury and Fatality	2
1.3 Injuries Sustained During a Rear-End Collision	4
1.3.1 Symptoms of Whiplash Injury	4
1.3.2 Introduction to the Anatomy of the Neck	5
1.4 The Role of the Vehicle Seat	7
1.5 Research Objectives	10
1.6 Overview of Thesis	11
1.7 Summary	12
2 Literary Review	14
2.1 Overview	14
2.2 Vehicle Seat Design Standards	15
2.3 Biomechanics of Whiplash	19
2.4 Anatomy of Whiplash	21
2.5 Injury Criteria	26
2.5.1 Neck Injury Criterion (NIC)	27
2.5.2 Neck Displacement Criterion (NDC)	28
2.5.3 Normalized Neck Injury Criterion (N _{ij})	30

2.5.4	Neck Protection Criterion (N_{km})	32
2.5.5	Inter-Vertebral Neck Injury Criterion (IV-NIC)	32
2.6	Seat Design Choices and Their Effect on Occupant Injury	33
2.6.1	Seat Back	34
2.6.2	Head Restraint	35
2.6.3	Seat Base	36
2.6.4	Crash Pulse	38
2.6.5	Occupant	39
2.7	Summary	40
3	Model Creation.....	42
3.1	Overview	42
3.2	Vehicle Collision Model	43
3.3	Seat Model	46
3.4	Modifications to the Seat and Dummy Model	47
3.5	Neck Injury Criterion Determination.....	50
3.5.1	NIC Calculation	50
3.6	Seat Model Verification.....	53
3.6.1	Rear Impact Dummy Evaluation Task Group (Kim et. al.)	53
3.6.2	National Highway Traffic Safety Administration (Kuppa et. al.)	54
3.6.3	Schmitt et. al	55
3.7	Summary	56
4	Simulation Procedure	57
4.1	Overview	57
4.2	Methods of Mitigating Injury Through Seat Base Design	58
4.3	Energy-Absorbing Foam	58
4.3.1	Microstructure	59
4.3.2	Mechanical Behavior of Energy-Absorbing Foam.....	60
4.4	Seat and Dummy Simulation with Foam Addition	62
4.4.1	Modeling of Energy-Absorbing Foam in LS DYNA.....	64

4.5	Optimal Foam Study Procedure	64
4.6	Detailed Energy-Absorbing Foam Description	66
4.6.1	IMPAXX™ Foam	67
4.6.2	Cymat™ Foam.....	68
4.6.3	Fraunhofer™ Foam.....	69
4.7	Summary	70
5	Results and Discussion	72
5.1	Overview	72
5.2	Relationship between Foam Geometry and NIC_{max}	73
5.3	Intermediate Collision Speed Evaluation	89
5.4	The Effect of Collision Speed on NIC_{max}	90
5.5	Peak Head Acceleration	91
5.6	Peak Torso Acceleration.....	93
5.7	Head Restraint Contact Forces.....	94
5.8	Seat Back Deflection.....	95
5.9	Occupant Kinetic Energy	96
5.10	Limitations.....	98
5.11	Summary	99
6	Conclusions	101
7	Safety System Design and Future Work.....	108
	Bibliography.....	113
	Appendix A: Acceleration Pulses.....	119
	Appendix B: Occupant Kinetic Energy	124

List of Tables

Table 2-1: NIC_{max} for Himmetoglu et. al. study [52]	37
Table 3-1: UBC Sled Simulation vs. Kim et. al. NIC [62]	53
Table 3-2: Seat and Dummy Simulation vs. Kuppa et. al. NIC	55
Table 4-1: Simulated foam types.....	65
Table 5-1: Optimal Foam Geometries.....	85
Table 5-2: Intermediate speed evaluation matrix using foams of Table 5	89

List of Figures

Figure 1-1: Cervical Spine (adapted from [23])	5
Figure 1-2: Flexion/Extension motion of the neck (adapted from [6])	6
Figure 1-3: Typical vehicle seat (adapted from [24])	7
Figure 1-4: Self-Aligning Head Restraint (SAHR - adapted from [2])	8
Figure 1-5: GM High Retention Seat frame structure (adapted from [25])	9
Figure 2-1: CMVSS #207 Testing Procedure (adapted from [26])	16
Figure 2-2: Phases of head and neck motion leading to whiplash from a rear-end collision (adapted from [30])	20
Figure 2-3: Facet joint (adapted from [32])	22
Figure 2-4: Anterior Longitudinal Ligament (adapted from [36])	23
Figure 2-5: Vertebral artery (adapted from [36])	24
Figure 2-6: Dorsal root ganglion (adapted from [41])	25
Figure 2-7: T1 and C1 vertebrae (adapted from [36]).	27
Figure 2-8: Neck Displacement Criteria Plots: a) Shearing vs. Rotation b) Shearing vs. Compression/tension (adapted from [2])	29
Figure 2-9: Previous FMVSS#208 Neck Injury Criteria [45]	30
Figure 2-10: Updated limits for the 50th percentile male dummy [45]	31
Figure 3-1: Vehicle collision model	44
Figure 3-2: C2500 Pickup truck model	45
Figure 3-3: Geo Metro Model	46
Figure 3-4: Seat and Dummy sled model updated from [31]	47
Figure 3-5: Head restraint upgrade: a) Old design b) New design	48

Figure 3-6: Hybrid III Dummy upgrade: a) old dummy b) improved dummy.....	49
Figure 3-7: Upgraded Hybrid III Neck: a) Rigid neck without vertebrae b) Updated neck with vertebrae	49
Figure 3-8: Low speed scenario measured only in a global coordinate system	51
Figure 3-9: Higher speed scenario measured in a local coordinate system	51
Figure 3-10: Conversion between global and local coordinate systems	52
Figure 4-1: Microstructure of Alporas TM Foam adapted from [65].....	59
Figure 4-2: Cross section of a) Open-cell foam b) Closed- cell foam (adapted from [65])	60
Figure 4-3: Typical stress vs. volumetric strain curve (adapted from [68])	61
Figure 4-4: Modified seat and dummy model	62
Figure 4-5: Rear-end collision simulation a) Pre-crush b) Post-crush	63
Figure 4-6: Optimal Foam Study Procedure	66
Figure 4-7: Measured dynamic stress vs. volumetric strain curves for IMPAXX TM foams (adapted from [74])	67
Figure 4-8: Measured stress vs. volumetric strain for Cymat 200	69
Figure 4-9: Measured stress vs. volumetric strain for Fraunhofer TM foam	70
Figure 5-1: Phases of an NIC plot (17 km/h rear-end collision).....	73
Figure 5-2: NIC _{max} vs. Foam radius for IMPAXX TM 300 foam at 17 km/h.....	75
Figure 5-3: NIC _{max} vs. Foam radius for IMPAXX TM 500 foam at 17 km/h.....	76
Figure 5-4: NIC _{max} vs. Foam radius for Cymat TM 200 at 65 km/h.....	76
Figure 5-5: NIC _{max} vs. Foam radius for Fraunhofer TM foam at 65 km/h	77
Figure 5-6: Relative time of foam crush completion	79
Figure 5-7: NIC _{max} vs. Relative crush time for IMPAXX TM 300 (17 km/h).....	80
Figure 5-8: NIC _{max} vs. Relative crush time for IMPAXX TM 500 (17 km/h).....	80

Figure 5-9: NIC _{max} vs. Relative crush time for Cymat™ 200 (65 km/h)	81
Figure 5-10: NIC _{max} vs. Relative crush time for Fraunhofer™ (65 km/h)	81
Figure 5-11: Relative crush time vs. Foam radius IMPAXX™ 300 (17 km/h)	83
Figure 5-12: Relative crush time vs. Foam Radius IMPAXX™ 500 (17 km/h)	83
Figure 5-13: Relative crush time vs. Foam radius Cymat™ 200 (65 km/h)	84
Figure 5-14: Relative crush time vs. Foam radius Fraunhofer™ (65 km/h)	84
Figure 5-15: Relative velocity with and without foam addition (17 km/h)	86
Figure 5-16: Relative velocity with and without foam addition (65 km/h)	86
Figure 5-17: Relative acceleration with and without foam addition (17 km/h)	87
Figure 5-18: Relative acceleration with and without foam addition (65 km/h)	87
Figure 5-19: NIC vs. time with and without foam modified seat (for 17 km/h collision)	88
Figure 5-20: NIC vs. time with and without foam modified seat (for 65 km/h collision)	88
Figure 5-21: Predicted NIC _{max} for selected collision speeds	90
Figure 5-22: Predicted NIC _{max} for selected collision speeds (modified collision ranges)	91
Figure 5-23: Peak Head accelerations for baseline vs. foam seat for: a) x-direction, b) z-direction	92
Figure 5-24: Torso accelerations for baseline vs. foam seat for a) x-direction b) z-direction	94
Figure 5-25: Peak resultant head restraint contact force	95
Figure 5-26: Peak seat back deflection of the baseline seat vs. seat with foam added	96
Figure 5-27: Occupant kinetic energy vs. time for a) 17 km/h b) 65 km/h	97
Figure 7-1: Millimeter-wave radar sensor [76]	110
Figure 7-2: Device functionality	112

Abbreviations and Acronyms

ATD	Anthropomorphic Test Dummy
AIS	Abbreviated Injury Scale
BC	British Columbia, Canada
BioRID	Biofidelic Rear Impact Dummy developed by Swedish Consortium
C1, C7	First and seventh vertebra in the neck
CAD\$	Canadian Dollars
CMVSS	Canadian Motor Vehicle Safety Standard
CPU	Central Processing Unit
FEM	Finite Element Model
FMVSS	Federal Motor Vehicle Safety Standard
GM	General Motors Corporation
Hybrid III	Standard Crash Test Dummy used for automotive testing
ICBC	Insurance Corporation of British Columbia, Canada (www.icbc.com)
IV-NIC	Inter-vertebral Neck Injury Criterion
LS-DYNA	General Purpose Transient Dynamic Finite Element Software Program
LSTC	Livermore Software Technology Corporation
NDC	Neck Displacement Criteria
NHTSA	U.S. National Highway Traffic Safety Administration
N_{ij}	Maximum Neck Tension Extension Criterion
N_{km}	Maximum Neck Shear Extension Criterion
OC	Occupant Condyles
RID	Rear Impact Dummy Neck
SAE	Society of Automotive Engineers
SAHR	Saab Active Head restraint or Self –Aligning Head restraint
T1	First Thoracic Vertebra
UBC	University of British Columbia
USD\$	United States Dollars

WAD	Whiplash Associated Disorder
WHIPS	Whiplash Protection System developed by Volvo Corporation
VA	Vertebral artery
ΔV	Delta-V or Differential Velocity
2D or 3D	Two or Three Dimensions
<i>in-lb</i>	Inch Pounds, Torque Measurement
<i>G</i>	Gravitational Acceleration of Bodies, Equal to 9.81 m/s^2
<i>Kph</i>	Kilometers per hour
<i>Lbf</i>	Pound Force
<i>Mph</i>	Miles per Hour
<i>Ms</i>	Millisecond
<i>Nm</i>	Newton-meter, Torque Measurement
Σ	Stress
<i>I</i>	Moment of Inertia
<i>x-axis</i>	Global Axis Parallel with the Longitudinal Vehicle Axis, Local Occupant Axis Parallel with the Anterior/Posterior Direction
<i>y-axis</i>	Global Axis Parallel with the Lateral Vehicle Axis, Local Occupant Axis Parallel with the Transverse Direction
<i>z-axis</i>	Global Axis Parallel with the Vertical Vehicle Axis, Local Occupant Axis Parallel with the Superior/Inferior Direction

Acknowledgments

This manuscript was made possible with the help and guidance of several individuals. Thanks are given to Dr. Douglas P. Romilly whose supervision, guidance, and support has been paramount to the success of this research. Among those who have contributed their time are Annie Zhang and Ali Forghani. This work could not have been done without the support of AUTO21 and NSERC. To my family, Raafat Mansour, Miranda Mansour, and Sarah Mansour, your undying support, encouragement, and love has motivated and inspired me throughout this work. Thank you all.

1 Introduction

This thesis describes the implementation, functionality, and feasibility of a new supplemental safety system for the vehicle seat which is capable of mitigating injury during a rear-end collision. In order to understand the significance of this device, it is first necessary to gain an appreciation for the severity and frequency of rear-end collisions, as well as a basic understanding of what injuries are sustained during this type of collision.

1.1 Overview

Rear-end collisions are one of the most common collision types in North America. Although the fatality rate is low (approximately 6.9% in 2008 [1]), they account for nearly 30% of all reported automobile injuries [2]. While many of these injuries are assessed as minor (AIS scale), the overall cost to society is significant, resulting in billions of dollars spent annually.

Many of those involved in a rear-end collision experience long term medical consequences [3]. Collisions that occur at higher speeds can prove fatal for the occupant being struck. Therefore, due to the financial strain on society, as well as the risk of occupant injury, methods of reducing injury during rear-end collisions continue to require investigation.

Most rear-end collisions occur at lower speeds relative to frontal impacts [4]. In a low speed rear-end collision the primary mode of injury is soft tissue damage to the neck, more commonly referred to as “whiplash” [5]. This term is typically associated with an injurious level of extension/flexion motion of the neck [4]. In high speed collisions, dynamic forces experienced by the occupant are larger due to an increase in the acceleration of the struck vehicle [6]. The most predominant safety device available to the occupant during a rear-end collision is the vehicle seat [4]. Investigations between seat design and occupant injury, beginning as early as the 1960’s, have generated several innovations including Volvo’s WHIPS seat [7], the SAAB Active Head restraint (SAHR) [8], and the GM High Retention seat [2]. Vehicle seat design relating to safety has predominantly been focused on the upper components of the seat (the seat back and head restraint). Little work has been conducted examining whether improvements to safety can be obtained through improved design of the seat base. This work

aims to provide evidence that a further reduction in injury risk can be achieved through the addition of a supplemental system to the seat base.

1.2 Incidence of Rear-End Collision Induced Injury and Fatality

Despite the improvements made to vehicle crashworthiness throughout the last few decades, the economic impact, number of injuries sustained, and number of fatalities due to rear-end collisions are still high. This section illustrates the prevalence and significance of rear-end collisions.

Economic Impact

Rear-end collision induced costs introduce a significant burden to society. Insurance companies are required to spend millions of dollars annually in order to facilitate the number of vehicle repairs and medical costs incurred by these collisions. A study conducted by Chappuis & Soltermann found that in 2008, Switzerland had the highest cost per whiplash related claim (€35,000). Following this was the Netherlands (€16,000), Norway (€6,050), Finland (€1,500), Germany (€2,500), France (€2,625), and Great Britain (€2,878). Of all the countries that participated in this study, the average cost per claim was €9,000 [9]. The Highway Loss Data Institute (HLDI) estimates that every year, insurers pay 1.7 million injury claims [10]. In 2008, total damages to property due to rear-end collisions involving transport vehicles was found to be \$1,284,000 USD with \$820,000 USD being for passenger vehicles [1].

Fatality

Despite the fact that rear-end collisions are responsible for less fatalities than side and frontal impacts, the amount of rear-end collision induced fatalities is still substantial. In 2008, the National Highway Traffic Safety Administration (NHTSA) found that 1,410 rear-end collision induced fatalities involving passenger vehicles occurred. This number was comprised of both single vehicle and multiple vehicle crashes. Similarly, the number of fatalities involving light trucks and large trucks were 1,313 and 697 respectively [1]. In 2007, there were 19 fatalities resulting from rear-end collisions in British Columbia, Canada [11].

Injury

Injuries sustained from a rear-end collision range from minor neck strain to severe neck trauma. In 2007, there were 3,410 injuries resulting from rear-end collisions in British Columbia, Canada alone [11]. In 2008, 497,000 people were injured in rear-end collisions in the United States [1].

A study examining the onset of injury after a rear-end collision showed that neck pain typically occurs within 12 hours for 77.6% of all accident victims, 12-24 hours for 13% of victims, 24-48 hours for 2% of victims, and 48 hours or later for the remaining 7% [12]. In 2007, the ICBC found that the locations on the body with the highest incidence of injuries as a result of a rear-end collision were the head (432), neck (5054), and back (1233) [11]. In Japan, the Institute of Traffic Accident Research and Data Analysis (ITARDA) reported that, in 2002, 45% of all vehicle-to-vehicle collisions were rear-end collisions resulting in 92% of those occupants reporting neck injuries [13]. Typically females aged 20 to 24 have the highest incidence of whiplash injuries [14].

Occupant Ejection

The dynamics of the struck occupant during a rear-end collision may lead to them being physically ejected from the vehicle seat to another location within the vehicle or ejected from the vehicle itself. Occupant ejection, although rare, can result in severe injuries and can often times be life threatening. The chance of experiencing fatal injuries is 40% more likely for those who are ejected from their vehicle seat than those that remain in it during a rear-end collision [15]. Huelke et. al. conducted a study which investigated the rate at which severe neck injury occurred for collisions where the struck vehicle experienced sufficient damage that it required towing. This study estimated that for those who remained in their vehicle seat, 1 in 300 occupants sustained severe neck injuries. However, for those who were ejected from the vehicle, this rate increased to 1 in 14 occupants [16].

Recovery Time

The amount of recovery time required for a whiplash injury varies from person to person. Recovery time is dependent on several factors including collision severity, occupant age,

previous neck injuries, etc. The amount of compensation that is paid to those who are unable to work due to rear-end collision induced injuries is substantial. From the perspective of employers, the unexpected absence of qualified individuals from the workplace may prove detrimental to a company's progress. Investigators in Quebec studied 2810 people claiming to have whiplash injuries due to motor vehicle collisions in 1987. This study found that 22% of people recovered within one week of the collision, 53% required more than four weeks to recover and 1.9% of the subjects required more than one year to recover [17]. Norris and Watt determined that 66% of subjects that had been involved in a rear-end collision had neck pain after two years [18]. Sterner and Gerdle stated that between 5 - 8 % of all occupants involved in a whiplash injury develop chronic symptoms severe enough to diminish their work capacity [19]. Hagan et. al examined the relationship between whiplash injury and lost wage payments. This study found that the mean recovery time for a minor whiplash injury was 10.6 days, 12.1 days for a moderate injury, 13.8 days for a severe injury, and 24.9 days for a very severe injury [20].

It is evident that while rear-end collisions yield a relatively low fatality rate, their prevalence and impact on society is significant. Rear-end collisions have, and continue to be, a real problem that must be addressed through further research in this field.

1.3 Injuries Sustained During a Rear-End Collision

In order to create a safety system capable of mitigating rear-end collision induced injuries and fatalities, an understanding of how the injury occurs must be gained. The most common injury resulting from a rear-end collision is whiplash. The term "whiplash" is associated with neck sprains and strains [21]. This injury occurs as a result of injurious levels of neck extension/flexion motion experienced by the occupant during a rear-end collision.

1.3.1 Symptoms of Whiplash Injury

Whiplash symptoms are similar to those symptoms seen in many other medical conditions, making it difficult to explicitly diagnose. The most common whiplash symptoms include: neck, shoulder, and back pain; headache, dizziness, and vertigo [19]. Other less common symptoms

include: blurred vision, loss of taste, smell, or hearing, fatigue, and blood in the urine or stool [22]. These symptoms do not necessarily manifest themselves immediately after the collision has taken place (they can arise 24-72 hours after the collision has occurred [22]). In many cases, these injuries can remain with an individual for years, reducing the quality of living of that individual.

1.3.2 Introduction to the Anatomy of the Neck

In order to gain an understanding of how whiplash can cause the symptoms described in the previous section, a basic understanding of the affected tissues within the body, specifically the neck and head, must be understood. A more detailed description of the anatomy involved in whiplash injury will be described in detail in Chapter 2. This section will briefly describe the basic anatomy of the neck.

The cervical spine (see Figure 1-1) is the portion of the spine found within the human neck making it a major focal point for analysis in whiplash causation. Many of the neck injury criteria that have been used to quantify whiplash injury are based on measuring the relative displacements, velocities, and accelerations between the vertebral disks found within the cervical spine. These formulations will be discussed in more detail in Chapter 2.

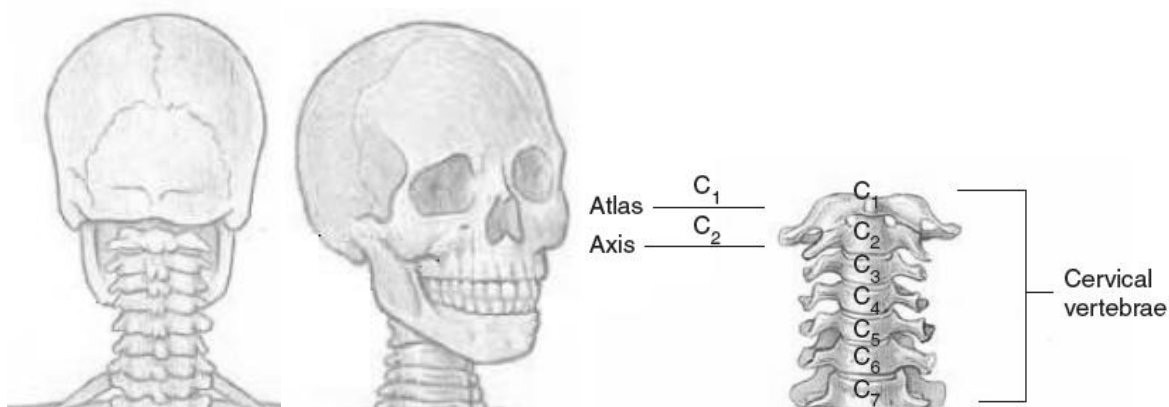


Figure 1-1: Cervical Spine (adapted from [23])

The cervical vertebrae are the smallest of the vertebra found in the spinal column [23]. These vertebrae are responsible for stabilizing the head, protecting the spinal column, and facilitating

movement of the head and neck. The first vertebra in the cervical spine (C1) is responsible for facilitating the articulation of the head in the sagittal plane (nodding up and down). The second vertebra (C2) facilitates the articulation of the head along the transverse plane (nodding left to right). The remaining five vertebrae (C3-C7) are only capable of articulation with respect to one another [23]. Rotation between vertebrae is made possible through the presence of synovial joints that are located between the adjacent vertebrae, which are held in place by ligaments.

The terms “flexion” and “extension” are used heavily throughout this thesis. An explanation of extension and flexion as they pertain to the neck is shown in Figure 1-2. The mean range of motion for the neck is different for all individuals. One study found that full range of motion of the neck varied from 89 degrees to 165 degrees [6]. Surpassing this range of motion can be seen as an injurious level of extension or flexion and may result in injuries to tissues in the neck.

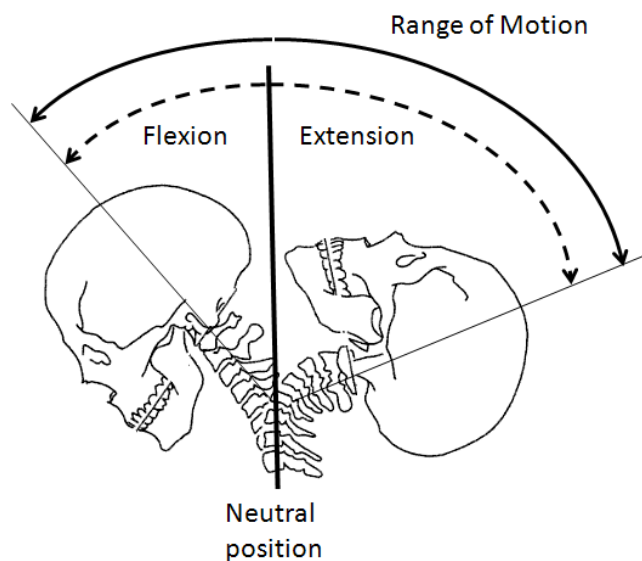


Figure 1-2: Flexion/Extension motion of the neck (adapted from [6])

Several muscles within the neck may be affected causing a whiplash injury. Some of these superficial muscles (closer to the surface of the neck) are the sternocleidomastoid and the trapezius. These muscles attach to the skull and shoulder girdle but are not connected to the individual vertebrae [21]. The sternocleidomastoid is responsible for flexing the vertebral column as well as rotating the head. The trapezius is responsible for rotating the scapula as well as drawing the head to one side [23]. Some of the muscles found deeper within the neck that

are connected to the vertebrae include the splenius, semispinalis, longissimus, scalene, and longus muscles. An understanding of the physiological limits of tissues within the neck has led to innovations in vehicle design which aim to ensure that these limits are not surpassed, thus eliminating whiplash.

1.4 The Role of the Vehicle Seat

The vehicle seat is the only safety device available to one experiencing a rear-end collision. This is due to the fact that it is not only capable of keeping the occupant within the seat during the collision (preventing occupant ejection); it can also act to limit the amount of relative motion between the neck and torso, thus reducing the risk of injurious flexion or extension. The three main components of the vehicle seat are shown in Figure 1-3.



Figure 1-3: Typical vehicle seat (adapted from [24])

Safety design modifications made to the vehicle seat have primarily focused on head restraint design, as proper positioning of the head restraint has been shown to prevent relative motion between the head and torso. Proper head restraint positioning is critical to whiplash mitigation. As a result, researchers have attempted to create a head restraint that is self-adjusting (i.e. it repositions itself in response to a collision) to eliminate the need for the occupant to manually adjust the head restraint to the correct position. One example of this innovation is the Saab Self-Aligning Head Restraint (SAHR) (see Figure 1-4). When the occupant comes into contact with the seat back during a rear-end collision, a force plate located within the seat back triggers

a linkage mechanism that causes the head restraint to move upwards and forwards towards the occupants head. By decreasing the back-set of the head restraint, the amount of extension experienced by the occupant's neck is reduced, thus reducing the amount of whiplash sustained [8].



Figure 1-4: Self-Aligning Head Restraint (SAHR - adapted from [2])

Research has also focused on seat back design, which acts to decelerate the torso during a rear-end collision. Seat back designs have typically employed one of two seat design ideals: providing either a yielding or a rigid seat. Historically, some researchers have argued that a yielding seat is safer during a rear-end collision, the idea being that by allowing the occupant to deflect the seat, it is possible to increase the amount of time for the torso to decelerate. This reduction in acceleration would mean that the dynamic loading on the occupant is also decreased. Those in favor of a rigid seat design argued that a yielding seat carries an increased risk of occupant ejection as the occupant may deflect the seat to the point where it is no longer capable of retaining the occupant within the seat. This is not only potentially fatal for the occupant but for passengers seated in the rear seats behind the occupant. A rigid seat acts to deflect less during loading reducing the risk of occupant ejection; however, this results in an increase the dynamic loading on the occupant [2].

In the late 1990's General Motors addressed both of these design methodologies and provided the "High Retention" seat design that employs the beneficial characteristics of both a yielding and a rigid seat design (see Figure 1-5). This design has a stiffer outer seat back frame with a yielding seat back center. The center compliant section of the seat back (predominantly foam) acts to absorb energy and gradually decelerate the torso during the collision, similar to a "catcher's mitt" in decelerating a thrown ball. As the occupant's inertia loads the seat, the stiffer outer frame prevents the occupant from deflecting the seat to the point at which occupant ejection is possible [25].



Figure 1-5: GM High Retention Seat frame structure (adapted from [25])

The vehicle seat is critical in mitigating injury during a rear-end collision as well as providing long term comfort for the occupant. Ergonomic factors must be combined with any safety device in order to provide a seat that is not only effective in protecting the occupant during a collision but is also comfortable and ergonomically-supportive to use for extended periods of time.

These technologies have focused on redesign of the seat back and head restraint. There have not been any safety systems that have been implemented for the seat base. This opportunity led to the research objectives of this thesis as defined in the following section.

1.5 Research Objectives

The overall objective of this research is to develop a means of utilizing the seat base as a contributing component to enhance occupant safety in a rear-end collision. The proposed approach is to develop a supplemental safety system that can act to dampen the effect of the acceleration pulse at the seat, reducing the overall impact of the collision to the occupant. In order to develop such a system, several research tasks were identified:

- 1) To obtain the means to assess the dynamics experienced by a seated occupant in a rear-end collision over a range of collision severities. This requires the development of finite element-based software simulation tools to quantify the vehicle response to a rear-end collision.
- 2) To use these tools to predict the extent of injury risk experienced by the occupant for a range of collision speeds with and without the use of the supplemental safety system. This will require that an injury criterion be adopted for assessment of occupant injury risk. This will give an initial baseline value of occupant injury for the original seat. The effectiveness of the supplemental safety system can be compared to the baseline value in order to test the efficacy of the device.
- 3) To develop relationships between the safety system design parameters and the reduced risk of occupant injury. This will involve utilizing the simulation results to develop a predictive relationship such that the level of injury can be estimated directly from a set of supplemental safety system parameters.
- 4) To determine the optimal characteristics of the safety system for a range of collision severities based on the trends seen in injury mitigation. The results from this portion of the work will lead into the development of the device itself.

Once these tasks have been completed, it may be possible to show that the addition of the proposed safety system can in fact further reduce the risk of injury to the occupant. Completing research tasks 1-3 will lead to the success of research task 4 by allowing for the optimal system characteristics to be determined through the development of simulation tools and developed

relationships. An understanding of the performance of the supplemental safety device can then lead to a prototype and physical testing.

1.6 Overview of Thesis

This thesis presents the relevant background information, the design approach based on simulation methods, and corresponding results obtained for the addition of a new supplemental safety system to the vehicle seat. The chapters that follow outline the relevant information regarding the work that has been previously conducted in this field, a description of the simulation tools that were created in order to model a rear-end collision, verification of these simulation tools, the implementation of the supplemental safety system, data analysis, and a discussion relating to the injury trends observed both with and without the implementation of the device. The final chapters will discuss the overall efficacy of the design and examine the future work that is required in order to progress the development of the device. The following is a breakdown of the thesis by chapters.

Chapter 2 discusses the current seat safety standards that exist today. This information is relevant due to the fact that new devices being implemented into the seat must adhere to these standards in order to be implemented. A description of the occupant dynamics experienced during a rear-end collision is provided in order to give an understanding of the different phases of occupant dynamics leading to a whiplash injury. Possible injury sites within the neck will also be discussed in order to provide an understanding of the specific injury mechanisms of whiplash. Several injury criterion have been previously created in order to quantify the amount of injury sustained to the occupant during a rear-end collision. These criteria will be discussed in detail in order to illustrate the rationale for selecting the one used in this research. Lastly, this chapter will outline the work that has been previously conducted relating to seat design parameters and occupant injury. This information is relevant as the system being developed in this study will work with existing systems that have been shown to reduce occupant injury.

In order to investigate the relationships between the seat and occupant (with and without the addition of the supplemental safety system) a numerical approach was taken. Chapter 3 will outline the development of the finite element models required to simulate a rear-end collision. Two models were created, one capable of simulating a vehicle collision, the other simulating a seat and dummy model. Utilizing both models will provide a detailed portrayal of the occupant dynamics for wide range of collision scenarios. This chapter will also discuss how the data from these simulations was used to determine the selected injury criterion (described in Chapter 2).

The supplemental safety system will be introduced in Chapter 4. The updated finite element model with the implementation of the supplemental safety device will be provided. In order to determine the optimal device parameters (i.e. geometry, mechanical behavior) a study was conducted at specific collision speeds. A final test plan involving testing the supplemental safety system at a variety of collision speeds is also outlined.

The results from the parametric study are provided in Chapter 5. This chapter will also summarize the efficacy of the device at a variety of intermediate speeds. Results are presented and discussed, outlining the importance of certain supplemental safety system characteristics. Relationships between the functionality of the safety device and the amount of injury sustained to the occupant will be discussed. These relationships include the effect of the supplemental device on selected injury criterion, occupant head and torso accelerations, kinetic energy, seat back deflection, and head restraint contact forces.

Conclusions regarding the influence of the supplemental safety system on occupant injury will be provided in Chapter 6. This chapter will summarize major findings from this investigation as well as outline the limitations of this study. The remaining work that must be conducted in order to implement this supplemental safety system will be outlined in Chapter 7.

1.7 Summary

This chapter has provided the evidence that rear-end collisions is an issue that affects many individuals. It has introduced some basic concepts relating the incidence and severity of rear-end collisions as well as the injury mechanism relating to rear-end collisions (i.e. whiplash and

occupant ejection). The importance of the vehicle seat and how it relates to rear-end collisions was also discussed. A need for additional improvements to the vehicle seat led to the development of the research objectives for this work.

In order to develop a system capable of further improving occupant injury response, an understanding of the exact problem must be attained through a comprehensive exploration of the available literature and previous work that has been conducted in this field. This information will lead to the many of the decisions and methods used in this research.

2 Literary Review

2.1 Overview

Currently, seat design standards exist which define a minimum strength for vehicle seats. These standards are a result of research that began as early as the 1960's. A detailed description of the seat design standards can be found in this section. This information is provided due to the fact that the supplemental safety system must adhere to current safety standards in order to be implemented.

The term "whiplash" is generally used to describe injuries levels of flexion/extension of the neck. As this is the primary mechanism of injury during a rear-end collision, researchers and vehicle seat manufacturers have focused on reducing this motion despite not knowing the exact injury site or mechanism within the neck. A description of the phases of a rear-end collision and how they relate to whiplash injury can be found in this section. The anatomy of the neck and potential injury sites within the neck are also described within this chapter.

Researchers have introduced several injury criterion which attempt to quantify the amount of injury sustained by an occupant who has experienced a rear-end collision. A detailed description of existing injury criterion can be found in this chapter. In order to test the efficacy of the supplemental safety system, the available injury criteria were individually considered with one being selected for this research.

Previous research has examined the relationship between certain seat characteristics and the injury response of the occupant. Some of these studies will be discussed in this chapter in order to gain an understanding of the previous work that has been done in this field. An understanding of how existing seat parameters can affect injury is crucial as the introduction of a supplemental safety system to the seat base may alter the motion of the occupant and thus alter the efficacy of the existing safety characteristics of the seat. Therefore, a description of past studies that have determined the relationship between seat parameters and occupant injury will be discussed in this chapter.

2.2 Vehicle Seat Design Standards

The supplemental safety system will be placed underneath the seat and will likely be fastened between the vehicle seat and the vehicle floor. The implementation of a supplemental safety system to the seat base will likely change the structural stability of the seat itself. It is important to ensure that the supplemental safety system still allows for the seat to adhere to federal regulatory requirements. Seats constitute a safety system within the vehicle and thus minimum requirements are defined by Transport Canada regarding various aspects of seat design. In Canada, seat requirements are dictated by the Canadian Motor Vehicle Safety Standard (CMVSS#207). This standard states that:

- A) Seat backs must be able to withstand a force of at least 20 times the weight of the seat applied in either a longitudinal forward or rearward direction through the center of gravity of the seat itself. This condition must be satisfied for any position to which the seat can be adjusted.

- B) In the seat's most rearward position, the seat back must be able to withstand a force that produces a moment of 373 Nm (3,300 in-lb) about the seating reference point for each designated seating position for which the occupant seat is designed (see Figure 2-1). This force is applied to the upper seat back or upper cross-member of the seat back. The moment is calculated by multiplying force P by moment arm D, for both the forward and rearward directions.

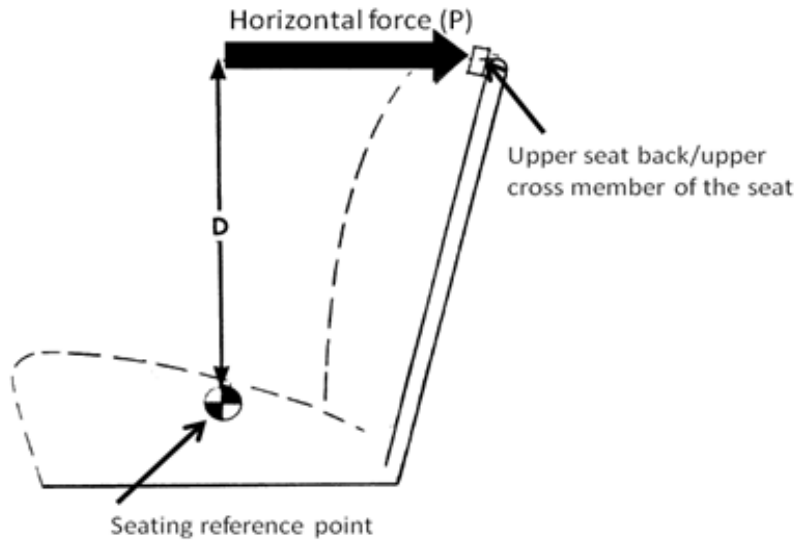


Figure 2-1: CMVSS #207 Testing Procedure (adapted from [26])

In the United States, automotive regulations are defined by the Federal Motor Vehicle Safety Standard (FMVSS). The specific standard that applies to seat anchorages is FMVSS#207. This standard is identical to CMVSS#207. In order to remain consistent, CMVSS#207 will be referenced throughout this document [26].

Seat designs were fairly primitive in the 1950's as they were designed to accommodate all body types and sizes in one structure. The seats were designed with strength of 3,559 N (800 lbs), with 1,779 N (400 lbs) resistances at each side of the structure. At this time it was assumed that the moment arm for occupant loading was 40.6 cm (16 in). This led to seat manufacturers designing seats that were capable of withstanding a moment of 723 Nm (6,400 in-lb) per side structure [25].

In 1961, General Motors undertook one of the first evaluations of seat performance in rear-end collisions. The intent of this study was to determine whether the 6,400 in-lb moment design specification was sufficient for preventing whiplash injury. This study compared the relation between seat strength and neck loads during a rear-end collision and found that an increase in seat back height would reduce the risk of injury for a larger proportion of occupants. This was a significant finding as at that point in time, head restraints were not used and seat back height

was significantly lower (i.e. only 55.9 cm (22 in) in height [25]) when compared to current vehicle seats.

In the early 1960's, the U.S federal government became invested in the issue of seat design. The Society of Automotive Engineers approved Recommended Practice J879 in 1963 [27]. This practice defined two test procedures for testing and evaluating seat strength. The first procedure was a static pull test performed on the seat back to evaluate anchor strength. The second procedure was a rearward moment applied to the seat back. In 1968, the U.S federal government issued a series of motor vehicle standards, including FMVSS#207.

In December of 1968, the National Highway Traffic Safety Administration (NHTSA) introduced the mandatory implementation of head restraints to all passenger vehicles. A minimum head restraint height requirement of 700 mm (27.5 in) above the seating references was also established and documented in FMVSS#202. The NHTSA also established the minimum requirement for rearward seat back strength (373 Nm) which can be found in FMVSS#207 [25].

In the 1970's, several new features were introduced to the vehicle seat. Bucket seats became much more prevalent due to their ability to allow for the occupant to adjust their distance away from the steering wheel. Seat back recliners were also introduced which gave occupants the opportunity to adjust their seat back angle [25].

In the 1970's to 1980's, minimum seat back strength was increased by some vehicle seat manufacturers. General Motors revised their design process by maintaining the seat back strength at 723 Nm (6,400 in-lb), however, implementing a maximum allowable seat back deflection angle of 10 degrees. They also determined that the seat back itself should return to within 5 degrees of the original preloaded angle once the load was removed [25].

At this point CMVSS#207 was performed with a static load only. In 1974, the NHTSA proposed to amend CMVSS#207 to include a dynamic rear impact test which would be similar to the moving barrier test that was used to test fuel tank integrity in FMVSS#301. The issue with this proposal was that while it would give a more realistic indication of seat behavior in an actual collision, this standard failed to address the types of injuries experienced, the number of such

injuries occurring, and a method of mitigating these injuries through proper design. Due to higher dynamic loads being applied to the seat, this standard would have enforced the need to design stiffer seats than the existing FMVSS#207 standards permitted. While several of the respondents at the time argued that doing this would actually increase injury, those who favored the amendments countered their argument by stating that ejection of the occupant through the rear window was a major concern and could be prevented by stiffer seats. Due to a lack of scientific studies on this matter and field accident data suggesting that occupant ejection only accounted for 4.5% of all rear-end collisions, it was decided on July 9th, 1976 that the NHTSA would take no action to amend FMVSS#207 [28].

No amendments were made to FMVSS#207; however, this petition paved the way for the implementation of a five year plan to prioritize rulemaking efforts in relation to seat design. Several desired outcomes of this plan included:

- Determining the types of trauma encountered in rear-end collisions and obtaining a more precise description of the nature of the collision.
- Determining which kinematic occupant parameters best correlate with injury and to investigate seat features that can assist to prevent this improper motion of the neck, head, and torso.
- Developing injury criteria and a head/neck model for simulation purposes.

In 1989 another petition was proposed to further modify FMVSS#207. This proposal attempted to improve the standard so that all seats must be able to withstand a force of 20 times the combined weight of the seat and the occupant (the original standard only included the weight of the vehicle seat). This petition also attempted to increase the minimum moment that the seat was able to withstand from 373 Nm (3,300 in-lb) to 6,327 Nm (56,000 in-lb) [29]. Saczalski had hoped that by implementing these changes, the risk of occupant ejection would decrease as the petition itself was based on four cases where the occupant had incurred serious/fatal injuries when ejected from the vehicle seat. This petition was declined due to various

researchers producing data that suggested that occupant ejection was not a significant problem in rear-end collisions [28].

While the standard remains unchanged since the mid 70's, in the early 1990's, General Motors conducted an in-depth study of seat design characteristics and their relation to occupant injury during a rear impact collision. This led to GM refining their minimum seat back strength from 373 Nm (3,300 in-lb) to 1,695 Nm (15,000 in-lb), nearly five times larger than the minimum found in FMVSS#207 [2]. However, Viano also determined that increasing seat back strength also meant an increase in seat back stiffness. This increase in stiffness was found to cause higher dynamic loads on the occupant's torso, which in turn caused greater neck deflections before coming into contact with the head restraint [2].

Currently, CMVSS#207 and FMVSS#207 do not take into account the mass and inertial loading due to the seated occupant. This is a problem due to the fact that the occupant mass is a direct contributor to the loading of the seat during a rear-end collision. As the load requirement is based on seat weight, this also means that lighter vehicle seats are not required to be as strong when compared to a heavier seat. This is an issue due to the fact that lighter seats will tend to experience a much higher degree of plastic deformation during a rear-end collision. In vehicles with lighter seats, the seat may also be more prone to failing, which may lead to the occupant being injured.

Before the supplemental safety system is implemented into the seat, it must be tested to ensure that the standards from CMVSS#207 are still maintained. This must be done in order to ensure that the device itself can gain the approval required to be implemented by auto manufacturers in Canada.

2.3 Biomechanics of Whiplash

An understanding of the motion of the neck and head during a rear-end collision is fundamental to the design of any injury mitigating device. The motion of the neck during a rear-end collision is well understood. Whiplash is attributed to injurious extension/flexion motion of the neck as

seen during a rear-end collision. The phases of neck motion as seen in a low speed rear-end collision are shown in Figure 2-2 and described below.

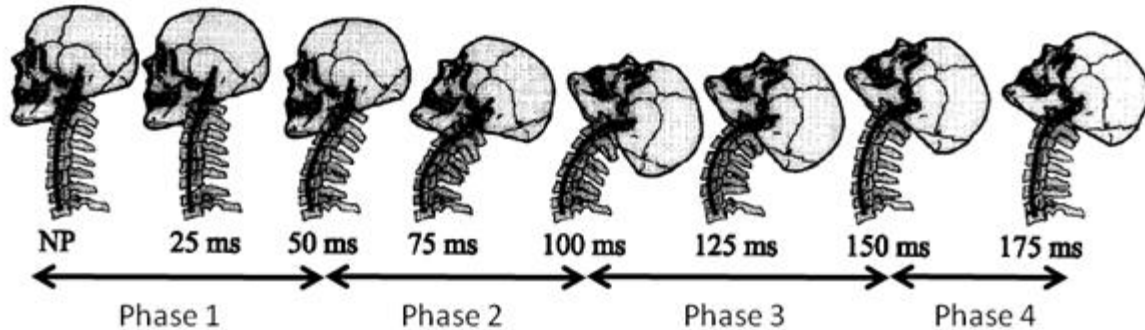


Figure 2-2: Phases of head and neck motion leading to whiplash from a rear-end collision (adapted from [30])

Phase 1: Head Retraction

Phase 1 typically occurs within the first 50 ms of the collision. The torso, having come into contact with the seat back, begins accelerating forward. The head, having not yet come into contact with the seat, has not experienced the effect of the crash pulse, and thus, experiences little forward acceleration. This causes the cervical spine to form an S-shape, placing a large strain on the tissues within the neck. Panjabi et. al. theorized that it is this phase of the collision that causes whiplash injury [30]. In Phase 1, the head is capable of translating up to 60 mm, relative to the T1 vertebrae, with no head rotation [30].

Phase 2: Head and Neck Extension

In Phase 2, the neck has reached a physical limit for which no further rear displacement can occur relative to the torso. The head begins to rotate with respect to the T1 vertebrae. Typically the head reaches its peak extension at 100 ms into the collision; however this is dependent on the occupant and the vehicle seat [30]. During this phase, head velocities and accelerations reach their peak values [30]. Velocity and acceleration magnitudes will depend on a variety of different parameters, including the seat configuration, occupant weight, gender, degree of cervical degeneration, neuromuscular response girth of neck, etc [31].

Phase 3: Rebound

During Phase 3 the head experiences a large forward acceleration due to the whipping effect generated from the torso, or contact with the head restraint. This phase typically occurs between 100 and 150 ms during the collision. The time at which the head makes contact with the head restraint is dependent on the occupant size, vehicle seat, and head restraint position [30].

Phase 4: Head and Neck Flexion

During this phase the head continues to move forward with respect to T1 and eventually flexion of the neck takes place. Figure 2-2 does not show the dynamics of the occupant after 175 ms. This is due to the fact that whiplash injuries typically occur within the first 150 ms of a collision.

Knowing that these phases occur throughout all rear-end collisions, it is possible to create a device that can activate during the critical injury causing phase. This is why an understanding of how the neck is moving, and the time frame at which it moves, is critical to the development of any supplemental safety device used for rear-end collisions.

While the motion of the head and neck during a rear-end collision are known, there is still a need to investigate further. Injurious flexion or extension can cause neck injury which can lead to a wide range of different symptoms. An understanding of what tissues within the neck are injured and how these tissue injuries manifest themselves into the symptoms experienced by the occupant must still be discussed.

2.4 Anatomy of Whiplash

Understanding the physiological implications of whiplash injury is important when developing any supplementary safety system. Different occupants may have different anatomical features (i.e. more muscle, stronger bones) which may lead to different injury responses from the same rear-end collision. The device must be designed to facilitate not just those individuals who possess healthy tissue, it must also be functional for those who may have experienced tissue degeneration over extended periods of time or have had previous irreversible damage to the

neck. An understanding of the anatomical cause of whiplash may provide insight into the development of this device, as the device itself may have to be altered or calibrated for different occupants.

Several theories have been developed attempting to explain the exact cause of whiplash related symptoms. Currently, researchers in this field believe that whiplash injury may occur to any one or a combination of the cervical facet joints, spinal ligaments, intervertebral discs, vertebral arteries, dorsal root ganglia, and neck muscles [21].

Cervical Facet Joint

The cervical facet joint (see Figure 2-3) is responsible for enabling movement between the vertebrae. When the neck is experiencing flexion, the facet capsule experiences tension, similarly, in neck extension, the facet capsule experiences compression.

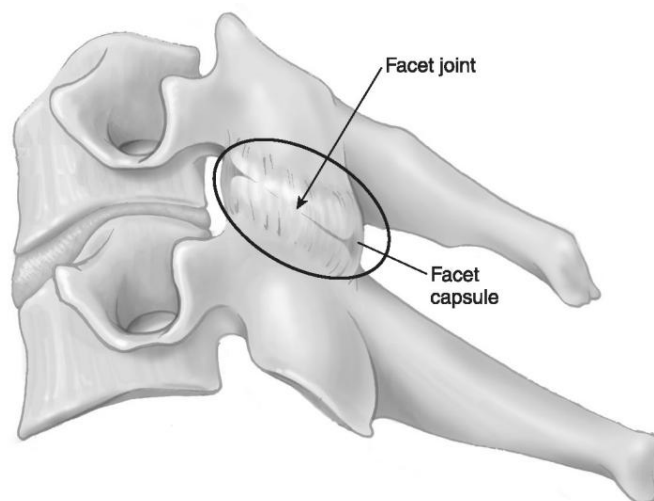


Figure 2-3: Facet joint (adapted from [32])

Cavanaugh et. al. suggests that there is significant biomechanical data that supports the idea that the overstretching of cervical facet-joint capsules is a possible source of whiplash injury [33]. Stemper et. al. found that during whiplash, lower cervical facet joints were exposed to increased distortions that could exceed tissue thresholds. This led to the finding of a strong correlation existing between facet-joint shear motion and segmental motion between vertebrae, which is typically seen during rear-end collisions. This study also concluded that

increased facet joint motions, particularly in the anterior joint regions, led to greater facet joint capsule distortion which may have led to neck injury [34]. By preventing injurious levels of flexion and extension during a rear-end collision, the amount of stress experienced by the facet capsule may be decreased, improving the overall injury response of the occupant.

Spinal Ligaments

The spinal ligaments assist with structural stability of the spine. There are two types of spinal ligaments, intertransverse and intersegmental. The intersegmental ligaments are responsible for holding the individual vertebrae together [35]. One of these ligaments is the anterior longitudinal ligament (ALL) (see Figure 2-4).

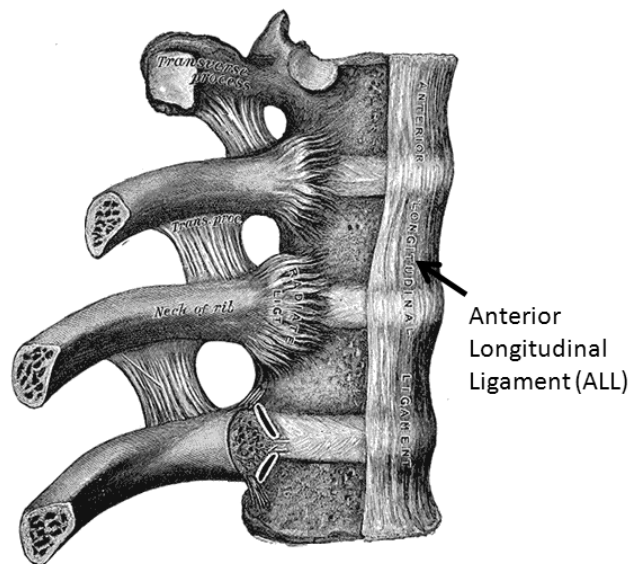


Figure 2-4: Anterior Longitudinal Ligament (adapted from [36])

Tominaga et. al. conducted a study attempting to determine the dynamic and mechanical properties of human cervical spine ligaments (specifically the ALL) following a whiplash injury. Using cervical spine specimens from cadavers ranging from 52 to 84 years old, the ligaments were divided into a control group and a whiplash exposed group. Both sets of ligaments were tested for failure force, elongation, energy absorption, and stiffness. The results from this study showed that the whiplash-exposed ligaments had a significantly lower failure force and less energy absorption capacity when compared to the control data. This may indicate that

irreversible damage is sustained by the neck after a whiplash collision [37]. This again illustrates the importance of whiplash mitigation systems within the seat as those affected by whiplash even one time, may never regain full functionality of the neck again.

Vertebral Arteries

The vertebral artery (see Figure 2-5) is one of two arteries that runs towards the head through the side projections of the neck vertebrae and then enters the skull [38]. It is responsible for supplying blood to the head, brain, and neck tissues [21].

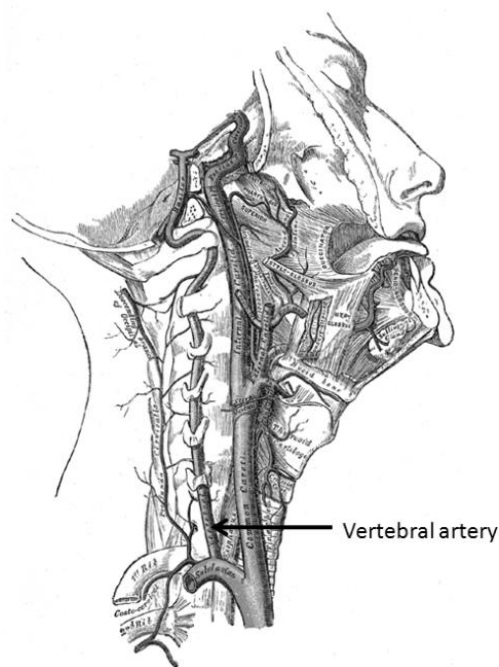


Figure 2-5: Vertebral artery (adapted from [36])

Vascular deficiency has been suggested as a possible explanation of many of the symptoms that are experienced by whiplash victims. The elongation of the vertebral artery (see Figure 2-5) can lead to a decrease in the diameter of the artery due to Poisson's ratio [39]. This can act to decrease blood flow to the brain. Nibu et. al. performed a study that attempted to quantify the amount of elongation in the vertebral artery (VA) during a whiplash simulation, with the use of an in vitro model. This study found that the maximum VA elongation experienced during a whiplash trauma was highly correlated with the horizontal acceleration of the test sled used to accelerate the seat and occupant. The sled was subjected to 2.5, 4.5, 6.5 and 8.5 g accelerations

and the VA was shown to exceed allowable elongation in all four cases [40]. The elongation of the VA can be prevented if the amount of flexion extension motion of the neck is limited. The addition of a supplemental safety system which will act to reduce relative motion between the head and torso may act to prevent VA elongation and thus eliminate symptoms such as headaches and vertigo.

Dorsal Root Ganglion

The dorsal root ganglion contains the cell bodies of many peripheral sensory nerves. Direct injury to this site may injure the nerve cell bodies, potentially explaining rare symptoms such as headache, vertigo, vision disturbance, and neurological disturbances of the upper extremities [21].

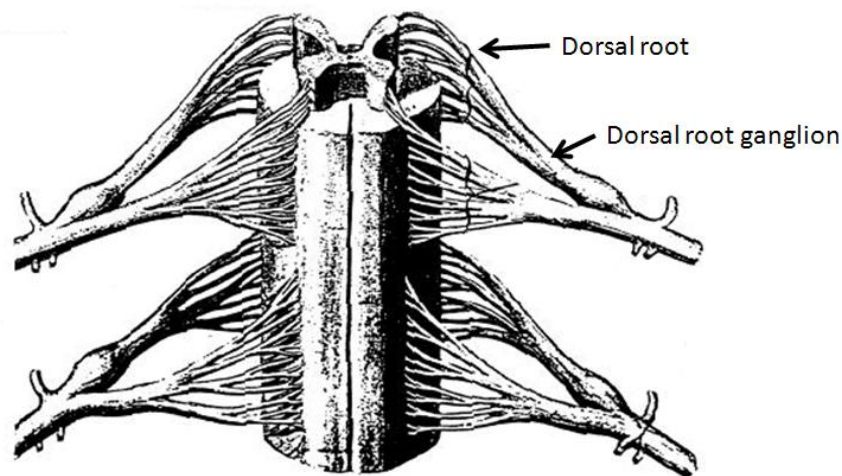


Figure 2-6: Dorsal root ganglion (adapted from [41])

Svensson et. al. stated that the inner volume of the spinal canal decreases during neck extension and increases during neck flexion [42]. They theorized that during extension-flexion motion, pressure gradients along the spinal canal are generated due to the incompressible nature of the fluids found within the spinal canal. These pressure gradients may act to generate injurious stresses and strains on the exposed tissue. The increase in pressure likely results in tissue damage such as that observed in the spinal ganglia found in the lower portion of the neck [42]. The addition of a supplemental safety system which further reduces whiplash injury may

act to reduce the pressure buildup within the spinal canal due to decreased flexion/extension motion. This will likely reduce the amount of injury sustained by the occupant.

Muscle

Muscle strain may play a more indirect role in the injury of other structures within the neck as opposed to the direct source of injury themselves [21]. Injury as a direct result of muscle strain it is likely due to the imposed lengthening of certain muscles due to the motions experienced in a rear-end collision, despite the active contraction of the same muscles. During the retraction phase (i.e. Phase 1), the anterior neck muscles (such as the sternocleidomastoid) contract while being lengthened, and during the rebound phase (i.e. Phase 3), the posterior muscles in the neck (such as the semispinalis capitis muscle) become the active muscles and are also lengthened [21].

While any one, or combination of, the tissues mentioned above may be responsible for the symptoms experienced by an occupant after a rear-end collision, damage to all of the aforementioned tissues is caused by rapid flexion/extension motion of the head and neck. The goal of this work is to develop a system that can further act to reduce the amount of extension experienced during a rear-end collisions, and while it remains unclear as to which tissue is the primary cause of injury, it can be expected that reduced head and neck motion will act to reduce injury.

2.5 Injury Criteria

The previous sections outlined the motion experienced by the occupant during a rear-end collision, as well as the possible injury sites of whiplash. These sections have reaffirmed the idea that limiting head flexion and extension motion during a rear-end collision is necessary in order to reduce occupant injury. However, unless injury can be quantified, it is not possible to determine whether or not improvements have been made to the seat design. Therefore, injury criteria must be used to assess the level of injury experienced by the occupant. These criterions generalize the level of injury based on easily measured parameters including displacements,

velocities, and accelerations of the head, vertebrae, and torso. A description of the criteria that exist and are currently being used by researchers in this field is found below.

2.5.1 Neck Injury Criterion (NIC)

The Neck Injury Criterion (NIC) was proposed by Bostrom et. al. in 1996 and is based on the hypothesis of Aldman (1986) and the findings of Swensson (1993) [5]. This criterion was based on a series of studies conducted on pigs which determined the pressure gradients of spinal fluid within the neck of the pig during flexion and extension. A relationship was formed between these measurements and the amount of permanent tissue damage found within the neck. NIC is a created parameter which utilizes this previously developed relationship from the pig studies to quantify neck injury in human subjects based on relative head and torso dynamics [42]. While several anatomical differences exist between humans and pigs, this criterion focuses on resultant pressure gradients caused by neck flexion/extension motion which occurs similarly for both humans and pigs. NIC can be calculated by quantifying the relative acceleration and velocities between the head and the torso (see Eq 1, 2 and 3 below) which are typically measured at the bottom (T1 vertebrae) and top (C1 vertebrae) of the neck (see Figure 2-7).

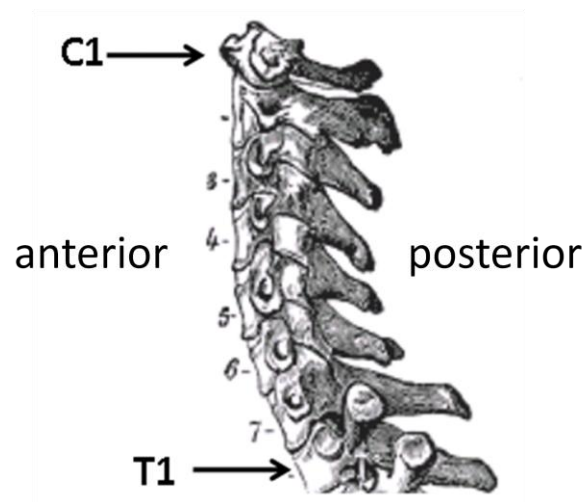


Figure 2-7: T1 and C1 vertebrae (adapted from [36]).

As the relative difference in velocity and acceleration between these two point increases, the likelihood of injury also increases. The equations used in this criterion are shown Eq. 1, Eq. 2, and Eq. 3.

$$NIC(t) = k \times a_{rel}(t) + (v_{rel}(t))^2 \quad (1)$$

$$a_{rel}(t) = a_{T1}(t) + a_{C1}(t) \quad (2)$$

$$v_{rel}(t) = v_{T1}(t) + v_{C1}(t) \quad (3)$$

Where $k = 0.2 \text{ m}$, and a and v are the acceleration and velocity of the T1 or C1 vertebrae in units of m/s^2 and m^2/s^2 respectively.

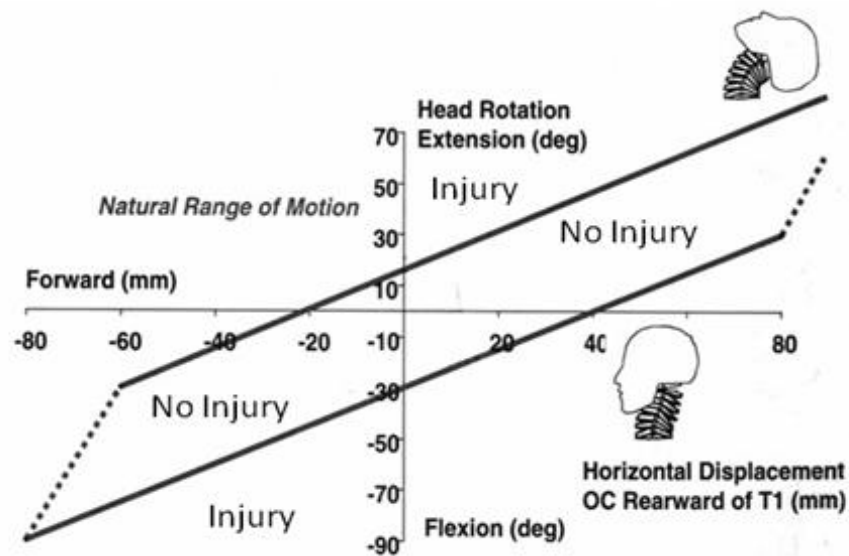
Bostrom et. al. determined that injury is sustained for NIC_{max} values greater than $15 \text{ m}^2/\text{s}^2$ [5]. While NIC remains the most commonly utilized criterion for rear-end collisions [43] it is not without limitations. The first limitation is that NIC_{max} can only be determined during the first 150 ms of the collision [44], which prevents NIC from indicating whether injury is occurring during the rebound phase. The second limitation is that this criterion does not take into account the tension/compression effect of the spine. This effect can act to influence the degree of injury an occupant is experiencing. NIC, only having been developed for low speed collisions, may also be less accurate at determining injury higher to severe collision speeds.

This criterion is one of the most commonly used by researchers and, as such, offers the ability to compare the results from this study to several others that exist. While it was not specifically designed to be used at high collision speeds, the basic principal of comparing the dynamics of the top and bottom of the neck are universal for all speeds as whiplash injury is caused by rapid flexion/extension motion regardless of acceleration pulse. Due to the ability to easily quantify NIC at any collision speed, and due to the fact that it is perhaps the most commonly used injury criterion on this field of study, this injury criterion was used in this study.

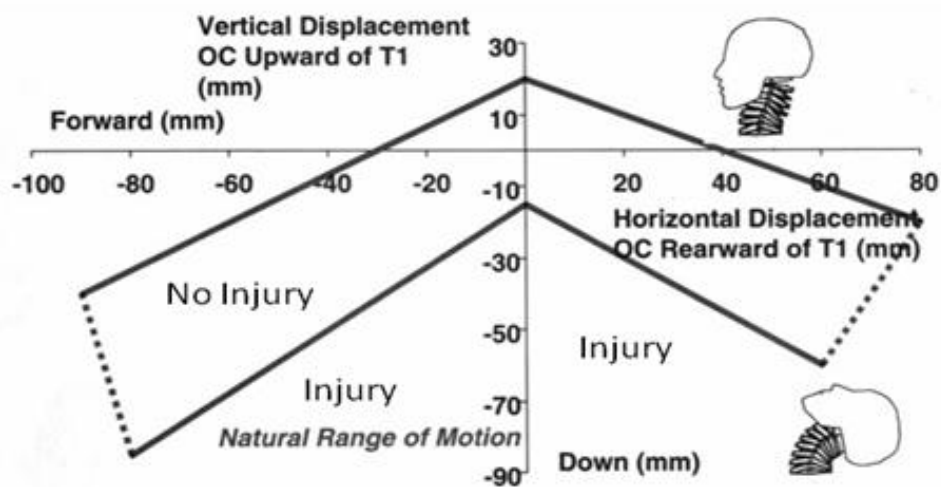
2.5.2 Neck Displacement Criterion (NDC)

This criterion was developed by the Lear Corporation and utilized in several previous whiplash studies, most notably, that of Viano [2]. This criterion attempts to determine the cumulative effects of neck compression, shear, tension, and bending moments that displace the head, by looking at head rotation and the relative x- and z- displacements with respect to T1. In applying this criterion, head displacements and rotations are bound to an acceptable range of motion as

previously determined through volunteer sled tests. The likelihood of injury increases as the head and neck trajectory approaches the limits of the defined corridors. These corridors, as previously defined for normal human motion, are shown in Figure 2-8.



a)



b)

Figure 2-8: Neck Displacement Criteria Plots: a) Shearing vs. Rotation b) Shearing vs. Compression/tension (adapted from [2])

NDC also has limitations. Since this criterion is based upon the physical limits of the neck, it does not account for age, gender, size of neck, and spinal degeneration. Secondly, the corridors themselves were defined only based on the 50th percentile male. It is for this reason that the corridors shown in Figure 2-8 are seen as a “fuzzy” tolerance limit as opposed to one that encompasses all occupants.

While NDC is useful at quantifying injury, even at high speeds, it has one major drawback. The implementation of a properly placed head restraint acts to limit the amount of head displacement experienced by the occupant, thus potentially giving the impression of a safe collision environment when in reality, high accelerations to the neck and head may cause injury even without the presence of large displacements. The supplemental safety system being developed in this study will act to work in conjunction with other safety devices, not to replace them. Therefore, this criterion was not used in this study,

2.5.3 Normalized Neck Injury Criterion (N_{ij})

Currently FMVSS#208, which is the standard for frontal crash protection, includes a neck injury criterion that examines tolerance limits for axial loads, shear loads, and bending moments. This criterion is based on the idea that axial loads (tension and compression) and bending moments (flexion and extension) can be plotted together to develop a corridor for which acceptable neck motion must fall within. The first iteration of this criterion is shown in Figure 2-9.

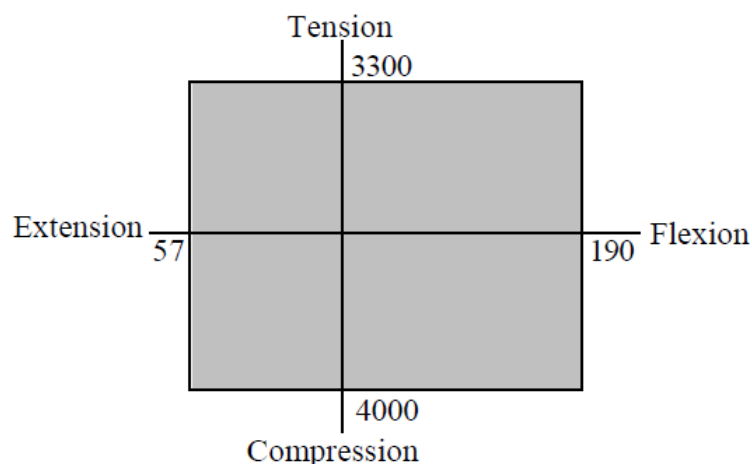


Figure 2-9: Previous FMVSS#208 Neck Injury Criteria [45]

This criterion was modified due to the fact that it failed to consider the combined effect of extension and tension, which could act to magnify the degree of injury experienced by the occupant. The concept of creating a neck injury criterion that was based on linear combinations of loads and moments was introduced by Prasad and Daniel in 1984. As a result, N_{ij} was developed. In this criterion the “ij” represents the indices for the four injury mechanisms (tension, compression, extension, and flexion). This leads to four different measures for this criterion: N_{TE} , N_{TF} , N_{CE} , and N_{CF} , where the first indices represent either tension or compression and the second indices represent either flexion or extension. The acceptable limits were updated to this modification. Figure 2-10 illustrates the updated limits for the 50th percentile male dummy [45].

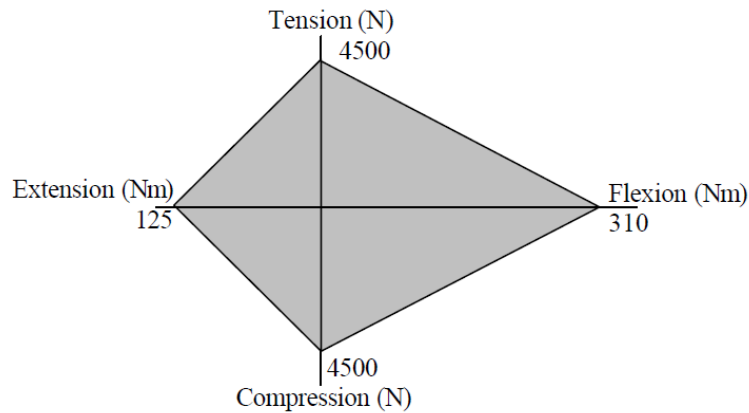


Figure 2-10: Updated limits for the 50th percentile male dummy [45]

It was necessary to normalize this criterion in order to allow for comparisons to be made between studies that utilized different ATDs. A normalized value of N_{ij} was determined by dividing each axis by the allowable limits of the particular dummy in use. This led to the more commonly seen equation for N_{ij} , shown in Eq. 4.[46].

$$N_{ij}(t) = \frac{F_Z(t)}{F_{critical}} + \frac{M_Y(t)}{M_{critical}} \quad (4)$$

Where $F_{critical}$ and $M_{critical}$ depend on the direction of the applied loading (i.e. causing flexion or extension) and on the dummy being used. An N_{ij} value of 1.0 marks the border between acceptable and not acceptable, according to the rating system of the Insurance Institute for

Highway Safety [46]. While this injury criterion may be indicative of injury, it was originally designed to assess severe injury in frontal collisions, not rear-end collisions. This criterion has also only been validated using a dummy representing a 3 year old subject and was then scaled in an attempt to be applicable to other sized dummies [44]. Based on the uncertainty associated with its applicability to the current research outlined above, this criterion was not selected for this study.

2.5.4 Neck Protection Criterion (N_{km})

Schmitt et. al developed a new injury criterion N_{km} , which is a modification of the N_{ij} criterion. Similar to the N_{ij} criterion, this criterion takes into account linear combinations of loads and moments [44]. However, the difference between N_{km} and N_{ij} is that N_{km} considers sagittal shearing forces to be the critical load case as opposed to axial forces. The equation for N_{km} is shown in Eq. 5.

$$N_{km}(t) = \frac{F_X(t)}{F_{int}} + \frac{M_Y(t)}{M_{int}} \quad (5)$$

Where F_{int} and M_{int} are the critical values that pertain to the specific dummy being used [44]. Similar to N_{ij} , the “k” and “m” in N_{km} are indices where “k” represents forward/rearward shear, and “m” represents extension/flexion moment [47]. Unlike NIC, there is no injury threshold for this criterion, and no correlation exists between this criterion and NIC_{max} , which may lead to potential design conflicts if both are used [44]. For these reasons, this criterion was not selected for this study.

2.5.5 Inter-Vertebral Neck Injury Criterion (IV-NIC)

While NIC values are shown to increase with increasing impact severity, there is still no definitive correlation between NIC and the amount of soft tissue injury experienced by the occupant. NIC, having been developed based on relative accelerations and velocities of the T1 and C1 vertebra only, does not take into account the response of tissue within the neck which may act to decrease the allowable threshold value of $15 \text{ m}^2/\text{s}^2$ defined by NIC [48]. As a result,

IV-NIC was developed based on the idea that inter-vertebral motion beyond physiological limits is the primary indicator of injury. IV-NIC(t) is shown in Eq. 6.

$$IV - NIC_i(t) = \frac{\theta_{dynamic,i}(t)}{\theta_{physiological,i}} \quad (6)$$

Where $\theta_{dynamic,i}(t)$ represents the dynamic inter-vertebral rotation during the collision and $\theta_{physiological,i}$ represents the physiological range of motion limit for the vertebra being examined. The physiological range of motion limit for every vertebra is tabulated and summarized by Panjabi et. al. [48]. IV-NIC has the ability to predict the intervertebral level, mode of loading, and severity of soft tissue damage to the spine during a whiplash injury [48] allowing it to model whiplash injury more precisely. However, this criterion is not validated and possesses no threshold injury value [44]. It also relies heavily on intervertebral interaction which may result in inaccurate predictions if the spine model used to produce IV-NIC is not accurate. As a result, this criterion will not be used in this study.

In conclusion, the neck injury criterion (NIC) was the injury criterion selected for this study because: 1) it has a proposed and validated threshold value for predicting neck injury (based on pig studies), 2) it does not have a strong dependence on vertebrae-to-vertebrae interaction, and 3) it has been accepted and has seen wide-spread use in previous research.

2.6 Seat Design Choices and Their Effect on Occupant Injury

The three main components of the vehicle seat are the seat base, seat back, and head restraint. While the focus of this work is on designing a supplemental safety system for the seat base, this device is intended to work in conjunction with other safety devices found in the seat back and the head restraint. Several studies have been conducted which examine design changes made to the seat and their effect on occupant injury. These studies, which have outlined trends based on seat design parameters and occupant injury, may give insight into how the seat base system could further mitigate injury.

2.6.1 Seat Back

While occupant comfort is a major focal point of seat back design, the seat back also serves two purposes relate to crashworthiness. The first is to prevent occupant ejection by ensuring that the occupant remains in the seat during the collision. The second is to reduce the amount of acceleration to the torso upon loading. Several studies have been conducted which examine the effect of design changes to the seat back to the risk of injury. These studies are discussed below.

Shin et al. conducted a study examining the effect of collapsing the seat back into two separate components during a rear-end collision. The collapse angle of the seat was varied in order to observe whether there was a relationship between seat back design and neck injury. A sled test was conducted at 33 km/h, employing the use of a 50th percentile Hybrid III dummy. The simulated sled test was validated against real test data. The effect of five separate seat design parameters on occupant injury was examined. These parameters were the head restraint back-set, seat back collapse angle, friction coefficient of the seat, the joint stiffness between the seat back and seat base, and the head restraint stiffness. This study found that an improved injury response could be achieved by increasing the friction coefficient between the dummy and the seat and by reducing the joint stiffness between the seat back and seat base [49].

Kaneko et al. aimed to optimize seat design parameters in order to generate an improved occupant response during a rear-end collision. This study employed the use of a BioRID II MADYMO model, utilizing NIC as an injury criterion. In order to validate the BioRID II MADYMO model, a hydraulic sled test was used with a BioRID II dummy. A parametric study was conducted to examine the effect of changing head restraint height, head restraint back-set, upper seat back stiffness, middle seat back stiffness, lower seat back stiffness, seat back frame stiffness, seat bracket stiffness, and seat cushion stiffness. This study found that, along with head restraint back-set, seat back middle stiffness was highly influential in the overall amount of injury experienced by the occupant [13].

Romilly and Skipper examined the effect of dual and single recliner stiffness, head restraint frame stiffness, seat back frame stiffness, inner seat back compliance, and the influence of

seatbelt application on occupant injury during a rear-end collision. This study employed the use of a seat and dummy model which was comprised of the Hybrid III 50th percentile occupant and a GM High Retention seat. A half-sine CMVSS 202 crash pulse, approximating a 17 km/h delta-V collision was used to model a low speed collision, and a higher severity crash pulse, approximating a 42.5 km/h delta-V was used to examine a high speed collision where occupant ejection may take place. This study found that the most influential seat structural components pertaining to the seat back were the recliner rotational stiffness and thoracic region compliance [50].

These studies suggest that:

- Increasing the coefficient of friction between the occupant and seat can reduce injury
- Reducing the joint stiffness between the seat back and seat base can reduce whiplash injury
- Thoracic region compliance is influential in the injury response of the occupant

2.6.2 Head Restraint

The head restraint acts to prevent relative motion between the head and the torso during a rear-end collision. Several studies have been conducted to determine the impact of head restraint characteristics and positioning on safety.

The study produced by Kaneko et al., previously discussed in relation to seat backs, showed that along with seat back middle stiffness, the most influential seat design parameter in preventing injury is the head restraint back-set [13]. Viano conducted a study that examined the effect of changing head restraint height and back-set on the overall injury response of a Hybrid III dummy. These tests simulated rear-end collisions of 12.9 km/h and 19.3 km/h. This study found that a 42% reduction in injury risk could be achieved by adjusting the head restraint to a proper height. This study also concluded that a reduced head restraint back-set could also lead to an improved injury response [2].

Svensson et. al. conducted a study investigating the influence of head restraint parameters on the injury response of a Hybrid III dummy fitted with a RID neck during a low speed rear impact

collision. Several combinations of seat designs were tested: seats with and without rods to stiffen the seat back, belts between side members, and an additional padding wedge between the occupant and seat. Head restraint back-set was also manipulated in order to determine its effect on injury. This study found that that head restraint back-set prior to impact had the largest influence on the overall dynamics of the neck. Smaller head restraint back-set resulted in smaller maximum rearward head displacements [51].

In the study conducted by Romilly and Skipper [50] (discussed in the previous section) it was found that an increase in head restraint frame stiffness could act to reduce occupant injury.

These studies suggest that:

- Decreasing the head restraint back-set can reduce injury
- Adjusting the head restraint to the correct height can reduce injury
- Increasing head restraint frame stiffness can reduce injury

2.6.3 Seat Base

Currently, seat base design has focused primarily on ergonomics, specifically relating to long term seating comfort. Few studies have examined the effect of utilizing the seat base to further mitigate injury.

Himmetoglu et. al. conducted a study investigating the effect of several anti-whiplash features added to the seat base. Several designs, which incorporate the addition of a spring-damper to the seat base as well as a pressure plate triggered active head restraint, were added to the seat. Six configurations were tested; these configurations are shown in Figure 2-11. In this study a 50th percentile male, multi-body human model was developed and validated against the response of seven human volunteers. The seats were tested at $\Delta V=16$ km/h with $a_{\text{mean}}=5g$ and $a_{\text{peak}}=10g$. The devices themselves were designed not to trigger for collisions that had a $\Delta V < 4.5$ km/h in hopes of preventing the device from activating during day to day routines.

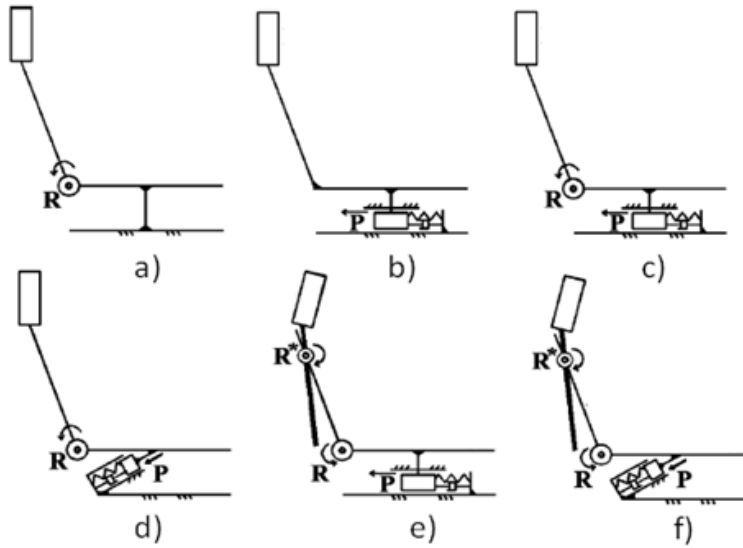


Figure 2-11: Anti-Whiplash seat configurations: a) rotational spring damper; b) spring damper; c) rotational spring damper with linear spring damper; d) rotational spring damper with tilted linear spring damper; e) rotational spring damper, active head restraint, linear spring damper; f) rotational spring damper, active head restraint, tilted linear spring damper (adapted from [52])

The values of NIC_{max} for all the configurations in this study are summarized in Table .

Table 2-1: NIC_{max} for Himmetoglu et. al. study [52]

Seat Design	NIC_{max}	%Improvement
Rigid seat (Baseline)	11.8	-
A	11.4	3.39%
B	11.13	5.68%
C	7.68	34.92%
D	7.06	40.17%
E	6.81	42.29%
F	6.28	46.78%

This study found that with the addition of a spring damper to the seat base (Figure 2-11b), minimal improvements in occupant response can be achieved. However, when a tilted spring

damper was used in the seat base in conjunction with a rotational spring damper in the seat back (Figure 2-11c), a 40.17% improvement was achieved. This indicates that the addition of a supplemental safety system in the seat base may act to reduce injury risk in conjunction with another safety device in the seat back or head restraint [52].

2.6.4 Crash Pulse

The acceleration pulse at the seat is a function of several parameters such as speed change, average acceleration, collision duration, displacement during the collision, and pulse shape [53]. Krafft et al. conducted a study that determined the effect of collision duration on the injury time experienced by the occupant. There was a significant difference in mean acceleration between rear impacts where the occupants sustained symptoms for more than and less than a month. For those who sustained injuries for more than a month, the mean acceleration was $5.3 \pm 0.6g$. For those who sustained injuries for less than a month the mean acceleration was $3.9 \pm 0.5g$ [54].

Siegmund et. al conducted a study examining the effect of collision pulse properties on selected injury criteria. This study employed the use of a BioRID II dummy tested in a linear sled that accelerated the seat and dummy forward. Fifteen different collision pulses were used, which were classified according to speed change, peak acceleration, collision duration, displacement during the acceleration and pulse shape. The results from this study indicated that for a specific seat, head restraint position, initial seating position, and dummy type, a strong correlation existed between NIC and speed change during the first 85 ms of the collision [53].

Sendur et. al. conducted a parametric study examining the effect of vehicle design on the four stages of whiplash injury: retraction, extension, rebound, and protraction. This study employed a multi-body model constructed in MSC.ADAMS and a 50th percentile male model with individual cervical and lumbar vertebrae. A seat model was produced that was comprised of a seat bottom, seat back, and head restraint. This study aimed to examine the effect of crash duration, head restraint back-set, head restraint height, and seat stiffness on occupant injury. The results indicated that during all four stages of the collision, the crash duration had the

greatest influence on occupant dynamics. The most notable phase was the retraction phase, where crash duration accounted for 70% of the influence [55].

These studies suggest that:

- Mean crash pulse acceleration is related to the duration of symptoms experienced by the occupant
- The speed change within the first 85 ms is related to the amount of injury sustained by the occupant
- Crash duration has the greatest influence on occupant injury

2.6.5 Occupant

Occupant size and pre-impact seating position may play a role in the injury response following a rear-end collision. While many studies utilize the 50th percentile male, representing the average occupant, several studies examined occupant related parameters more closely.

Women typically experience higher rates of whiplash than men [56]. One study showed that women are 1.5-2 times more likely to experience whiplash when compared to men [57]. Viano theorized that this trend is caused by the relative differences in torso and head mass between men and women, which can directly relate to the accelerations and displacements experienced by the torso. Women also typically have a lower neck stiffness when compared to men [2].

Krafft et. al [56] examined the rates of whiplash injury for front and rear seated occupants during a rear-end collision. The results from this study were based on reported neck injury data from Folksam, a Swedish insurance company. This study found that there was a higher risk of permanent disability for female rear seat passengers than for female front seat passengers, female rear seat passengers than for male occupants, female occupants than for female front seat passengers, female rear-seat passengers than for male rear-seat passengers, and female occupants than male occupants [56].

These studies suggest that:

- Women are more likely to experience whiplash than men

- The injury response of the driver compared to other occupants within the vehicle differ

In conclusion, the results that relate the most to the implementation of a seat base supplemental safety system for the seat base are:

- *The implementation of a spring-damper system to the seat base in conjunction with other safety devices in the seat back and head restraint resulted in reduced injury:* This indicates that there is potential to assist other systems through redesign of the seat base.
- *Crash duration has the greatest influence on occupant injury:* This indicates that by manipulating or delaying the response of the crash pulse through the implementation of an intermediate device in the seat base, further improvements to occupant injury can be made.
- *The speed change within the first 85 ms is related to the amount of injury sustained by the occupant:* This may indicate that the supplemental safety system should be triggered during the first 85 ms to counter the sudden change in speed.
- *Women are more likely to experience whiplash than men:* This may suggest that women will benefit more from the addition of a supplemental safety system.

2.7 Summary

The seat must adhere to government regulations (CMVSS#207) after the implementation of a supplemental safety system to the seat base. This means that the supplemental safety system must function without compromising the structural integrity of the seat. With a good understanding of the dynamics experienced by the occupant, and several theories as to the exact injury causing mechanism within the neck, several injury criteria have been defined in order to quantify injury. Neck Injury Criterion (NIC) will be used in this study due to its wide use in this type of research as well as its simplicity in derivation. It is apparent that significant research in this area has been conducted; however, this research has focused primarily on redesign of the seat back and head restraint. Previous research does indicate several concerns that do apply to the implementation of a seat base system, specifically that crash pulse

duration, speed change within the first 85 ms, and occupant size all affect occupant response. These factors will be taken into consideration during the development of the seat base system. The development and application of the design tools required to model a rear-end collision will be discussed in the next chapter.

3 Model Creation

3.1 Overview

As outlined in Chapter 1, one of the initial research tasks defined was to obtain the means to assess the dynamics experienced by a seated occupant in a rear-end collision over a range of collision severities. This required the development of two finite element-based software simulation tools to quantify the vehicle response to a rear-end collision.

The first simulation employs the use of two vehicle models acquired from the National Crash Analysis Center (NCAC) [58]. This simulation represents a severe rear-end collision, and the results provide the acceleration pulse of the struck vehicle at the driver seat for any impact velocity. The acceleration pulses generated from this simulation are used as an input for the second simulation.

The second simulation consists of a seat and dummy model that employs the use of the Hybrid III 50th percentile dummy seated in a GM High Retention seat. Originally created by Skipper and Romilly [31], this simulation has been updated to include a properly adjusted head restraint and a more advanced Hybrid III dummy with a neck composed of separate vertebrae as opposed to one rigid part. This second simulation utilizes the acceleration pulse acquired from the first simulation as an input, and then generates occupant displacement, velocity, and acceleration data. This data is then used to determine the Neck Injury Criterion (NIC) which was previously discussed in Chapter 2.

While the GM High Retention Seat model used by Skipper and Romilly was originally created using Unigraphics NX from UGS, Patran from MSC Software Corporation, and LS-DYNA from Livermore Software Technology Corporation (LSTC), this research employs the use of LS-DYNA only. LS-DYNA (and LS-PrePost) is a general-purpose non-linear transient dynamic explicit finite element program.

This chapter outlines the development, specifications, and intended use of both simulations, and indicates how the output occupant dynamics data will be used to derive NIC correctly. The

injury outcome from the use of these models, for specific crash scenarios that have been previously studied, will be compared in order to determine the efficacy and reliability of these models in the absence of physical testing.

It is noted that throughout this thesis, the global x-direction is taken as the vehicle longitudinal axis (anterior direction of the occupant), the global y-direction is along the vehicle lateral axis (transverse direction of the occupant), and the global z-direction is parallel with the vehicle vertical axis (superior direction of occupant).

3.2 Vehicle Collision Model

In order to determine the dynamics of the struck occupant during a rear-end collision, it is necessary to determine the acceleration pulse of the vehicle seat on which they are seated. The acceleration pulse is a function of impact velocity, the amount of energy removed from the collision through crush zones, the mass of the vehicles, as well as the mass of the occupant and seat. Therefore, a model capable of modeling a rear-end collision (see Figure 3-1) was created in order to generate an acceleration pulse at the driver seat that reflected a severe crash scenario for a variety of different impact velocities. While the FMVSS#202 half-sinusoidal pulse is typically used in rear-end collision studies, this study aims to show that the supplemental safety device is functional for a variety of different collision pulses representing several collision speeds, not just one. The FMVSS#202 pulse cannot simply be scaled to represent other collision speeds; therefore it was necessary to produce this model to generate these acceleration pulses. It is noted that the pulses that have been generated from this model contain several peaks and valleys (see Appendix A). It is believed that these peaks and valleys represent the effect of several individual crush zones being triggered during the collision. In reality, it is more likely that the actual collision pulse will resemble that of the vehicle crush model output and not the uniform half-sinusoidal pulse of FMVSS#202.

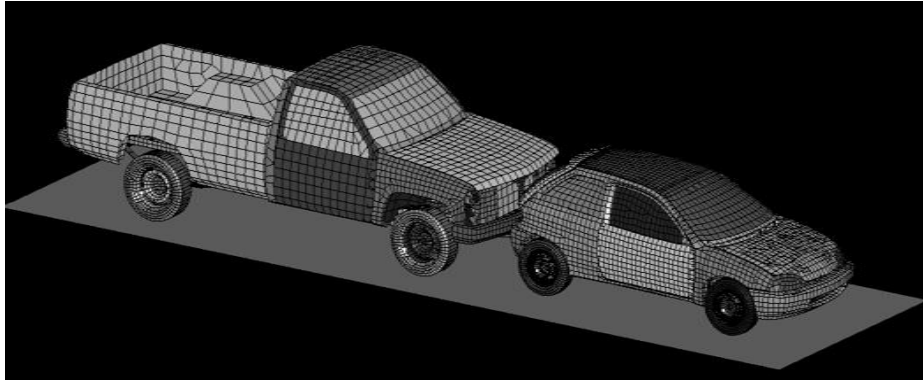


Figure 3-1: Vehicle collision model

This model utilizes two finite element vehicle models produced by the National Crash Analysis Center (NCAC) [58]. This model is composed of a large bullet vehicle (Chevrolet C2500 all-purpose pickup truck) hitting a small target vehicle (Geo Metro). The software package used to create this model is LS-DYNA which is a general purpose transient dynamic finite element program capable of simulating complex real world problems. This software package was selected based on the fact that it is heavily used in automotive design problems. The crash model is capable of facilitating any impact velocity or impact angle. This study will only examine a direct rear-end collision. A description of the vehicle models used in this model is found below.

Chevrolet C2500 Model (Bullet Vehicle)

While clearly many rear-end collisions occur with smaller bullet vehicles, the supplemental safety device is expected to reduce occupant injury for severe crash scenarios, thus a large bullet vehicle (i.e. the Chevrolet C2500 light-truck) was selected for this study.

The Chevrolet C2500 light-truck vehicle model consists of a frame, cab, and a box bolted together. The chassis frame supports the engine, transmission, power train, suspension and accessories of the vehicle as seen in Figure 3-2.

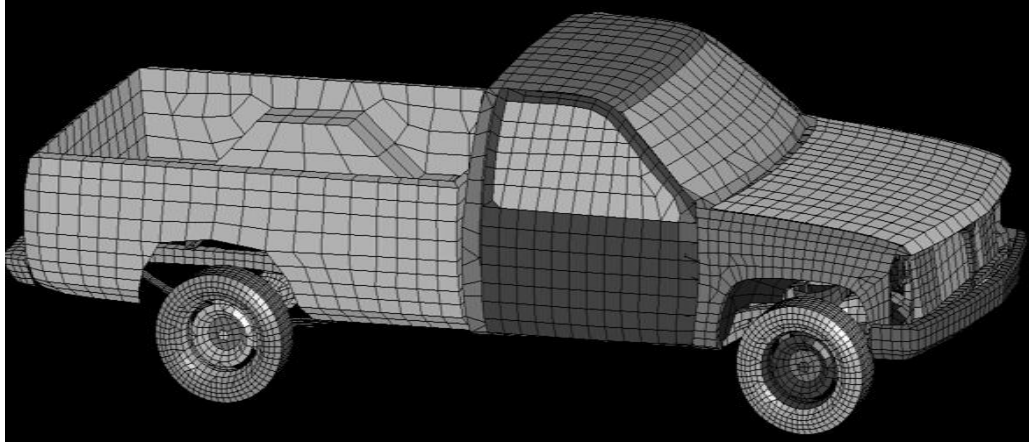


Figure 3-2: C2500 Pickup truck model

The mass of the simulated truck model is approximately 1,857 kg (4,093 lb). The actual curb weight of a 2000 C2500 pickup truck is 2,080 kg (4,586 lb) [59]. The difference in vehicle weight can be attributed to the fact that the simulated vehicle model represents a simplified model which does not contain many of the components found in the interior of the vehicle. This model consists of 10,500 elements which is less elements, when compared to the to the more advanced C2500 model which contains 58,313 elements. The simplified model was chosen in order to reduce computational time as computational time increases significantly with an increase in element number.

Geo Metro Model (Target Vehicle)

The Geo Metro (Figure 3-3) model used in this study is a simplified model based on a more complex vehicle model currently available from the NCAC. Similar to the C2500 pick-up, this simplified model was created in order to reduce the computational time required for the crash model simulation.

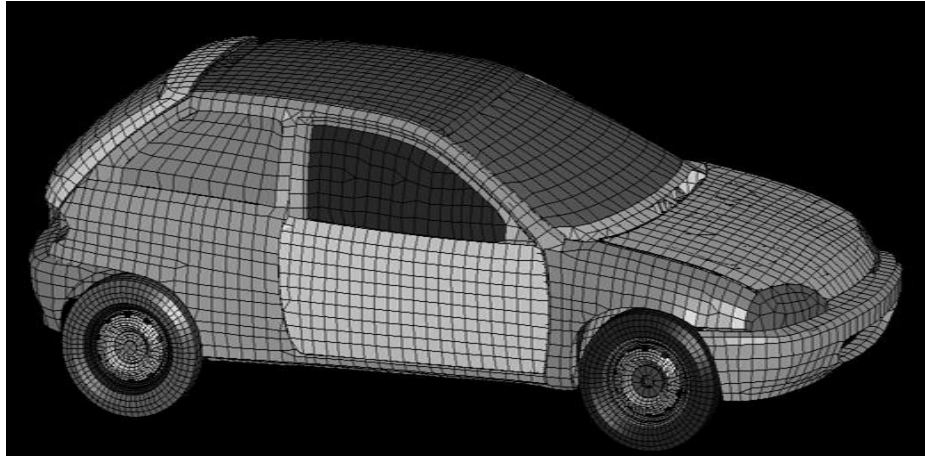


Figure 3-3: Geo Metro Model

This model consists of 16,100 elements, which is a 92% reduction in the amount of elements, when compared to the more advanced Geo Metro model which contains 193,200 elements. The mass of the simulated Geo Metro model is approximately 812 kg (1,789 lb), while the actual curb weight of a 1997 Geo Metro is 831 kg (1,832 lb) [60].

While both the C2500 pick-up truck model and the Geo Metro models can only offer an approximate indication of a true vehicle response during a collision, these models have been heavily used in industry and academia, and are considered as some of the most detailed vehicle models available to researchers.

3.3 Seat Model

Occupant dynamics can be determined with the seat and dummy model (see Figure 3-4) and the acceleration pulse at the seat (acquired from the crash model). Skipper and Romilly produced a seat and dummy model capable of simulating the interior environment of the struck vehicle during a rear-end collision [31]. The seat is modeled after the GM High retention seat. This model was used in previous work which examined the relationship between seat structural parameters and occupant injury during a rear-end collision [50]; however, has been updated to better facilitate this study. These updates included the addition of a more advanced 50th percentile Hybrid III dummy, a properly positioned head restraint with a more realistic tilt angle, and more stable material models. This seat and dummy simulation is capable of

determining seat and occupant displacements, velocities, and accelerations based on a specific crash pulse.

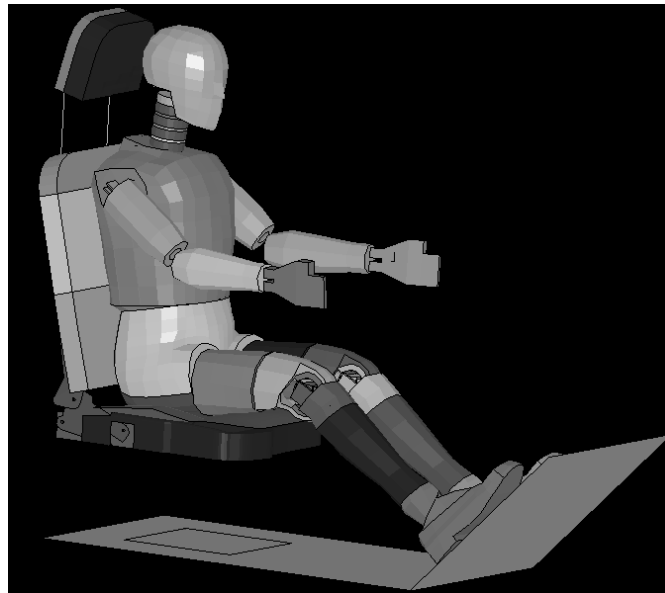


Figure 3-4: Seat and Dummy sled model updated from [31]

3.4 Modifications to the Seat and Dummy Model

In order to further improve the accuracy of the Skipper-Romilly seat and dummy model, several adjustments were made.

A properly positioned head restraint was implemented in order to simulate an “ideal” head restraint position as the effects of varying head restraint positioning were not the goal of this research. This ideal position is when the midline of the head restraint is in line with the ear of the occupant [61]. The head restraint was also tilted forward in order to better match the head restraint found on a GM High Retention seat. The foam found in the head restraint was also made thicker to more accurately depict the actual head restraint. The head restraint, before and after the modifications, are shown in Figure 3-5.

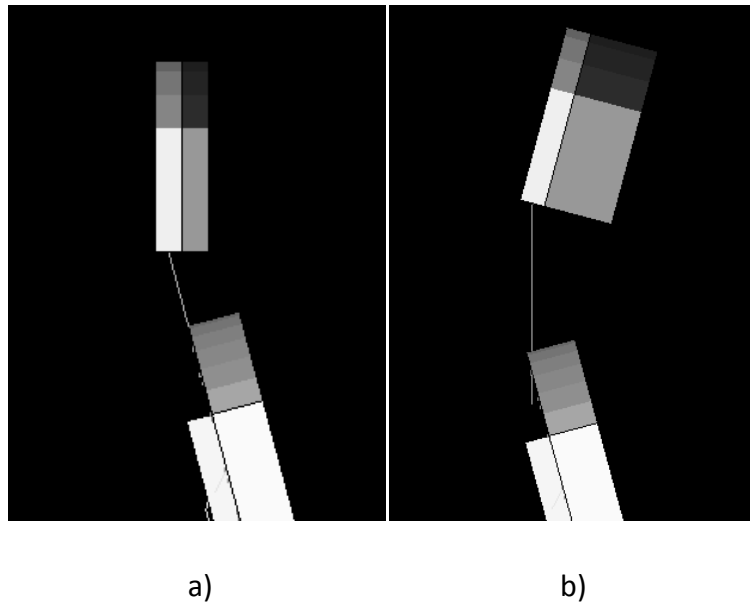
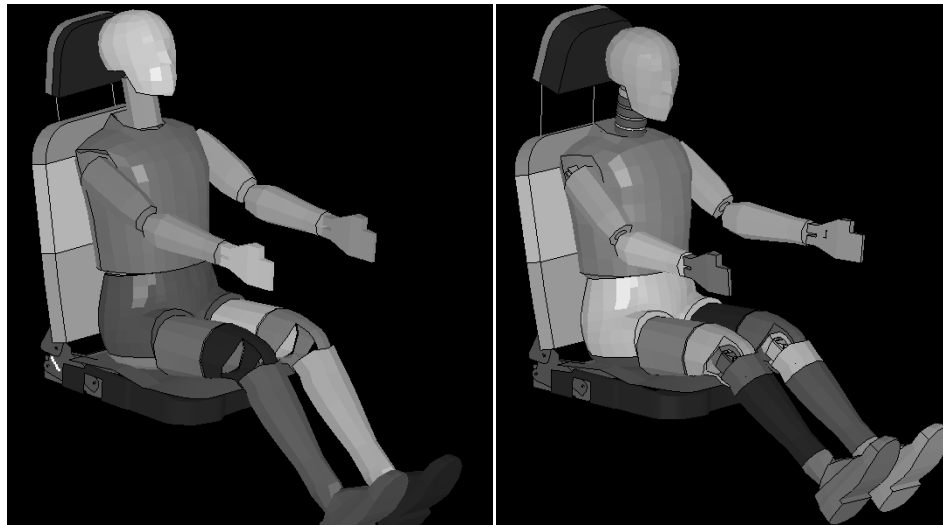


Figure 3-5: Head restraint upgrade: a) Old design b) New design

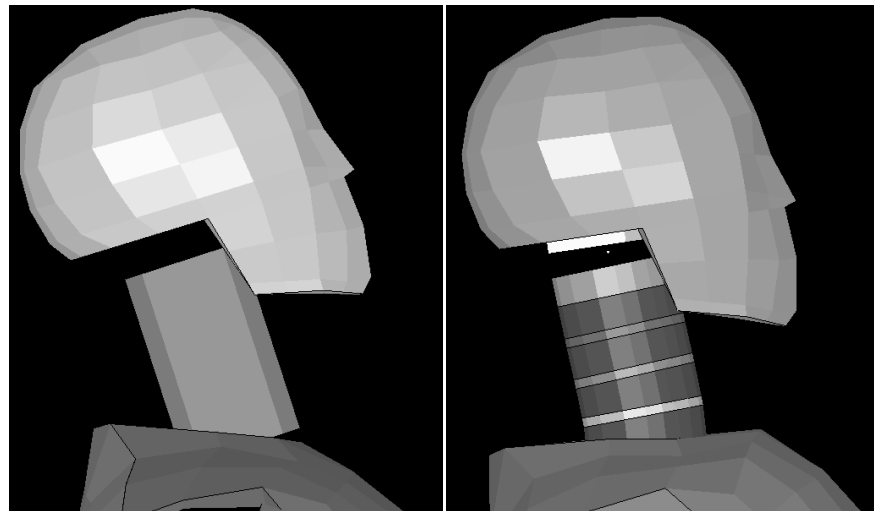
A more advanced Hybrid III simulated dummy was implemented into the seat and dummy model, with the new neck structure shown in Figure 3-6. The neck was originally modeled as one rigid piece (Figure 3-7a) which limited the amount of extension/flexion motion due to an inability of the vertebrae to rotate with respect to one another. The updated neck is modeled as separate vertebrae (Figure 3-7b) which allows for more humanlike neck behavior due to the neck's ability to now bend. In addition, changes to the LS-Prepost interface allows for these dummies to be positioned more accurately than in the previous simulations. The previous, as well as updated, 50th percentile Hybrid III dummies can also be seen in Figure 3-6.



a)

b)

Figure 3-6: Hybrid III Dummy upgrade: a) old dummy b) improved dummy



a)

b)

Figure 3-7: Upgraded Hybrid III Neck: a) Rigid neck without vertebrae
b) Updated neck with vertebrae

The models used in this study were run on a desktop personal computer with a 2.83 GHz Intel 2 Quad core CPU. Each run of the vehicle crash model required approximately 2 hrs and 45 min to complete, while each run of the seat and dummy model required approximately 1 hr and 45 mins to complete.

3.5 Neck Injury Criterion Determination

The acceleration pulse at the seat generated from the first simulation crash model was used as input to the seat and dummy model which then provided estimates of the occupant displacements, velocities, and accelerations of the torso, neck, and head. In the previous research conducted by Skipper and Romilly [31], a macro enabled spreadsheet was developed which extracted the displacements, velocities, and accelerations of the neck from the seat and dummy model, and determined NIC as a function of time. For low speed collisions, accelerations and velocities can be determined in global coordinate system as the occupant's torso does not experience significant rotation. The previous research of Skipper and Romilly [31] was conducted primarily at low collision speeds; therefore, the post processor extracted and processed global displacements, velocities, and accelerations. This work examines both low and high speed collision scenarios, requiring several modifications to be made to the post processor.

3.5.1 NIC Calculation

In order to calculate the Neck Injury Criteria (NIC), the accelerations and velocities as a function of time were acquired for the top (C1) and bottom (T1) of the neck. For low collision speeds (where little torso rotation occurs), the x-direction velocities and accelerations can be measured in a global coordinate system (see Figure 3-8). However, during higher collision speeds, the torso will load the seat back with a sufficiently large force to cause it to deflect. In this scenario the head will experience velocities and accelerations in the forward/rearward directions, as well as the downward/upward directions. The coordinate system for which linear shearing motion between the top and bottom of the neck is measured will now be changing as a function of time. This requires that these velocities and accelerations be calculated with respect to a localized system as opposed to a global system (see Figure 3-9).

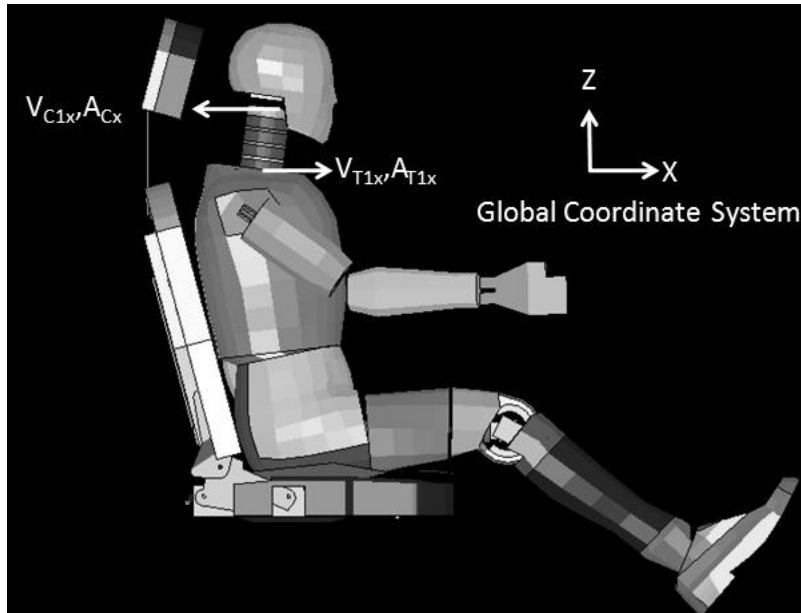


Figure 3-8: Low speed scenario measured only in a global coordinate system

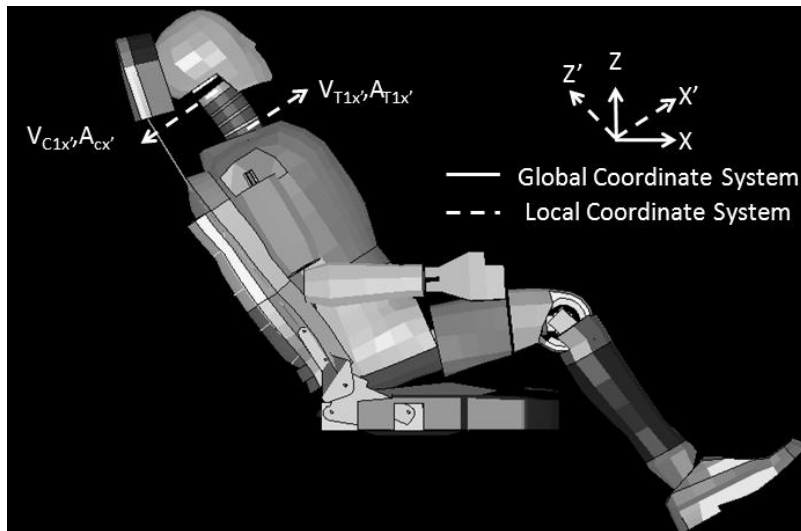


Figure 3-9: Higher speed scenario measured in a local coordinate system

The previous post-processor determined the vector sum of the velocities and accelerations at the top and bottom of the neck, in the global system. These values were calculated as a function of time and were used to determine NIC throughout the collision. This method may not have generated proper values of NIC due to the fact that the vector sums determined at both the top and bottom of the neck were not necessarily in the same direction.

The conversion from global to local coordinates is shown in Figure 3-10. The “neck vector” between T1 and C1 is first computed and the angle that this vector forms with the global x axis is determined. Assuming a nearly perpendicular relationship between the bottom of the neck and the torso, the angle between the torso and the neck vector is calculated as $(90^\circ - \theta)$ if in flexion or $(\theta - 90^\circ)$ if in extension. This angle is then used to separate the global velocities and accelerations into corresponding local components.

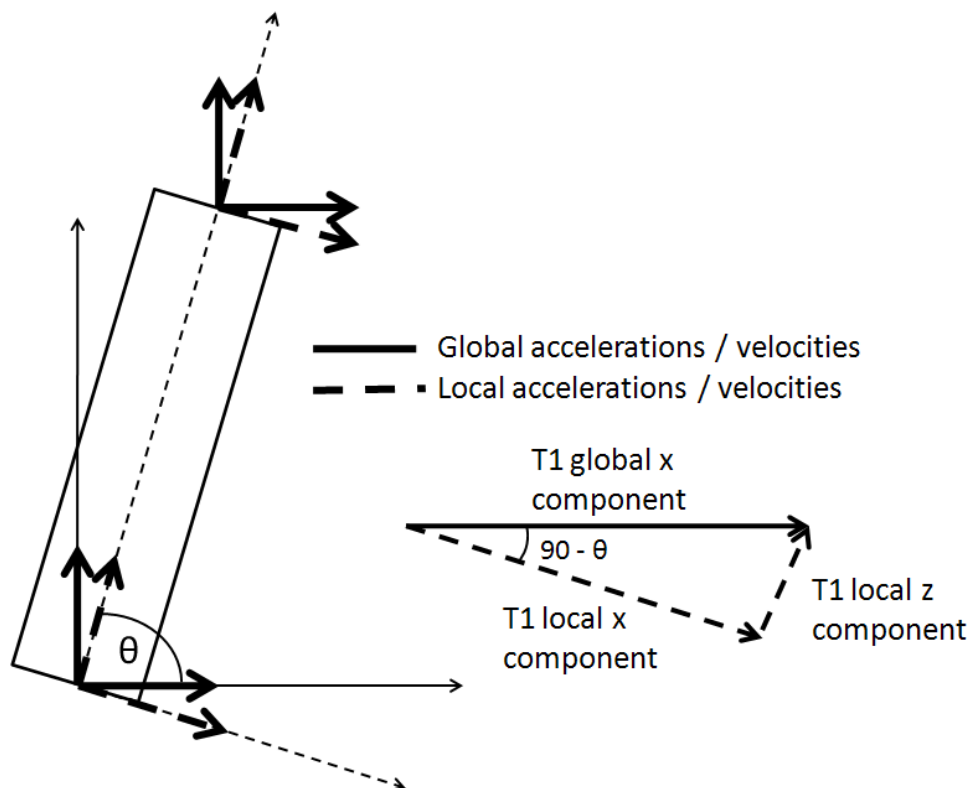


Figure 3-10: Conversion between global and local coordinate systems

The adjustments made to the NIC calculation process will ensure that NIC is being determined properly independent of the seat back angle. This is paramount to this work due to the fact that as seat-back rotation increases, the amount of x-direction velocity and acceleration in the neck may be decreasing with an increase in z-direction velocity and acceleration. In this case, using only x-directional values will generate an NIC value that does not reflect the true situation.

3.6 Seat Model Verification

There is a need to ensure that the output data from the first simulation vehicle crash model (i.e. the acceleration pulse) and the second simulation seat and dummy model (i.e. the occupant displacements, velocities, and accelerations) are accurate. Accurate models capable of producing realistic baseline models will ensure that the occupant injury response predicted with the implementation of the supplemental safety system can be trusted. It is costly to physically test the GM High Retention seat with a Hybrid III Dummy as this would require the use of an experimental crash facility. However, several researchers, who have had access to such facilities, have conducted similar experiments in order to validate their research. This section compares the results that they have acquired from physical testing and compares this to the output generated from the simulations created in this research.

3.6.1 Rear Impact Dummy Evaluation Task Group (Kim et. al.)

Kim et. al. conducted a study comparing the performance of the Hybrid III, BioRID II and Rid2 ATDs in low-severity collisions. The acceleration pulse used in the Kim et. al. study was implemented into the updated seat and dummy model created for this study. The collision scenario was a 17 km/h collision with a head restraint in the upward position. A comparison of the results from both studies is shown in Table [62].

Table 3-1: UBC Sled Simulation vs. Kim et. al. NIC [62]

	UBC Sled Simulation	Kim et. al. Study
Seat type	GM High retention	Not stated
NIC (m^2/s^2)	9.24	11±0.25
Peak head acceleration (g)	18.71	16±1
T1 x-acceleration (g)	9.42	8±1
External head impact F_x forces (N)	620.62	475±25
External head impact F_z forces (N)	195.82	90±10
Head restraint contact time (ms)	104	130
Head restraint back-set (mm)	70	115±5

The results shown in Table indicate that the injury response produced by the seat and dummy simulation are within the same range as those produced by Kim et. al. The discrepancy between the two sets of results may be attributed to the neck properties of the simulated Hybrid III ATD. While the 50th percentile Hybrid III simulated ATD has been modeled as closely as possible to the real Hybrid III ATD, the injury response of the simulated dummy may differ from that of the real dummy.

The fact that the seat and dummy simulation used in this study has a smaller head restraint back-set explains why the simulated ATD head comes into contact with the head restraint sooner than that of the real dummy. A smaller head restraint backset may also explain why the value of NIC_{max} is slightly lower than that of the study produced by Kim et. al.

The amount of seat back deflection in the study produced by Kim et. al. may affect results seen in Table . The seat used in the study produced by Kim et. al. may have allowed for more deflection, which may not only explain the delay in head restraint contact time, but also the fact that the forces experienced by the head hitting the head restraint are lower. As the occupant deflects the seat further, the dynamic loads experienced on the occupant are decreased. NIC has been shown to be heavily influenced by seat design characteristics. Since the simulation employs the use of a different seat than that specified by Kim et. al., it is to be expected that differences in data will arise.

3.6.2 National Highway Traffic Safety Administration (Kuppa et. al.)

The NHTSA conducted a study which determined the injury response of the Hybrid III 50th percentile male ATD during a rear-end collision. The dynamic sled test defined in FMVSS#202 was utilized in this study. The same acceleration pulse defined in FMVSS#202 was implemented into the UBC simulation in order to compare the injury response of the simulated Hybrid III compared to that of an ATD. The acceleration pulse defined in FMVSS#202 has a duration of 90 ms and a peak acceleration of approximately 9 g. This study chose to examine the performance of two seats belonging to; the 1999 Ford Taurus and the 2001 Ford Taurus. The results from this study and from the sled and dummy simulation are summarized in Table 1.

Table 1-2: Seat and Dummy Simulation vs. Kuppa et. al. NIC

	Seat and Dummy	1999 Taurus (Kuppa)	2001 Taurus (Kuppa)
Head restraint back-set (mm)	70	85	85
Head restraint contact time (ms)	78.0	120.5	111.7
NIC _{max} (m ² /s ²)	14.49	19.5	23.9

The GM high retention seat combined with an optimally positioned head restraint may be the reason why the NIC value achieved by this simulation is lower than that of the study produced by Kuppa et. al. However, these results are within the same range [63].

3.6.3 Schmitt et. al

Schmitt et. al conducted a study where 37 sled tests, with several different vehicle seats, were tested. This study employed the use of the Hybrid III 50th percentile male ATD and tested the seats at a ΔV of approximately 15 km/h. This study found that, on average, the seats produced a NIC_{max} value of $18.1 \pm 5.0 \text{ m}^2/\text{s}^2$ with a minimum value of $10.2 \text{ m}^2/\text{s}^2$ (obtained for a seat with whiplash protection).

The baseline value obtained for a 17 km/h collision in the seat and dummy simulation was $13.61 \text{ m}^2/\text{s}^2$ which falls within the range described by Schmitt et. al. [64]. The results generated from the seat and dummy simulation used in this study are closer to that of the seats with whiplash protection (i.e. properly positioned head restraint) used in the Schmitt study. This again, indicates that the simulation is performing accurately enough to perform parametric studies.

While physical validation is not possible at this point in time in this research, there is evidence, based on the previously mentioned studies, that the simulations produced for this research do in fact produce output data that is within the same range as those studies that have provided experimental test results. Discrepancies in results are expected due to the fact that these studies were conducted with different seats, and occupant dynamics is known to be heavily dependent on seat characteristics.

3.7 Summary

This section has outlined the creation and verification of two simulations that are used to determine occupant dynamics for a range of rear-end collision speeds. These two simulation tools were created using LS-DYNA and have been shown to be capable of producing reasonably similar results to previous studies that have implemented the use of physical test data in order to validate their research.

This section has also described the process of determining the value of Neck Injury Criterion. This process involved converting global velocities and accelerations to a local coordinate system in order to properly track NIC independent of the amount of torso rotation experienced by the occupant. This allows for a more accurate depiction of NIC, especially at higher collision speeds.

The tools that have been described in this section will allow for the determination of baseline NIC, acceleration, head restraint contact force, seat back deflection, and occupant kinetic energy values. These values will be shown and discussed in more detail in Chapter 5.

The next chapter (i.e. Chapter 4) outlines the concept of the supplemental safety system as well as its implementation into the seat and dummy model. This new model employs the use of energy-absorbing foam to the seat base as a means of removing impact energy and delaying the acceleration of the occupant. A description of the test process used in order to find the best characteristics of the supplemental safety device will also be described in Chapter 4.

4 Simulation Procedure

4.1 Overview

Chapters 1-3 have discussed the frequency and severity of rear-end collisions, previous studies relating to vehicle seat crashworthiness, and the tools capable of simulating a rear-end collision that have been developed for this work. In this chapter the supplemental seat base safety system will be addressed. The supplemental seat base safety system employs the use of energy-absorbing foam which is implemented into the seat base to absorb impact energy and delay the acceleration of the occupant during a rear-end collision.

Energy-absorbing foam has been used in industry for a variety of different applications including those relating to vehicle crashworthiness. The mechanical performance of energy-absorbing foam is characterized by the relative density, foam type (open or closed), density of the bulk material, and geometry. These factors will be discussed in detail within this chapter.

An updated version of the seat and dummy model will also be introduced in this chapter. This updated model includes the addition of energy-absorbing foam placed at the rear of the seat base.

Several foam types and geometries have been tested in order to indicate whether the addition of foam can act to improve the dynamic response of the occupant and thus, reduce the amount of injury sustained by the occupant. The test plan used in this research will also be outlined in more detail at this point.

4.2 Methods of Mitigating Injury Through Seat Base Design

While both the seat back and head restraint are capable of absorbing energy as the occupant collides with the seat, there is potential for the seat base to play a role in this process. Introducing an energy-absorbing system into the seat base could result in less impact energy being transferred to the remaining components of the seat and thus to the occupant, potentially resulting in an improved injury response. Several mechanisms capable of absorbing energy already exist. These include spring damper mechanisms, hydraulic cylinders, pneumatic cylinders, and deforming members. While any one, or a combination of these mechanisms may act to successfully reduce occupant injury, this research is focused on examining the effect of adding deforming members to the seat base.

Himmetoglu et. al. (see Chapter 3) showed that the addition of spring damper elements to the seat base, with no additional safety elements, achieved only minimal reduction in NIC (i.e. <10% improvement) [52]. Alternatively, the addition of a hydraulic or pneumatic system would likely increase the cost and weight of the seat due to the mandatory addition of a reservoir tank underneath the seat. As a result, utilizing deformable members within the seat base was selected as it was deemed a potentially effective and affordable solution to this design problem.

This work will determine whether the addition of energy-absorbing foam in the vehicle base can improve the overall safety of the occupant in both low and high speed rear-end crash scenarios. While the implementation of any device into the seat base requires a great deal of design work, this paper will focus primarily on showing that injury mitigation is possible through the use of the simulations previously discussed in Chapter 3.

4.3 Energy-Absorbing Foam

As energy-absorbing foam will be used to create the supplemental seat base safety device, an understanding of how these foams behave must first be understood. Energy-absorbing foams have been used in engineering applications for 50 years [65]. These materials exhibit exceptionally high impact energy absorptive capabilities while being extremely lightweight [66].

Factors that contribute to the mechanical response of these foams include production methods, relative foam density, as well as microstructural configuration [65]

4.3.1 Microstructure

The microstructural feature that predominantly affects the mechanical performance of the energy-absorbing foam is the ratio of foam density to bulk material density [65]. This property is known as the volume fraction or relative density. Typically, the relative density of aluminum foam ranges from 0.03 to 0.3 [65]. The stiffness of the foam increases as relative density increases. The cross section of one aluminum foam used in industry is known as AlporasTM and is shown in Figure 4-1.

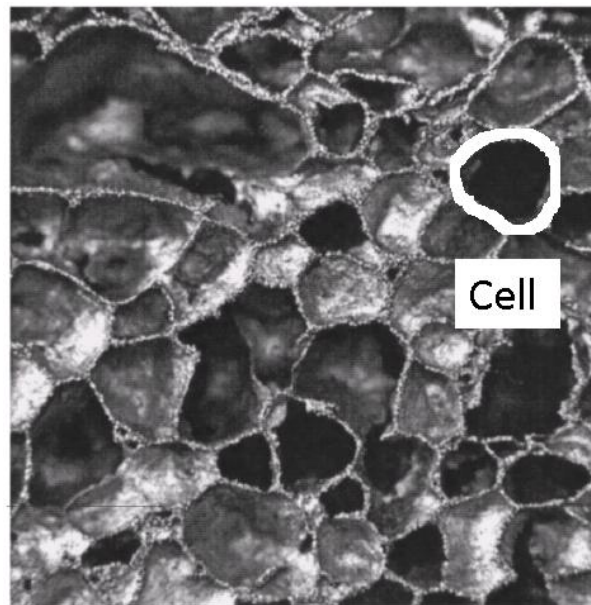


Figure 4-1: Microstructure of AlporasTM Foam adapted from [65]

The encircled portion of Figure 4-1 is referred to as the cell. The shape of these foam cells are typically circular or ellipsoidal with sizes ranging from 2 to 10 mm [65]. The ratio of cell wall thickness to cell wall length can affect the overall mechanical response of the foam; however, it is not as significant as the effect of relative density [67].

Energy-absorbing foams can either be classified as open-cell (see Figure 4-2a) or closed-cell foams (see Figure 4-2b). Open-cell foams contain cells that are not completely separated by cell

walls; several interconnecting pathways can be made between all of the voids within the foam. Closed-cell foams have clear borders between all of the voids.

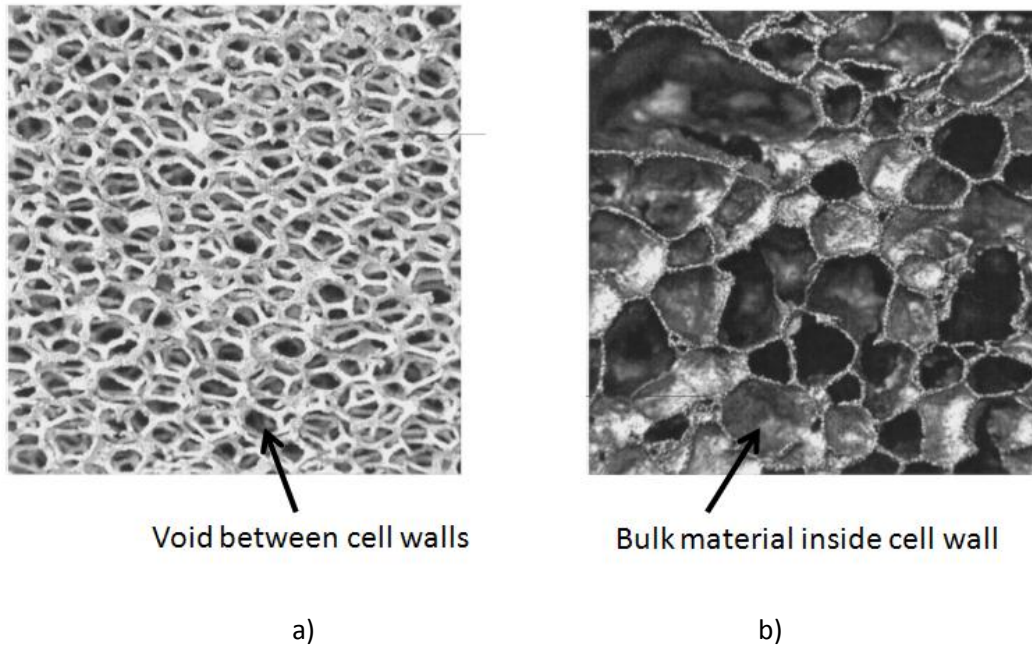


Figure 4-2: Cross section of a) Open-cell foam b) Closed- cell foam (adapted from [65])

Open-celled foam is typically used in applications requiring heat dissipation due to the ability of air and other coolants to pass through the cell voids [65], whereas closed-cell foams are more commonly used in energy dissipation applications due to increased strength and stiffness.

4.3.2 Mechanical Behavior of Energy-Absorbing Foam

The mechanical behavior of the energy-absorbing foam is of significant interest to this research as it will dictate the amount of crush, and thus, the amount of energy removal that can be achieved for a particular foam. Maintaining control over the mechanical properties of the foam will allow for the supplemental safety system to be more predictable.

The stress vs. volumetric strain curve (see Figure 4-3) of energy-absorbing foams can be separated into three phases.

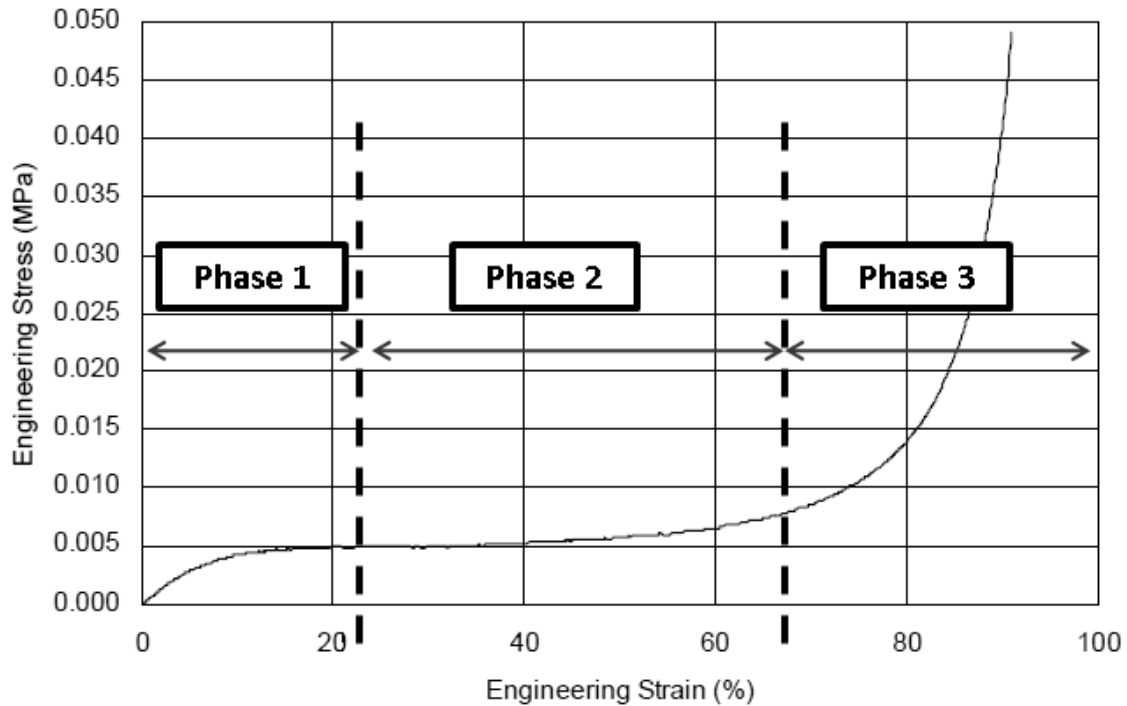


Figure 4-3: Typical stress vs. volumetric strain curve (adapted from [68])

In Phase 1, the foam will deform elastically until the yield stress is achieved. If the load is released, the foam is capable of returning to its original geometry with little permanent strain. In Phase 2, the cells begin to collapse by either plastic collapse, buckling, or fracture depending on the cell wall thickness, length, and size of the cell itself [65]. As a result, the foam continues to crush without an increase in impact force. Phase 2 is referred to as the “crush plateau”. Once the cells within the foam have collapsed fully, additional force is required to deform the foam further [68]. Phase 3 is known as the “densification zone”. The transition point between Phase 2 and 3 is known as the densification percentage. If the foam has a predicted densification percentage of 0.75, the volume of the foam will be reduced by 75% before it enters the densification zone.

While altering the stress vs. volumetric strain curve in order to achieve desired injury mitigation properties may prove successful, designing specialized foam adds additional costs. Therefore, the stress vs. volumetric strain curve is not a parameter in this study. Alternatively, several real foams that are currently being sold by manufacturers will be utilized instead. The geometric

properties of any given foam will be manipulated in this study in order to test evaluate effect of changing cross section and foam length.

4.4 Seat and Dummy Simulation with Foam Addition

As previously stated in Chapter 1, one of the research goals was to assess the efficacy of a supplemental seat base safety system and to develop relationships between the safety systems parameters and injury response. The simulation tools developed for this research (see Chapter 3) were developed to be capable of modeling a rear-end collision and are, therefore, able to provide a baseline value of occupant injury to which simulation results using the supplemental safety device can be compared with for evaluation.

The seat and dummy model has been modified to include the addition of four energy-absorbing foam rods situated between the seat base and the vehicle floor. The acceleration pulse generated from the first simulation vehicle collision model is now applied to the back plate of the foam device as opposed to the seat base itself (see Figure 4-4) with the front plate of the device now in contact with the vehicle seat. This simulates the effect of an intermediate device between the vehicle floor and vehicle seat.

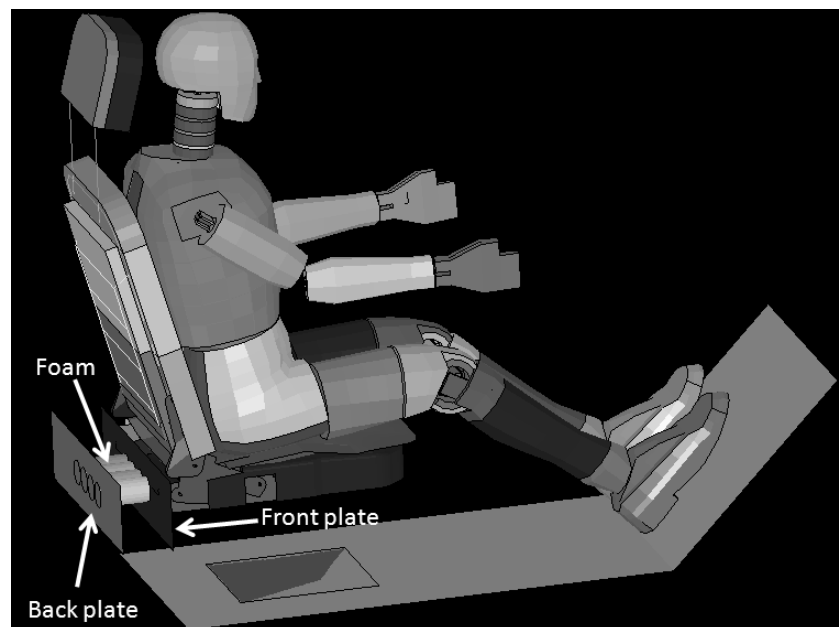


Figure 4-4: Modified seat and dummy model

This is a simplified model designed to determine whether energy-absorbing foam is effective in mitigating injury. The foam has been modeled as four cylinders due to the fact that cylinders allow for two simple parameters (radii and length) to be altered. Future designs will see the device being placed underneath the seat as opposed to behind it. Creative design will be required in order to ensure that the four cylindrical foam rods do not interfere with other seat components such as the motorized components responsible for adjusting the seat.

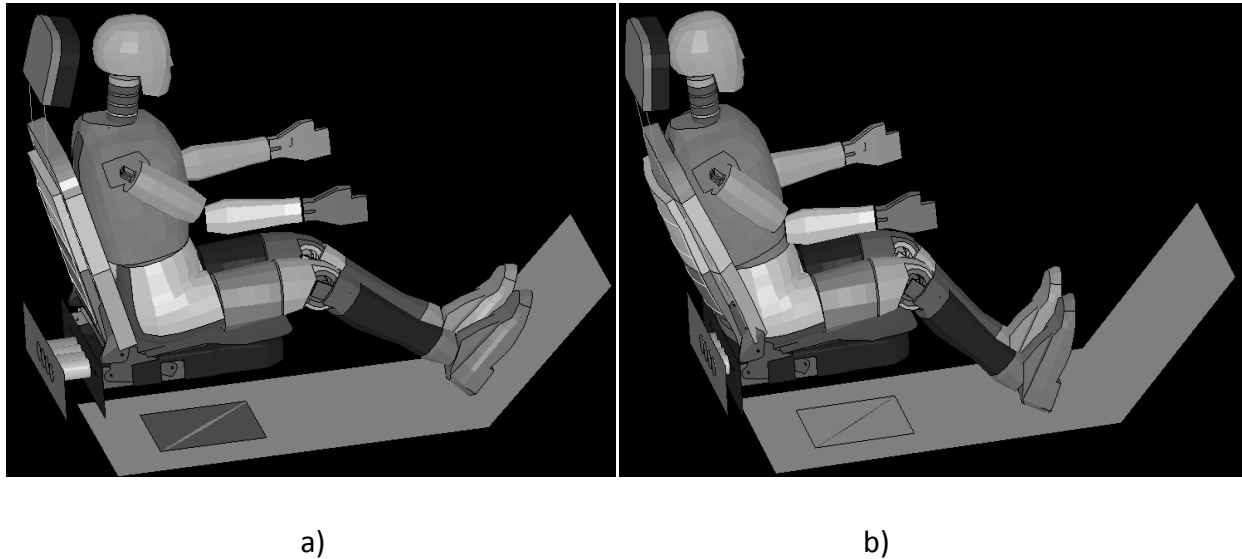


Figure 4-5: Rear-end collision simulation a) Pre-crash b) Post-crash

Figure 4-5 shows the supplemental safety system before and after a rear-end collision has occurred. As a result of the acceleration pulse now being applied to the back plate, the foam initiates crushing before the seat base is affected by the acceleration pulse. This acts to delay the increase in acceleration experienced by the seat. This alters the occupant dynamics and acts to delay the sudden ramp up of occupant acceleration. This may not only act to reduce the dynamic loading experienced by the occupant, but may also reduce the amount of injury sustained by the occupant. By comparing the results from the modified seat and dummy model (see Figure 4-4) and comparing these results to the original seat and dummy model (see Chapter 3), it will be possible to determine: 1) whether the addition of energy-absorbing foam is acting to mitigate injury and 2) how changes to the foam geometry and characteristics will affect occupant injury response.

4.4.1 Modeling of Energy-Absorbing Foam in LS DYNA

Modeling energy-absorbing foam can be achieved with the use of several “Material Cards” found in LS-DYNA. Material Card 63 was selected as it is one of the simplest material models for energy-absorbing foam [69]. This material card allows the user to implement the stress vs. volumetric strain curve, relative density, modulus of elasticity, and Poisson’s ratio of the foam. It has been shown to be useful when the application requires no recovery of the foam, which is the case for this application [68]. One limitation of Material Card 63 is that it does not take into account rate dependency when implementing the stress vs. volumetric curve. The foams that are being used in this study have been shown to have little to no strain rate dependence (discussed later in this chapter). It should also be noted that for closed cell foams, a Poisson’s ratio close to zero is recommended due to the foam typically compressing along the axis of loading as opposed to laterally [70].

4.5 Optimal Foam Study Procedure

In addition to determining whether the supplemental safety system is capable of mitigating injury, it is necessary to determine whether one foam type and geometry utilized in this device is capable of mitigating injury for an entire range of collision speeds. Based on the general characteristics of energy-absorbing foam behavior, it is unlikely that one foam type will be sufficient for all collision severities. For minor collisions, foam that is too stiff may operate entirely in the elastic zone (Phase 1), preventing energy removal from taking place. Similarly, during high impact collisions, foam that is too compliant may activate well before the acceleration pulse has begun increasing, potentially reducing the foams ability to affect the occupant dynamics. As a result, two foams will be implemented into the supplemental seat base safety system; one foam for lower collision speeds ranging from 5 km/h to 17 km/h, and one for higher collision speeds ranging from 18 km/h to 65 km/h. Since the effect of foam addition was unknown during the commencement of this research, the speed ranges chosen for this study are arbitrary. Should the low speed foam show successful injury mitigation for impact speeds greater than 17 km/h, or alternatively, should the high speed foam show successful

injury mitigation for collision speeds less than 17 km/h, the speed limits for the activation of these foams may be altered.

Several foams possess the potential to mitigate injury if utilized in this application. However, In order to focus this research, two foams were selected for each collision severity range (see Table 2). Four different foam types (two per collision range) were tested at the upper limits of both low and high speed collision ranges (17 km/h and at 65 km/h respectively).

Table 2-1: Simulated foam types

Impact Velocity Range	Foam Name	Relative Density (kg/m ³)	Yield Stress (MPa)	Densification Strain (%)	REF
5-17 km/h	IMPAXX™ 300	35	0.75	75	[71]
	IMPAXX™ 500	43	0.50	75	[71]
18-65 km/h	Cymat™ 200	200	1.00	80	[72]
	Fraunhofer™	520	7.50	40	[73]

The foam cylinders will be tested at different foam radii and foam lengths in order to determine the most beneficial foam geometry for both low and high collision severities (5-17 km/h and 18-65 km/h). Due to the spatial limitations within the seat base, limits were placed on both the length and radius of the foam rods. Foam lengths were tested at 3, 3.5, and 4 inch values (7.62, 8.89, and 10.16 cm respectively). A 4 inch (10.16 cm) displacement limit was placed on the foam in order to prevent injury to rear passengers seated behind the occupant. During a rear-end collision, the entire vehicle will accelerate forward causing the foam to be compressed between the vehicle floor (modeled as a single plate situated between the simulated seat (see Figure 4-4)) and the detached driver seat. While the foam is crushing, the vehicle floor will continue accelerating, however, there will be a delay in the acceleration of the occupant seat. This delay will cause the driver seat is experiencing rearward translation relative to the rear seated passenger.

The foam radius was varied from 1 inch to 1.75 inches, with several intermediate values in between. The foam radius must be sufficiently small such that the device can be realistically implemented into the seat base. In order to determine the optimal foam dimensions for a specific foam type, different combinations of foam length and radius were simulated using the modified seat and dummy model.

The foam configurations that demonstrated the greatest amount of injury reduction (one foam per collision speed range), based on foam type and geometry, will be tested at intermediate collision speeds to determine the overall efficacy of the foam over the entire range of speeds (see Figure 4-6). These foams will then be implemented into the overall seat base safety system. In order for a foam to be selected, it must show effective injury reduction at each intermediate speed.

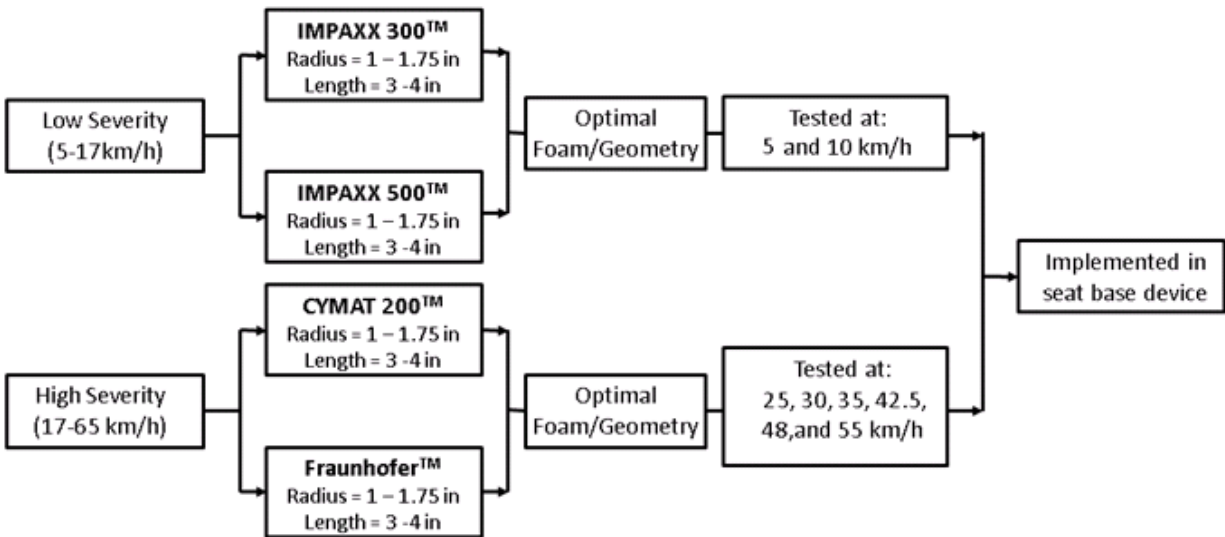


Figure 4-6: Optimal Foam Study Procedure

4.6 Detailed Energy-Absorbing Foam Description

The foams used in this study have been selected based on several factors including availability of mechanical data, strain rate insensitivity, and a stress vs. volumetric strain curve that allowed for the foam to achieve crush at the speed for which it is being tested. This section will describe these foams in detail.

4.6.1 IMPAXX™ Foam

IMPAXX™ foam is a closed-cell extruded polystyrene-based thermoplastic foam that was developed specifically for energy absorption in automotive applications [74], and has been selected as a potential foam for this study. It is produced by continuous extrusion which is done in order to ensure that there are constant material properties throughout the foam [74]. IMPAXX™ foam has also been shown to have constant mechanical properties over a wide range of operating temperatures [74].

While the stress vs. volumetric strain curves are readily accessible through the data sheets provided by the DOW Company [71], dynamic stress vs. volumetric strain curves were required in order to better model the foam for a vehicle collision. Slik and Vogel determined the average dynamic response for IMPAXX™ 300, and IMPAXX™ 500 using a drop tower with a flat impactor test set up [74]. The measured stress strain curves obtained from this study for IMPAXX™ 300 and IMPAXX™ 500 are shown in Figure 4-7.

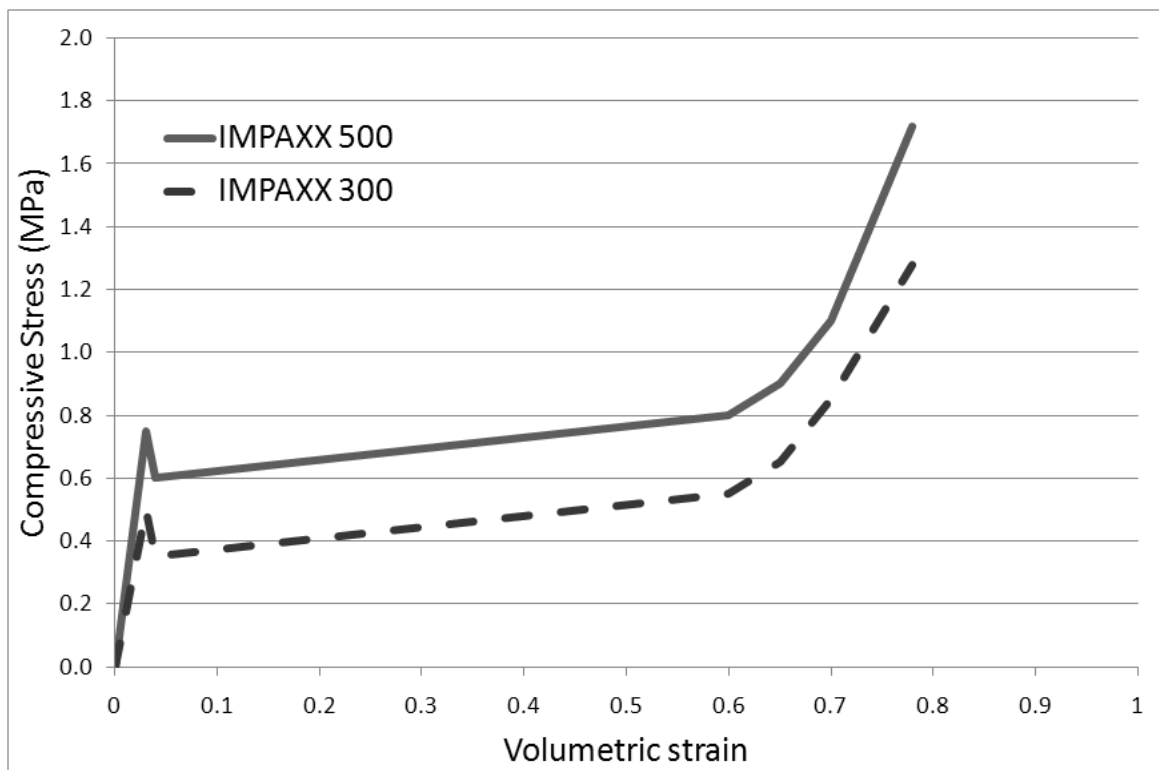


Figure 4-7: Measured dynamic stress vs. volumetric strain curves for IMPAXX™ foams (adapted from [74])

The study produced by Silk and Vogel also employed the use of a numerical model created in LS-DYNA. This model employed the use of Material Card 63, and attempted to match the load vs. displacement curve generated from the simulation to that from the real impactor test. This study found that LS-DYNA using Material Card 63 was very effective at matching the load vs. displacement curve generated from the physical test set up [74].

This indicates that not only is this foam an acceptable choice for this study based on the fact that the average dynamic behavior curves have been acquired, it can also be modeled accurately using Material Card 63.

4.6.2 Cymat™ Foam

Cymat™ foam is a closed-cell aluminum foam that can be manufactured into 3-D shapes by utilizing a low pressured casting process which is commonly used to make aluminum wheels [72], and is the second foam adopted for this study. This foam is typically used in automotive, transport, and military applications which is why it was selected for this work. Cymat Technologies states that the Cymat™ foam is insensitive to strain rate effects [72]. Ruan et. al. [75] examined the compressive behavior of Cymat™ foam at low to medium strain rates. This study employed the use of an MTS machine capable of applying a compressive load at strain rates of 10^{-3} to 10^{+1} s^{-1} . This study concluded that the plateau stress of the foam was insensitive to the strain rate. The researchers also concluded that the relative density played a larger role in the deformation characteristics of the foam at higher dynamic loadings [75].

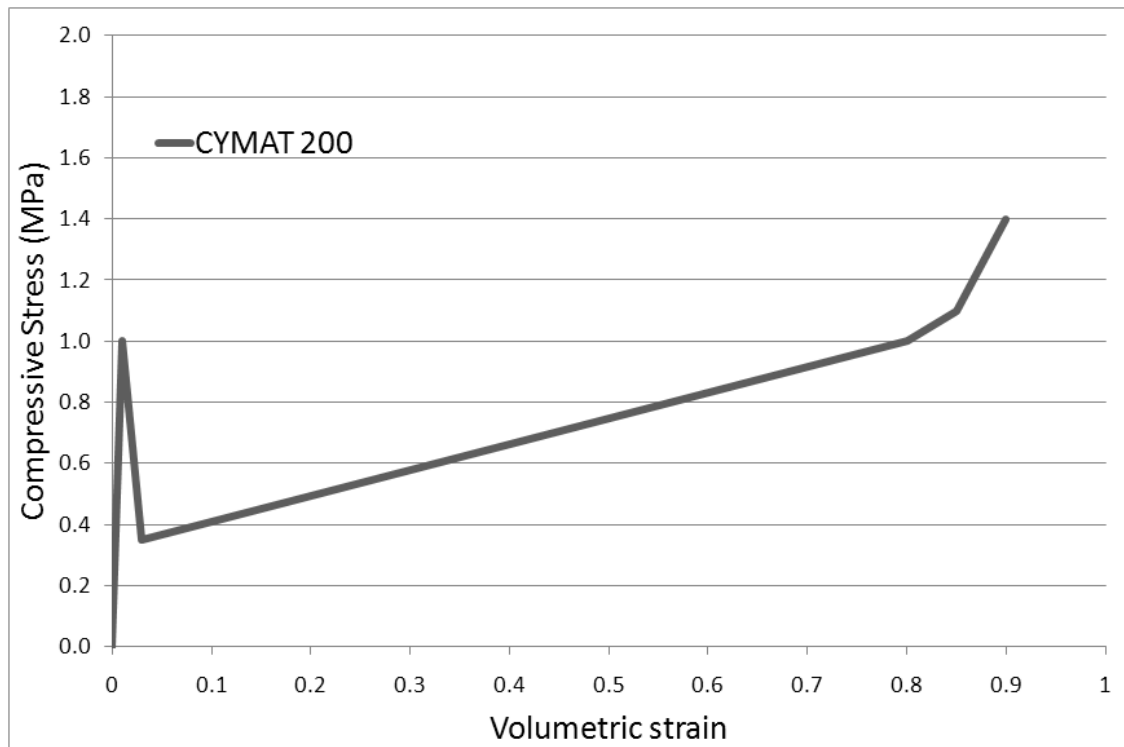


Figure 4-8: Measured stress vs. volumetric strain for Cymat 200

The stress vs. volumetric strain figures for CymatTM 200 were produced based on the data found in the Cymat Technical Manual [68] and implemented into the modified seat and dummy model.

4.6.3 FraunhoferTM Foam

FraunhoferTM foam is a closed-cell aluminum foam that is prepared using powder metallurgical techniques and was also considered for use in this research study. The foam was created by combining 6061-Al alloy powder and TiH₂ as a foaming agent [73]. Hall et. al. conducted a study that examined the compression characteristics of FraunhoferTM foam at both quasi-static as well as high dynamic strain rates. This study concluded that this foam exhibits little to no strain rate sensitivity. They found that the crush behavior of the foam was dictated primarily by relative density [73]. The stress vs. volumetric strain curve (see Figure 4-9) that was implemented into the model was that of a high dynamic strain rate.

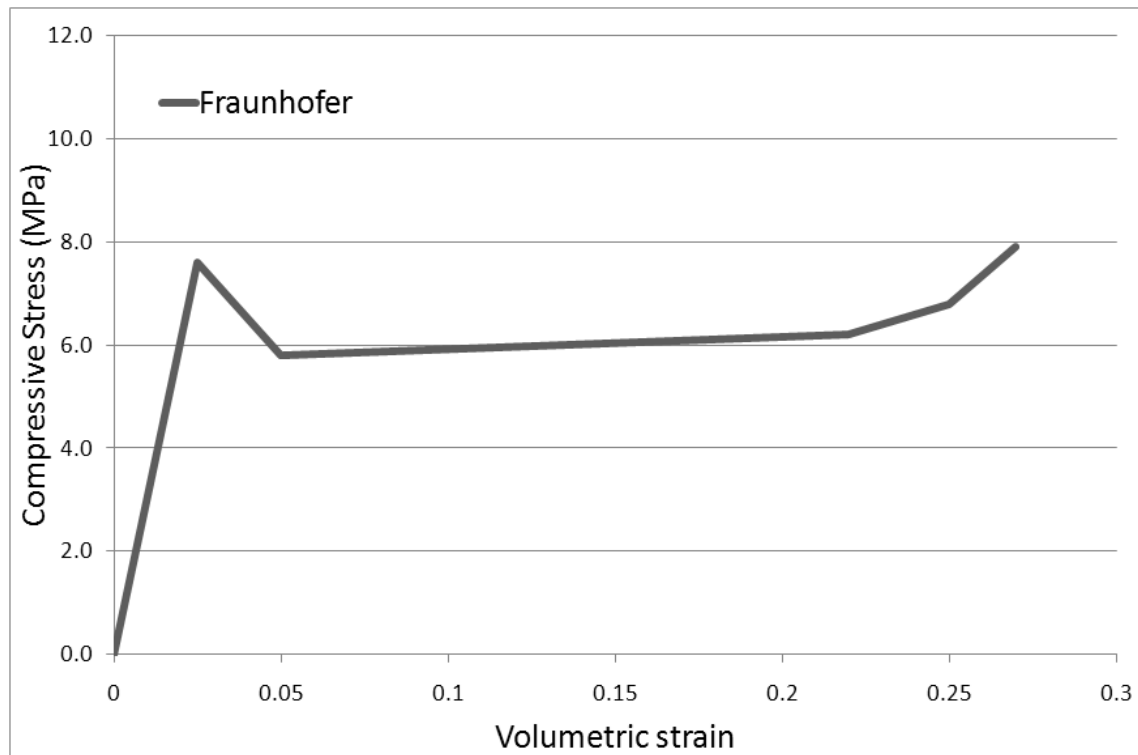


Figure 4-9: Measured stress vs. volumetric strain for Fraunhofer™ foam

The mechanical characteristics of the Fraunhofer™ foams used in this study (Figure 4-9) have been acquired from physical test data which is indicative of a true, as opposed to ideal, response of the simulated foam. However, it is acknowledged that when dealing with materials of this nature, uniformity is paramount to the functionality of the foam. Manufacturing processes rarely produce two components that perform identically and as such, assessment requires a degree of flexibility in the performance of these foams. In order for this supplemental safety device to be implemented, the injury response should not be overly sensitive to small differences in foam mechanical properties.

4.7 Summary

This chapter outlines the concept of utilizing energy-absorbing foam to absorb impact energy from a rear-end collision in the intent of reducing occupant injury. The method of determining optimal foam type and geometry was outlined illustrating spatial as well as safety limitations in foam selection. The supplemental safety system will employ the use of two foams (one for low speed and one for high speed collisions). These foams must mitigate injury for the entire speed

range for which they are defined; low speed being 5-17 km/h, and high speed being 18 – 65 km/h. The foam type and geometry that has been shown to mitigate injury most successfully will be implemented into the final supplemental safety system.

A detailed description of the foams used in this study has also been provided in this chapter. The stress vs. volumetric strain curves, modulus of elasticity, relative density, and densification percentage are provided as well as a discussion on the strain rate sensitivity of the foam itself. All of the foams used in this study have been shown to be strain rate insensitive based on experimental test data provided by previous researchers.

The next chapter will present the results of the optimal foam study for both low and high speed collisions. Trends relating to foam type and geometry and Neck Injury Criterion (NIC), head and torso accelerations, head restraint contact forces, seat back deflection, and kinetic energy will also be discussed.

5 Results and Discussion

5.1 Overview

The previous chapters have outlined the work required to complete the first two research tasks, which were: 1) to develop the tools to assess the dynamics experienced by a seated occupant in a rear-end collision, and 2) to use these tools to predict the extent of injury risk experienced by the occupant both with and without the supplemental safety device. The first research task was achieved through the development of the vehicle crash model and the seat and dummy model (see Chapter 4). The second task was achieved by firstly, utilizing the Neck Injury Criterion (NIC) (see Chapter 2) to quantify the extent of injury, and secondly, modifying the seat and dummy model to include the addition of energy-absorbing foam between the seat and the seat base (see Chapter 4).

The third defined research task was to develop relationships between the safety system design parameters and occupant injury. In this chapter, the relationships between foam parameters (i.e. type, radius, length, etc.) and injury risk (as defined by NIC_{max} , head and torso accelerations, head restraint contact force, seat back deflection, and occupant kinetic energy) will be presented and discussed.

5.2 Relationship between Foam Geometry and NIC_{max}

Multiple foam geometries were tested in order to determine which geometrical configuration would result in the greatest reduction of NIC_{max} when compared to the baseline value (i.e. the seat and dummy model results without the supplemental safety system). This section outlines the relationships between the foam geometry parameters and the NIC_{max} reduction for the specific foam types outlined previously in Chapter 4. NIC_{max} is representative of the peak difference in head and torso movement, making it a significant indicator of occupant injury. However, it is important to understand how the NIC plot is generated and how it relates to the dynamics of the occupant during the collision. NIC is based on the relative difference between the first thoracic vertebra (T1) and the first cervical vertebra (C1). Figure 5-1 illustrates the different stages of an NIC plot (e.g. shown here for a 17 km/h rear-end collision).

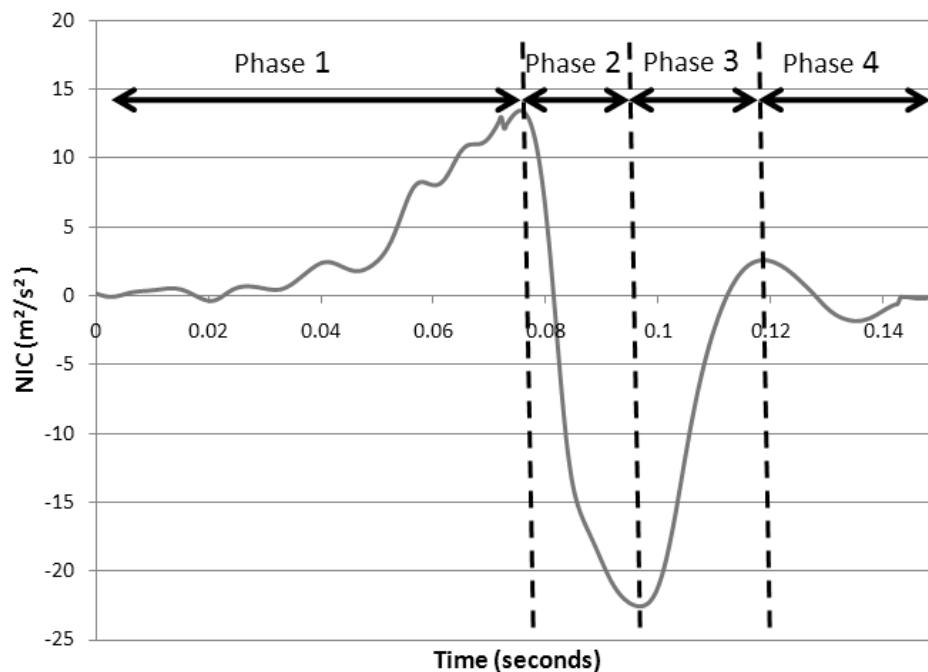


Figure 5-1: Phases of an NIC plot (17 km/h rear-end collision)

In Phase 1, the acceleration of the T1 vertebra increases in the positive x-direction due to the interface force between the seat back and the occupant's torso due to inertial loading. The C1 vertebra, having not yet come into contact with the seat, experiences little to no acceleration during the early stages of Phase 1. As a result, the relative acceleration and velocity (T1–C1) are

positive values. NIC_{max} occurs at the end of this phase. The magnitude of NIC_{max} , as well as the time at which it occurs, are heavily affected by the location of the head restraint, neck anatomy, and seat back properties.

In Phase 2, the head has either come into contact with the head restraint, or can no longer tolerate the increasing displacement from the torso. This causes a sudden acceleration of the head (i.e. the C1 vertebrae) in the positive x-direction resulting in the “whipping” effect. As Phase 2 continues, the accelerations experienced by the head and neck (C1 vertebrae) surpass those of the torso (i.e. the T1 vertebrae). As a result, the T1-C1 relative acceleration becomes negative.

In Phase 3, both the head (C1 vertebrae) and torso (T1 vertebrae) have experienced positive x-acceleration. At this point, head acceleration approaches equilibrium with respect to the torso. As a result, the T1-C1 relative acceleration approaches zero (i.e. the head and torso are now essentially moving at the same speed).

In Phase 4, the head (C1 vertebrae) surpasses the torso (T1 vertebrae) which causes the neck to go into flexion. This can occur due to the deceleration of the occupant’s torso due to contact with the seat belt or steering column. The head, not having come into contact with any vehicle structures, will keep moving forward causing the T1-C1 relative acceleration to once again become negative. If there is significant seat back deflection, as seen in higher severity collisions, the allotted collision time used in the analysis (150 ms) may not be sufficient in capturing the recoil. As a result, NIC will remain negative throughout Phase 4 as the torso and neck have not yet come to equilibrium with the vehicle. It should be noted that understanding how the dynamics of the occupant affect NIC is critical when examining NIC_{max} , as these values are only capable of quantifying injury risk, not indicating at what point during the collision event the injury actually took place.

As per the test plan (see Chapter 4), collision simulations with the supplemental safety system installed were run at 17 km/h and 65 km/h, both utilizing two different foam types. The radii of these foams were varied between specified limits (see Chapter 4) in order to determine the optimal geometry. The results from this test plan are shown in the Figure 5-1 to 5-4. These

figures outline the NIC_{max} vs. foam radius values simulated at 3, 3.5, and 4 inch (7.62, 8.89, and 10.16 cm respectively) foam lengths for each foam type. Note that the baseline values of NIC_{max} (i.e. seat and dummy model results without the presence of foam) for both the 17 km/h and 65 km/h are labeled on the figures in order to show the relative amount of improvement to occupant injury. It is also important to note that the results found in this chapter are based on computations which may be affected by the selected time step, computer employed to determine the data points, and material models selected. As such, the results provided are meant to be seen as predicted injury response, requiring physical validation in the future.

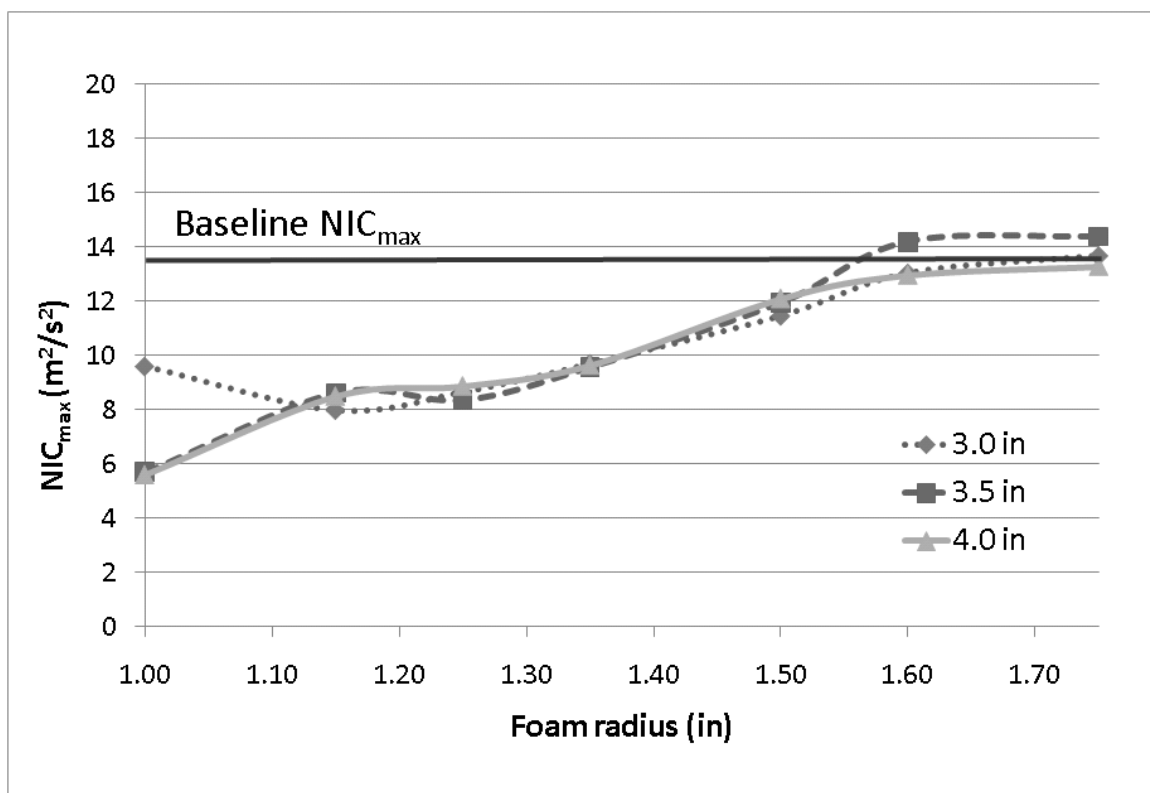


Figure 5-2: NIC_{max} vs. Foam radius for IMPAXX™ 300 foam at 17 km/h

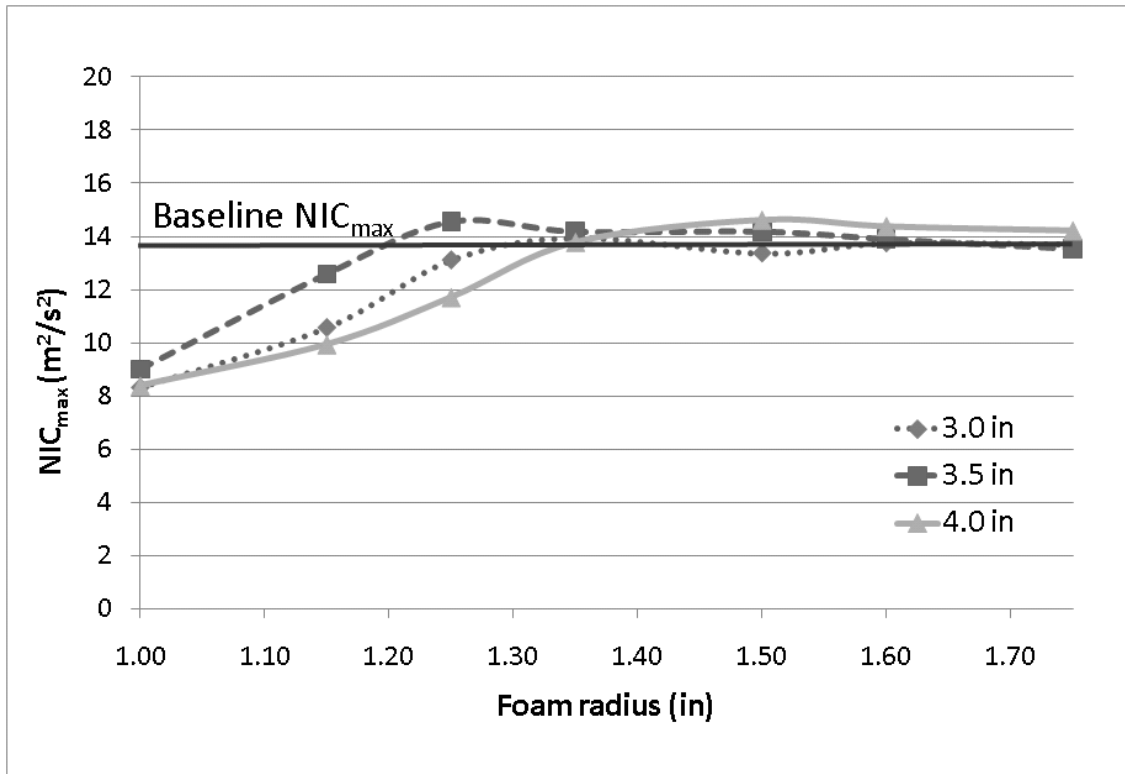


Figure 5-3: NIC_{max} vs. Foam radius for IMPAXX™ 500 foam at 17 km/h

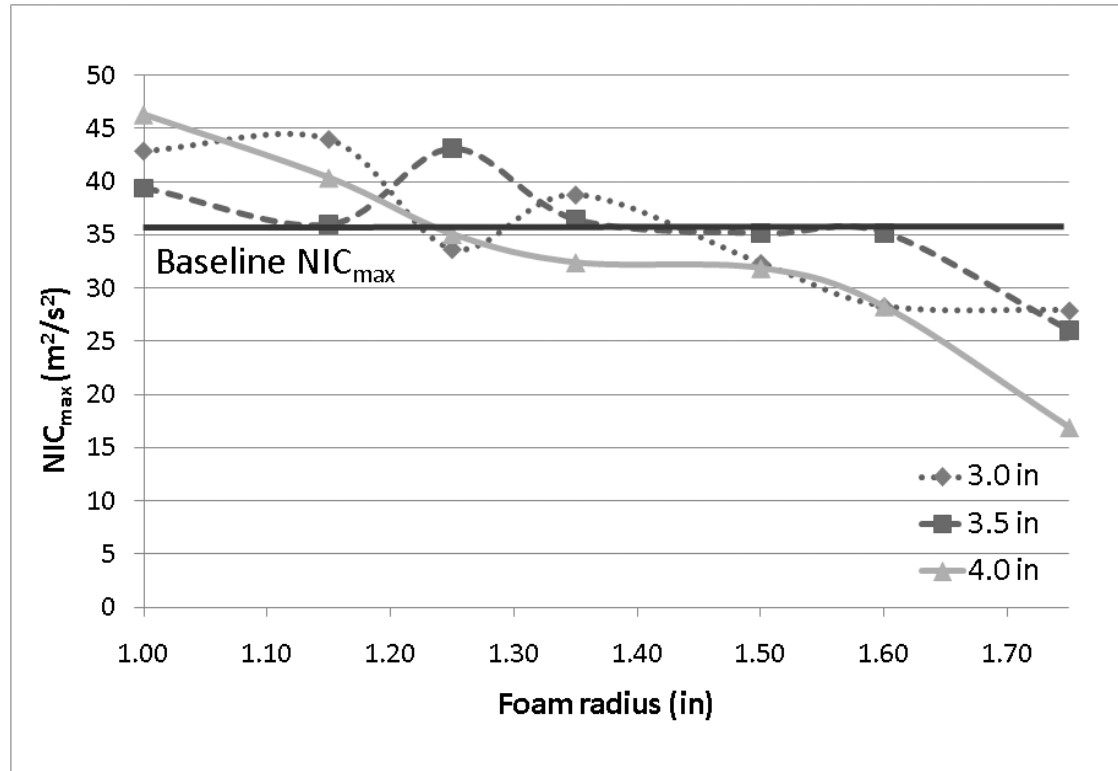


Figure 5-4: NIC_{max} vs. Foam radius for Cymat™ 200 at 65 km/h

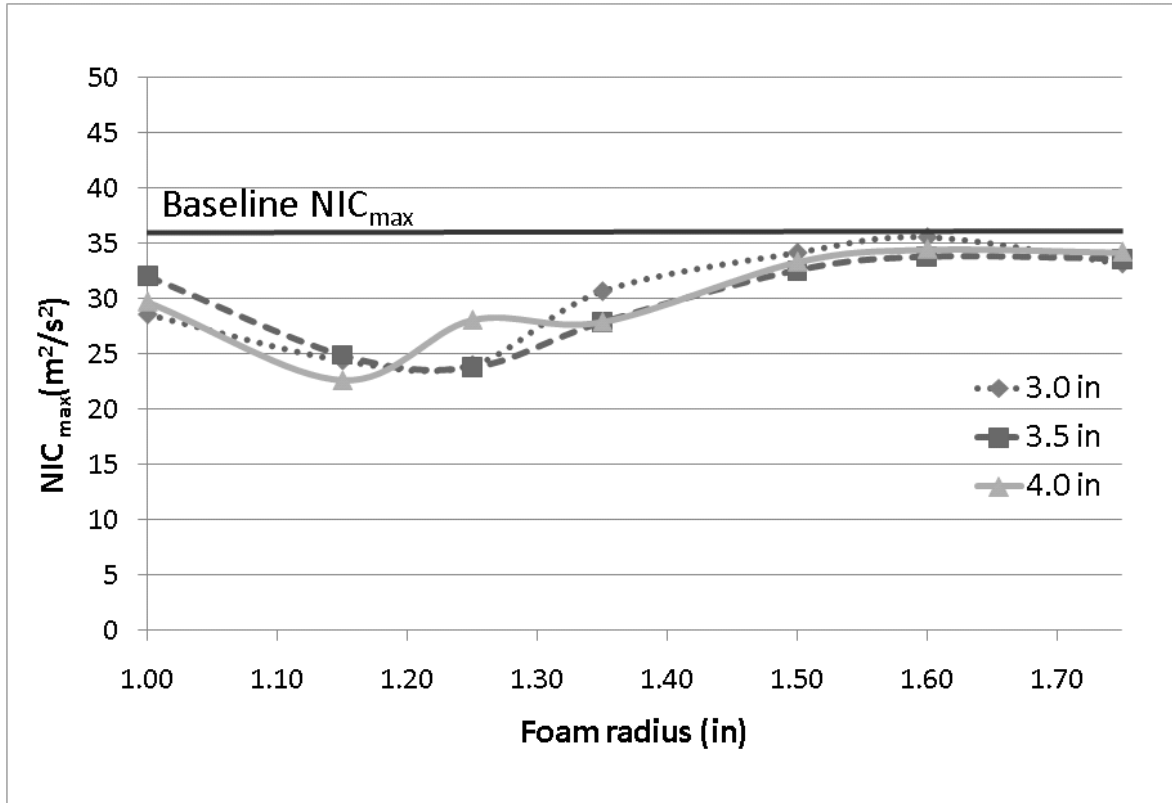


Figure 5-5: NIC_{max} vs. Foam radius for Fraunhofer™ foam at 65 km/h

The NIC_{max} vs. foam radius trends differ for all four foams. However, all four foams demonstrate the capability of reducing NIC_{max} given a specific foam geometry. It is noted from the results that the foam length does not significantly impact the amount of injury reduction predicted. This may indicate that the range of foam lengths was not sufficiently large as to capture the effect of foam length (due to spatial and safety constraints) or that NIC_{max} is insensitive to the percentage of foam being crushed (i.e. insensitive to foam volumetric strain).

The stiffer foams with higher relative densities (i.e. IMPAXX™ 500 and Fraunhofer™) appear to mitigate injury predominantly at lower radii, whereas, foams with lower relative densities (i.e. IMPAXX™ 300 and Cymat™ 200), have optimal ranges that occur at higher foam radii. This may indicate that foam components that are too stiff (as a result of a foam cross-sectional area that is too large, or a crush plateau stress that is too high) may not be beneficial at mitigating injury. Similarly, foam components that are not stiff enough (as a result of a foam cross-sectional area

that is too small, or a crush plateau stress that is too low) may also not be beneficial at mitigating injury.

As the radius increases for IMPAXXTM 300, IMPAXXTM 500, and FraunhoferTM, (see Figure 5-2, Figure 5-3, and Figure 5-5 respectively) the value of NIC_{max} moves towards the baseline value of NIC_{max} (i.e. the results for the seat without the supplemental safety system). This reaffirms the idea that any foam that is too rigid does not have a significant effect on injury mitigation. In the case of CymatTM 200 (see Figure 5-4) the plot indicates that this foam may be overly compliant for smaller radius values. This trend is not seen in the FraunhoferTM foam (i.e. Figure 5-5), likely due to the fact that the FraunhoferTM foam has a higher relative density. This may indicate that as the foam becomes too compliant, the value of NIC_{max} becomes much less predictable, even surpassing the baseline value.

The trends shown in Figure 5-2 to Figure 5-5 illustrate that there may be a relationship between the time in which the foam is crushing and the likelihood of injury. Therefore, in order to test this prediction, the time of foam crush completion (measured relative to the end time of the crash pulse) was examined. In order to quantify this value; a new parameter Δt (see Figure 5-6) was defined.

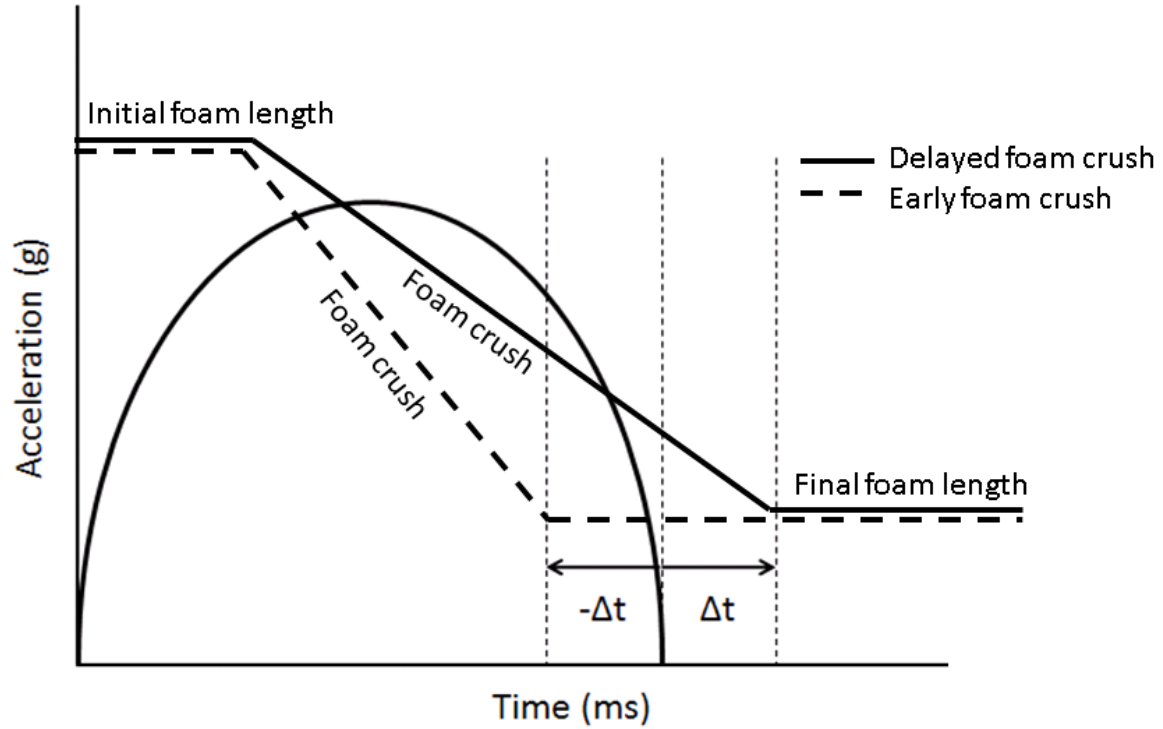


Figure 5-6: Relative time of foam crush completion

The relative time of foam crush completion (Δt) to be referred to hereafter as the relative crush time is defined in Eq. 7:

$$\Delta t = t_{\text{foam}} - t_{\text{pulse}} \quad (7)$$

Where t_{foam} is the time at which the foam is no longer crushing and t_{pulse} is the time at which the acceleration pulse has concluded. Foam configurations that conclude crushing after the acceleration pulse has finished will have a positive value of Δt , and alternatively, those that finish crushing before the acceleration pulse has concluded, will have a negative value of Δt . Using this parameter, NIC_{max} vs. The relative time Δt was determined for the simulations using all four foams and the results plotted against NIC_{max} below to identify if indeed a relationship exists (see Figure 5-7 to Figure 5-10).

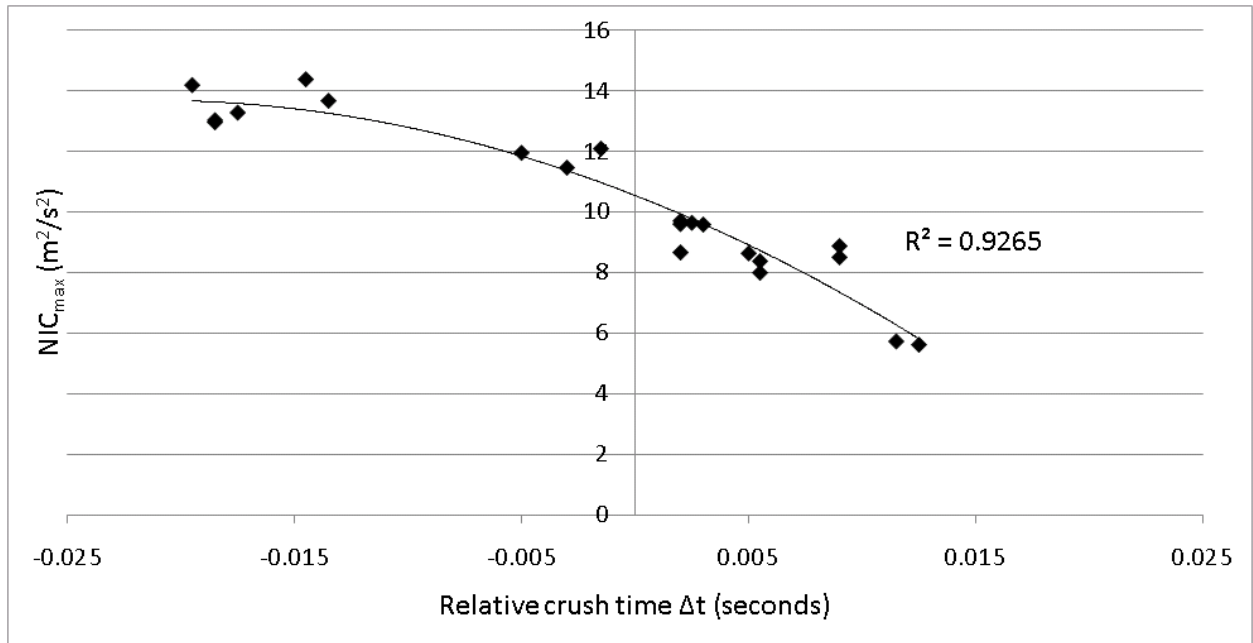


Figure 5-7: NIC_{max} vs. Relative crush time for IMPAXX™ 300 (17 km/h)

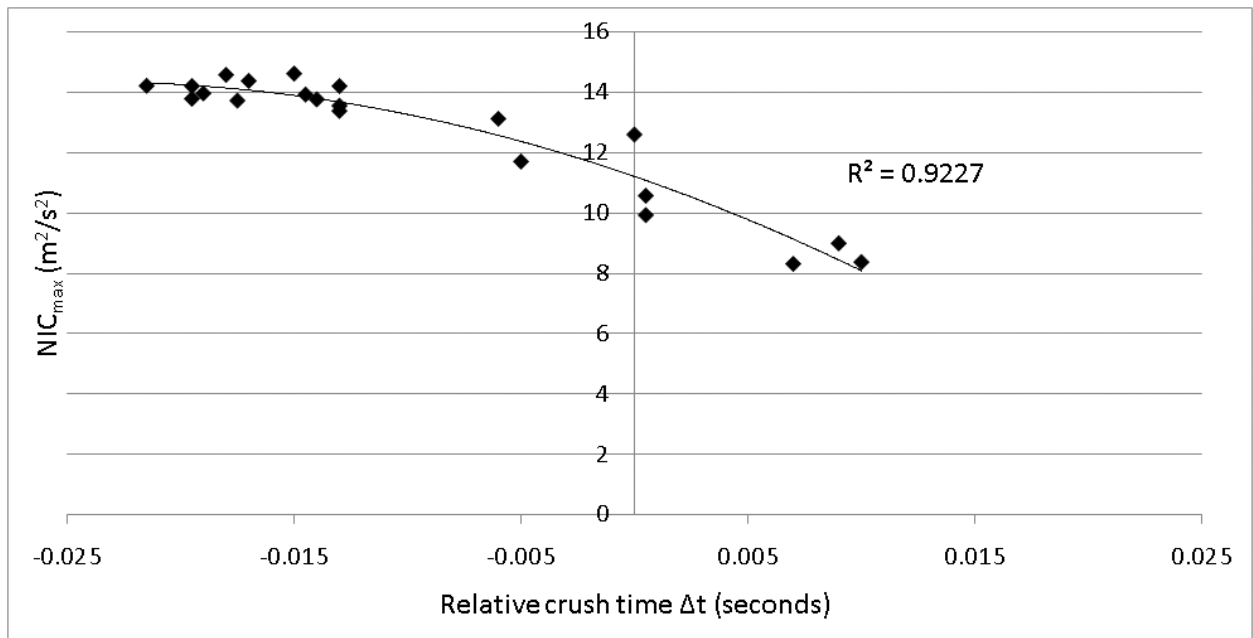


Figure 5-8: NIC_{max} vs. Relative crush time for IMPAXX™ 500 (17 km/h)

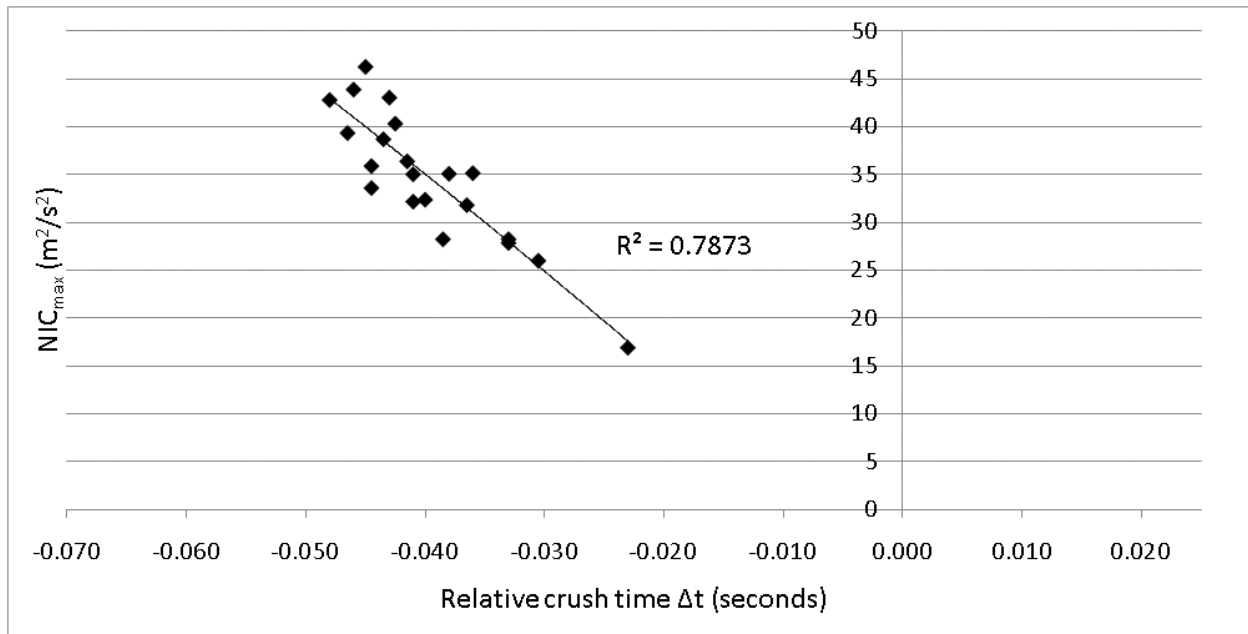


Figure 5-9: NIC_{max} vs. Relative crush time for Cymat™ 200 (65 km/h)

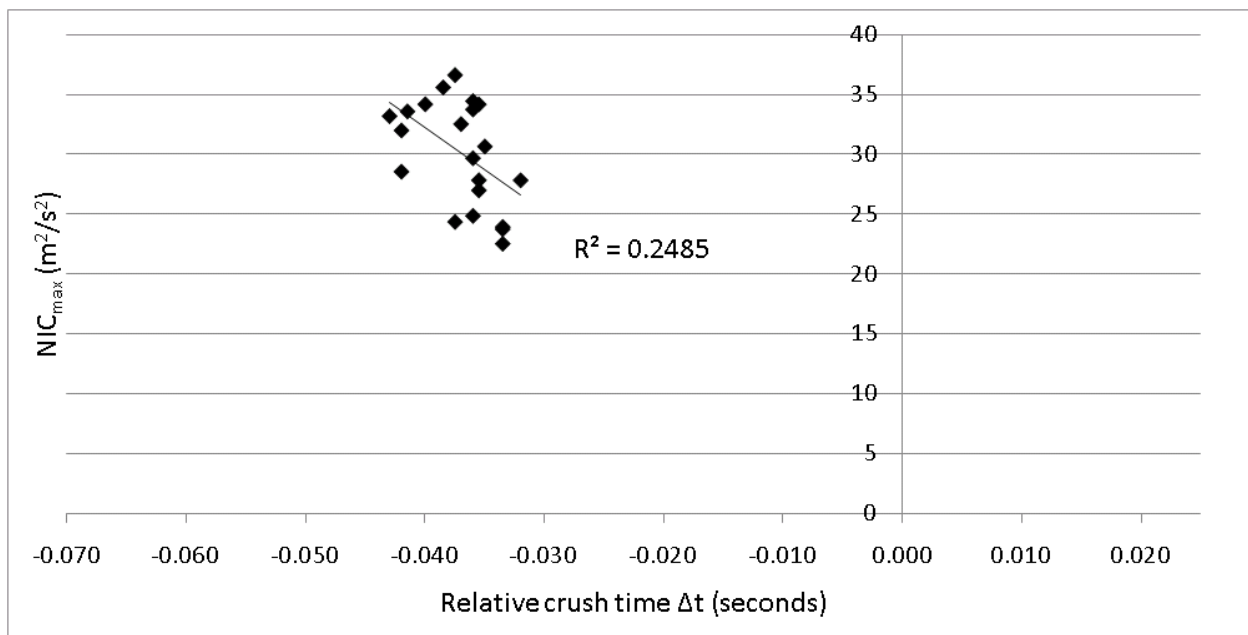


Figure 5-10: NIC_{max} vs. Relative crush time for Fraunhofer™ (65 km/h)

The trends shown in Figure 5-7 to Figure 5-9 indicate a reasonably strong relationship between the time at which the foam has concluded crushing (as defined by Δt) and NIC_{max} . This is

indicated by a second degree polynomial fit with R^2 values of 0.9265 and 0.9227 for IMPAXXTM 300 and IMPAXXTM 500 foams respectively (17 km/h), and a linear fit with an R^2 value of 0.7873 for the CymatTM 200 foam (65 km/h). For those collisions where the foam is actively crushing for the duration of the acceleration pulse, NIC_{max} values are reduced. These results suggest that the safest collision scenarios are those in which foam crushing extends beyond the conclusion of the acceleration pulse.

In the case of the FraunhoferTM foam, a weaker relationship was found between the relative time of foam crush and NIC_{max} injury (i.e. a linear fit with an $R^2 = 0.2485$) as shown in Figure 5-10. For foams with small radii, the decrease in the relative crush time is a result of the foam crushing too quickly. Whereas, for foams with larger radii, decreased relative crush time is a result of little to no crush being achieved. This is not seen in the CymatTM foam (see Figure 5-13) due to the fact that the radii have not become sufficiently large to prevent plastic deformation.

The aforementioned trends are important as they indicate a reasonably strong correlation between the timing of events during the collision and the predicted amount of injury as determined by NIC_{max} values. While this provides an improved understanding of the mechanics related to potential performance of the supplemental safety system, it also indicates that both in-depth design and calibration of this device for a range of different occupants and seats will likely be necessary, as these factors may also affect the timing of events during the collision.

As the time interval for foam crushing is known to be related to foam geometry, the relative foam crush time (Δt) vs. foam radius relationships were examined for all four foams. By first relating NIC_{max} to the relative foam crush time (Eq. 4), and then relating the relative foam crush time to foam radius, insight can be gained into how geometric changes to the foam will affect injury risk directly. The relative foam crush time vs. foam radius trends are shown in Figure 5-11 to Figure 5-14 for the various foams employed in this research study.

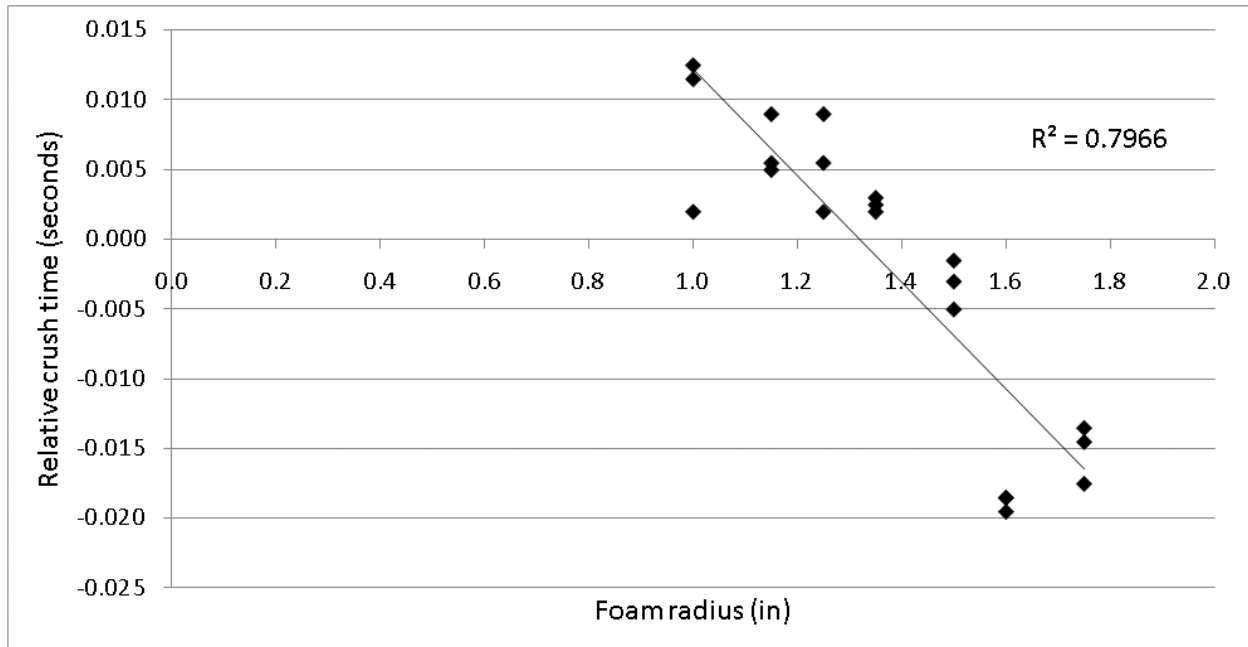


Figure 5-11: Relative crush time vs. Foam radius IMPAXX™ 300 (17 km/h)

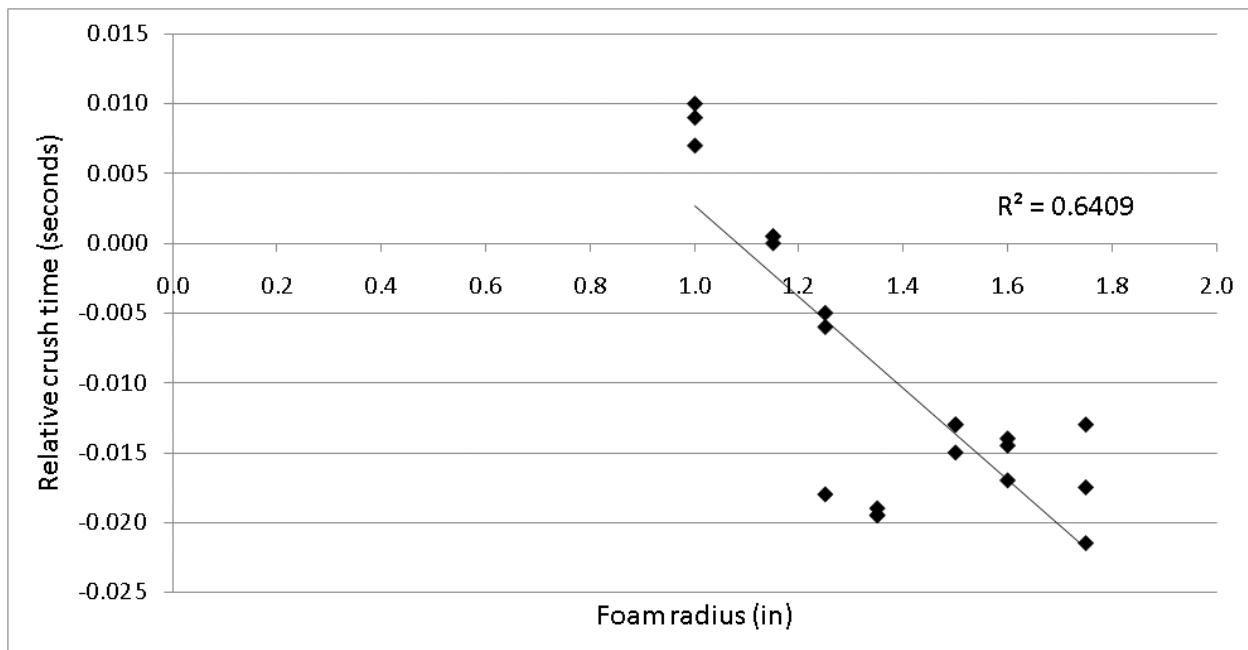


Figure 5-12: Relative crush time vs. Foam Radius IMPAXX™ 500 (17 km/h)

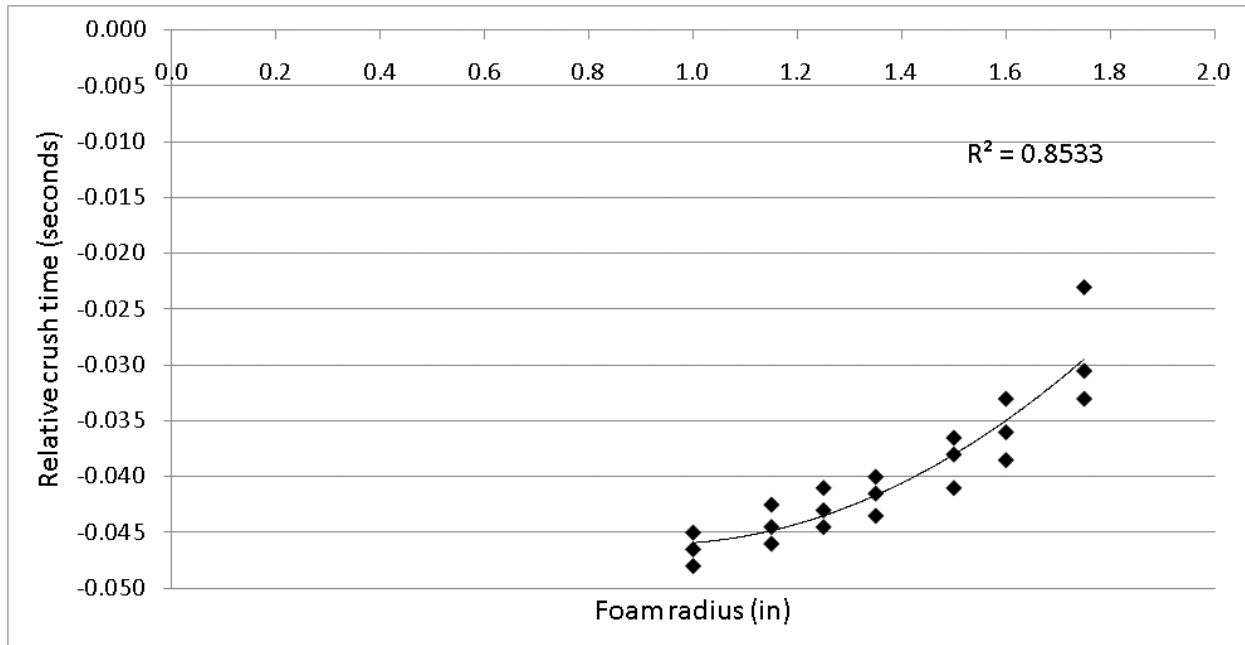


Figure 5-13: Relative crush time vs. Foam radius Cymat™ 200 (65 km/h)

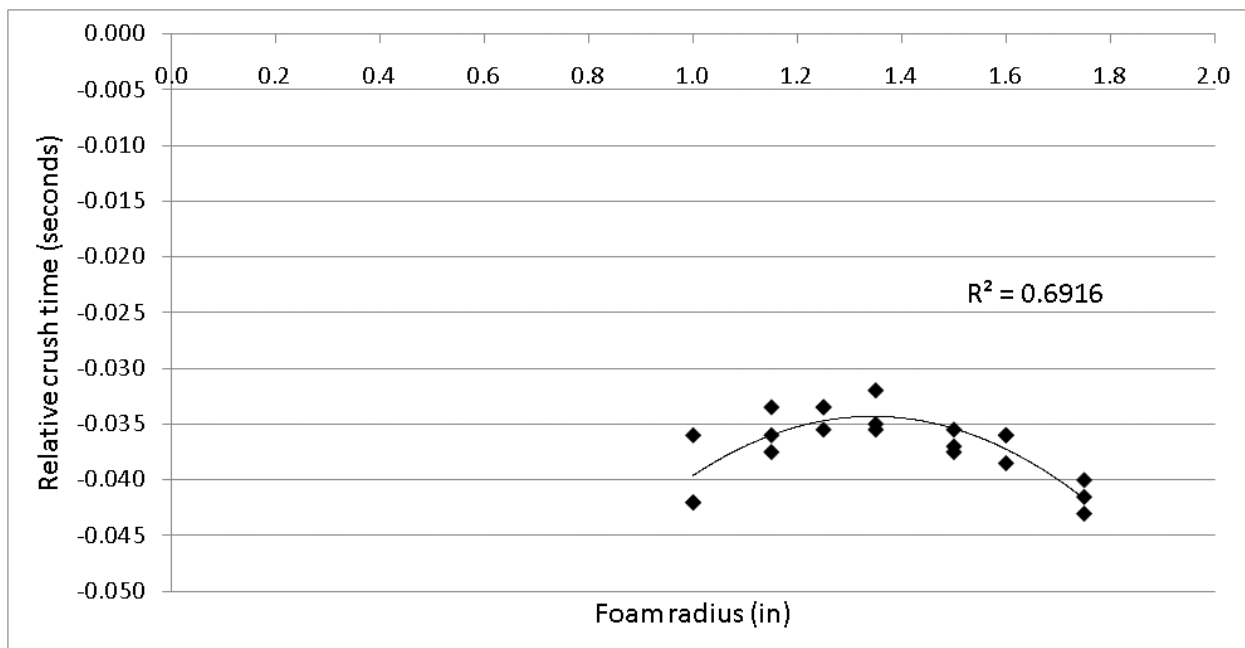


Figure 5-14: Relative crush time vs. Foam radius Fraunhofer™ (65 km/h)

Upon reviewing the results, it can be seen that both the IMPAXX™ 300 (Figure 5-11) and IMPAXX™ 500 (Figure 5-12) foams utilized for the 17 km/h simulations indicate a general trend of decreasing relative crush time with increasing foam radius. In contrast, the results for the Cymat™ 200 (Figure 5-13) foam used for the 65 km/h simulations shows an increase in relative

crush time as the radius increases. This indicates that at higher collision speeds, foam that is too compliant may act to fully crush too quickly, thus reducing the overall effectiveness at reducing injury risk. In higher severity collisions, foam that is more rigid will act to delay and extend the crushing interval and mitigate injury more effectively. Fraunhofer™ foam (see Figure 5-14) shows an increase in relative crush time up to a specific radius (1.35 in), followed by a decrease in relative crush time as the radius increases. Again, this indicates that, the Fraunhofer™ foam becomes too stiff at larger radius values (due to an increased cross-sectional area) which acts to reduce the amount of crush achieved, resulting in a decrease in the relative crush time Δt .

While the results outlined in this section give insight into how to properly select a foam geometry for a selected foam type, it is clear that the trends vary significantly depending on foam type and collision severity. Based on this study, the foam type and geometry that provided the maximum predicted decrease in NIC_{max} were selected for use in a proposed initial supplemental safety system prototype device, and are provided in Table 3 below.

Table 3-1: Optimal Foam Geometries

Collision Speed	Foam Type	Radius	Length
17 km/h	IMPAXX™ 300	1.00	4.0
65 km/h	Cymat™ 200	1.75	4.0

In order to gain a further understanding of the effect of energy-absorbing foam on injury mitigation, the NIC plots for the 17 km/h and 65 km/h collision simulations (both with and without foam) are shown below in Figure 5-19 and Figure 5-20. Since NIC is composed of the relative velocity and acceleration between the top and bottom of the neck, these values are also shown (both with and without foam) in Figure 5-15 to Figure 5-18.

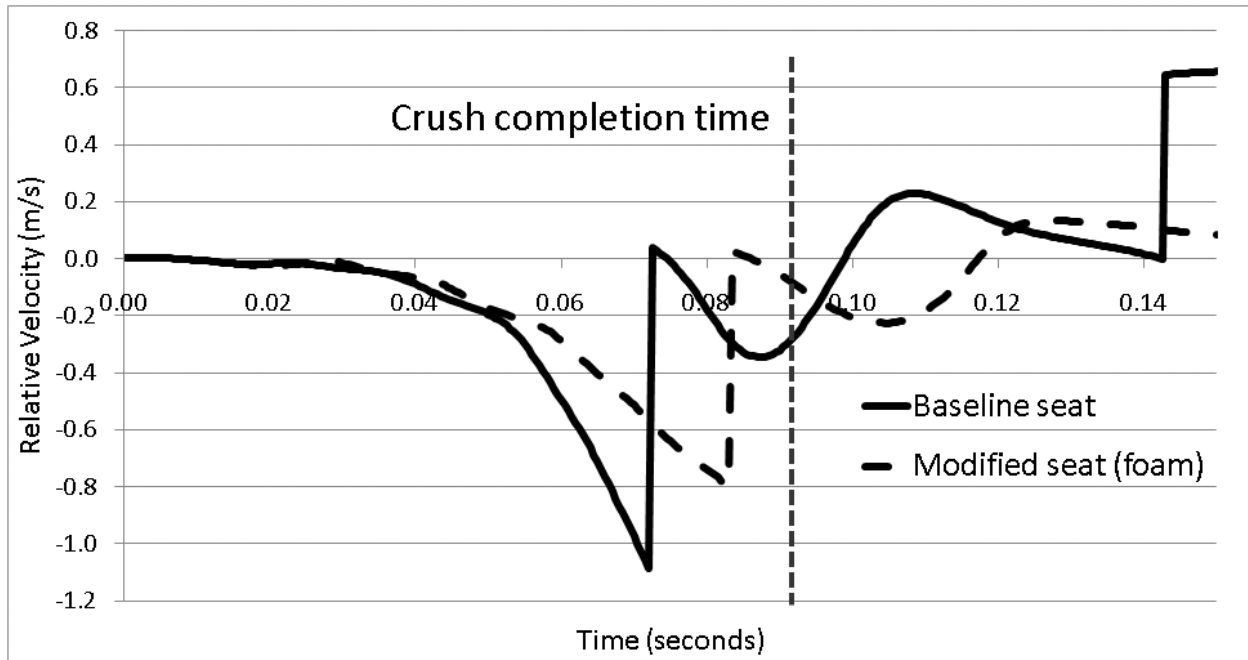


Figure 5-15: Relative velocity with and without foam addition (17 km/h)

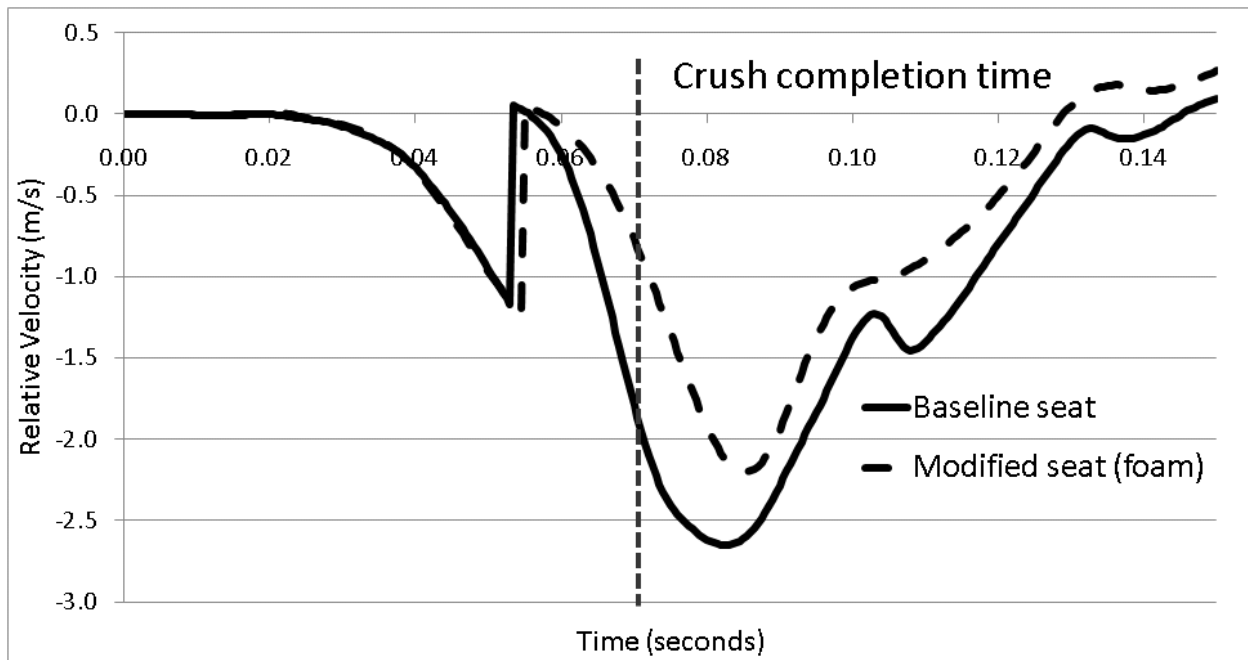


Figure 5-16: Relative velocity with and without foam addition (65 km/h)

Figure 5-15 and Figure 5-16 indicate that the magnitude of the relative velocity does not play a significant role in the determination of NIC. However, it is evident that the addition of foam does act to reduce the peak values of relative velocity for both collision speeds. The

discontinuity that is evident at both collision speeds is a result of the head coming into contact with the head restraint, suddenly changing the direction of the relative velocity.

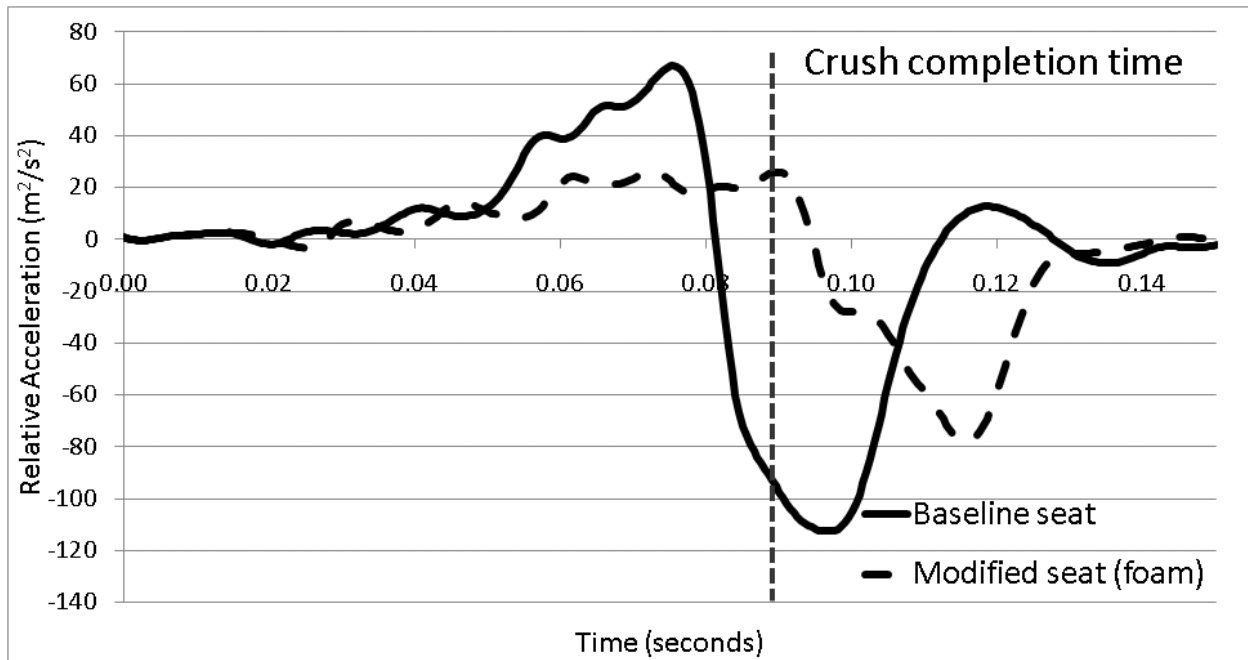


Figure 5-17: Relative acceleration with and without foam addition (17 km/h)

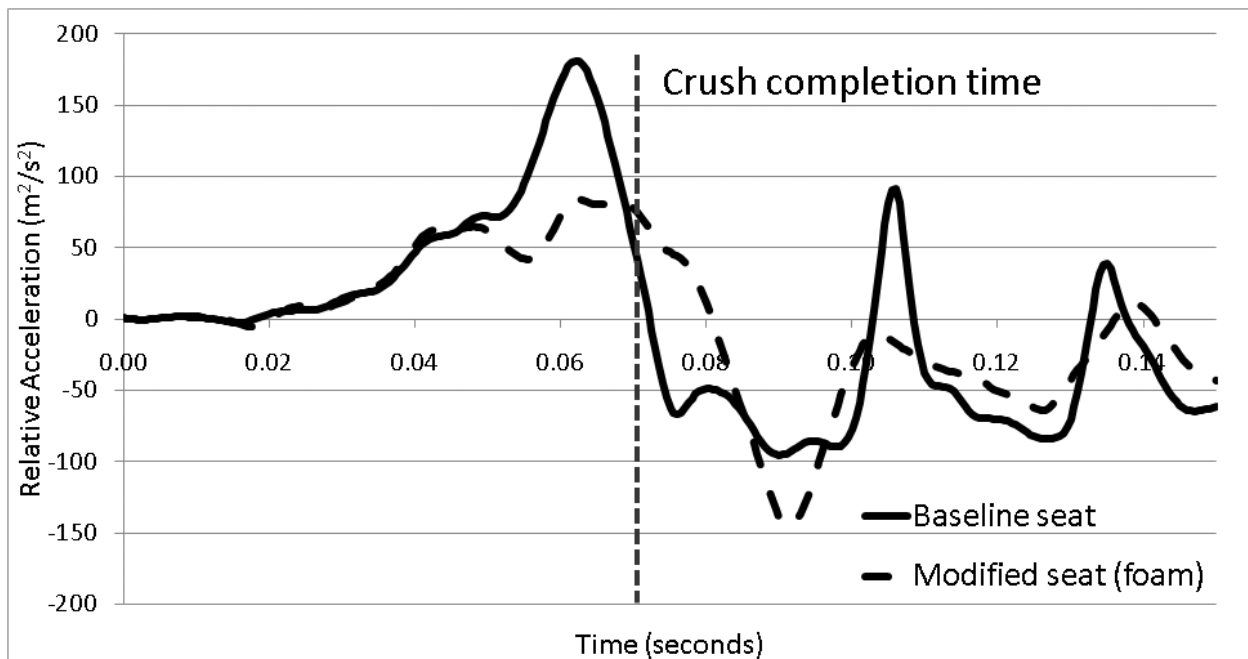


Figure 5-18: Relative acceleration with and without foam addition (65 km/h)

The relative acceleration between the top and bottom of the neck is the primary determining factor in the determination of NIC. It is evident that the addition of foam to the seat base acts to reduce the peak acceleration values at both 17 and 65 km/h collision speeds.

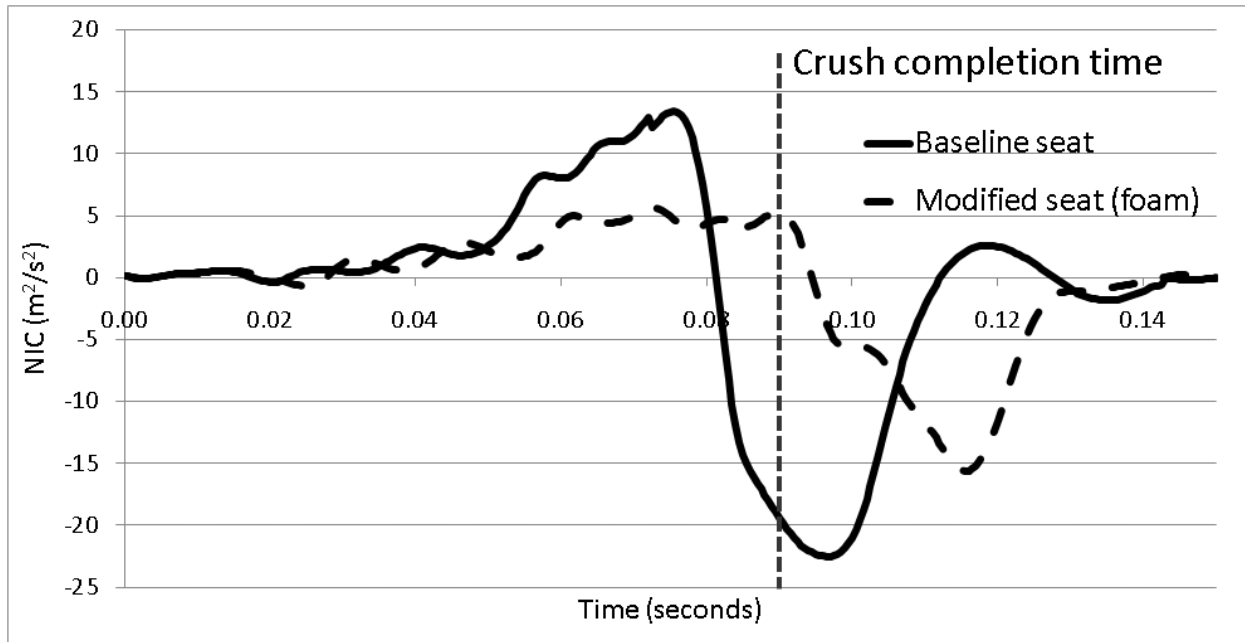


Figure 5-19: NIC vs. time with and without foam modified seat (for 17 km/h collision)

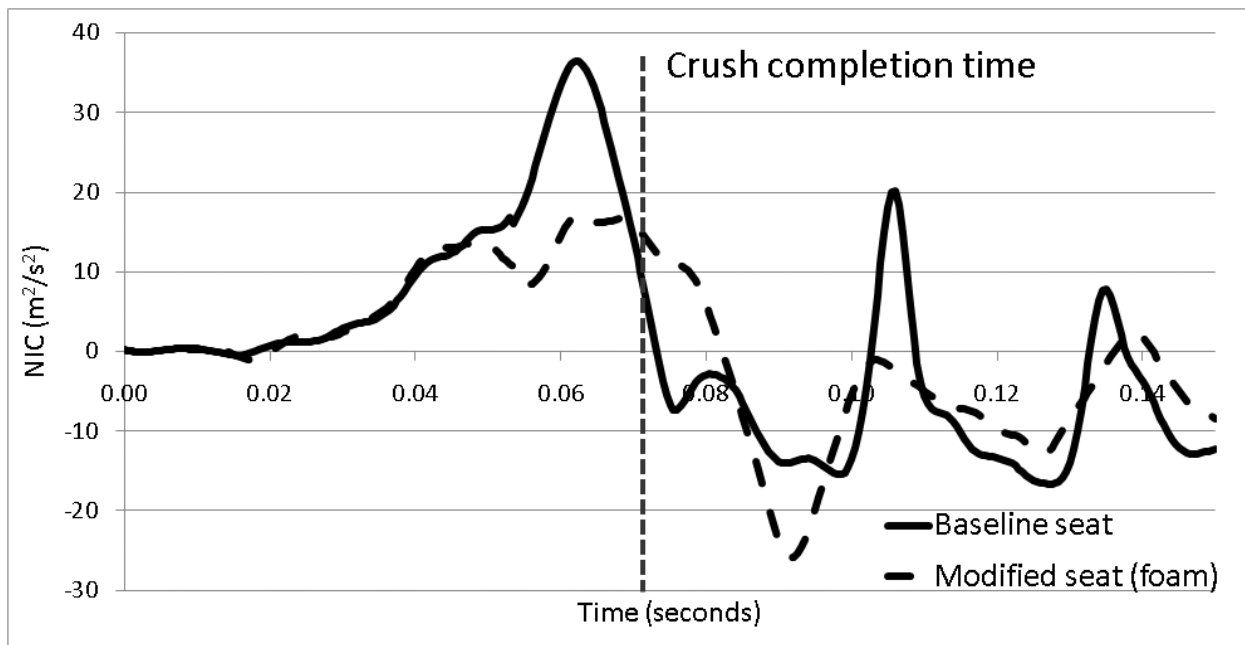


Figure 5-20: NIC vs. time with and without foam modified seat (for 65 km/h collision)

Both the 17 km/h and 65 km/h collision simulation NIC plots indicate that the presence of energy-absorbing foam acts to reduce the first peak of the baseline contour (i.e. where NIC_{max} occurs in the baseline case). In the case of the 17 km/h collision, the presence of the energy-absorbing foam device shifted the entire NIC contour to the right, indicating that the foam addition both reduced and delayed the peak related to maximum occupant injury risk. In each of the modified seat NIC curve predictions, the maximum value of NIC was both significantly reduced and occurred prior (and notably close to) the time of foam crush completion.

5.3 Intermediate Collision Speed Evaluation

To be a truly useful consumer vehicle safety device the supplemental safety system must be effective at mitigating injury for a wide range of collision speeds. Therefore, the foams that were found to be the most beneficial in reducing injury in both the 17 km/h and 65 km/h collision simulations (see Table 3) were further assessed over a broader range of collision speeds to verify their effectiveness (see Table).

Table 5-2: Intermediate speed evaluation matrix using foams of Table 5

Range	Collision Speed	Foam Type	Radius	Length
Low speed range (5-17km/h)	5 km/h	IMPAXX™ 300	1.00	4.0
	10 km/h	IMPAXX™ 300	1.00	4.0
	17 km/h	IMPAXX™ 300	1.00	4.0
High speed range (18-65km/h)	25 km/h	Cymat™ 200	1.75	4.0
	30 km/h	Cymat™ 200	1.75	4.0
	35 km/h	Cymat™ 200	1.75	4.0
	42.5 km/h	Cymat™ 200	1.75	4.0
	48 km/h	Cymat™ 200	1.75	4.0
	55 km/h	Cymat™ 200	1.75	4.0
	65 km/h	Cymat™ 200	1.75	4.0

In the following sections, NIC_{max} , head and torso acceleration, head restraint contact force, seat back deflection angle, and occupant kinetic energy will be presented for the collision speeds indicated in Table (both with and without the foam device).

5.4 The Effect of Collision Speed on NIC_{max}

The NIC_{max} values obtained for the selected collision simulations listed in Table are shown in Figure 5-21 below.

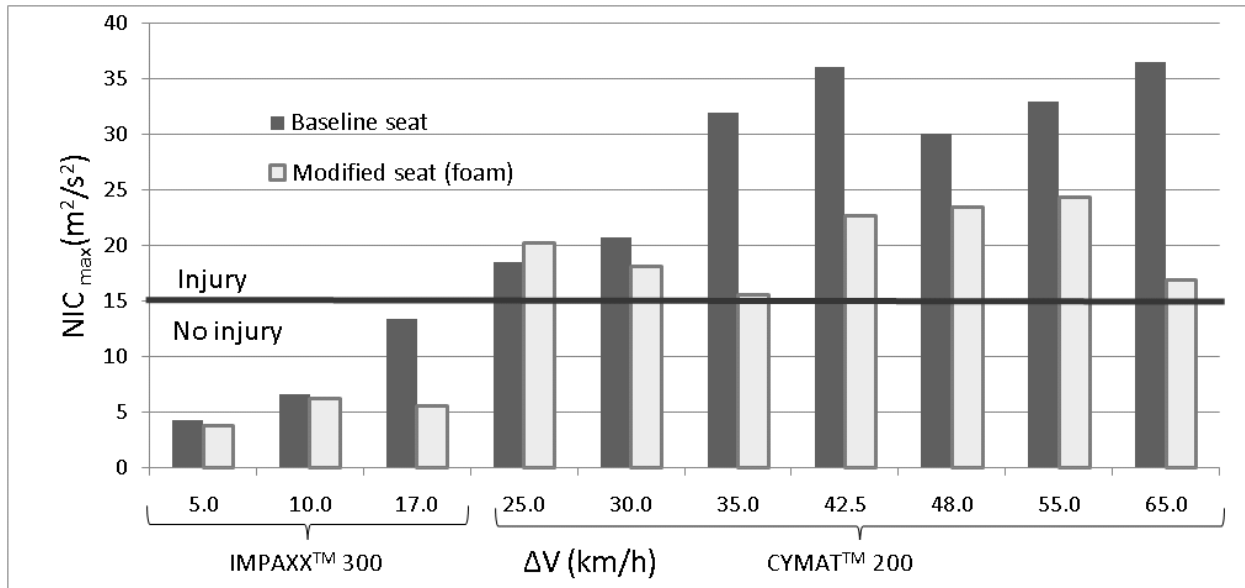


Figure 5-21: Predicted NIC_{max} for selected collision speeds

The results comparison shown in Figure 5-21 predict that the supplemental safety system will reduce NIC_{max} for all collision speeds examined with the exception of the 25 km/h collision. This exception may indicate that the Cymat™ 200 foam is not sufficiently compliant at this collision speed to alter the dynamics of the occupant, and thus the use of IMPAXX™ 300 foam may need to be extended up to this collision speed range. As was previously stated, the collision severity ranges were arbitrarily chosen and thus, are susceptible to change based on the findings from this study. Therefore, the low speed range was extended to include the 25 km/h and 30 km/h collisions so that a greater amount of foam crush could be achieved at these collision speeds. The predicted NIC_{max} values using the IMPAXX™ foam for the extended low speed collision speed range are shown in Figure 5-22.

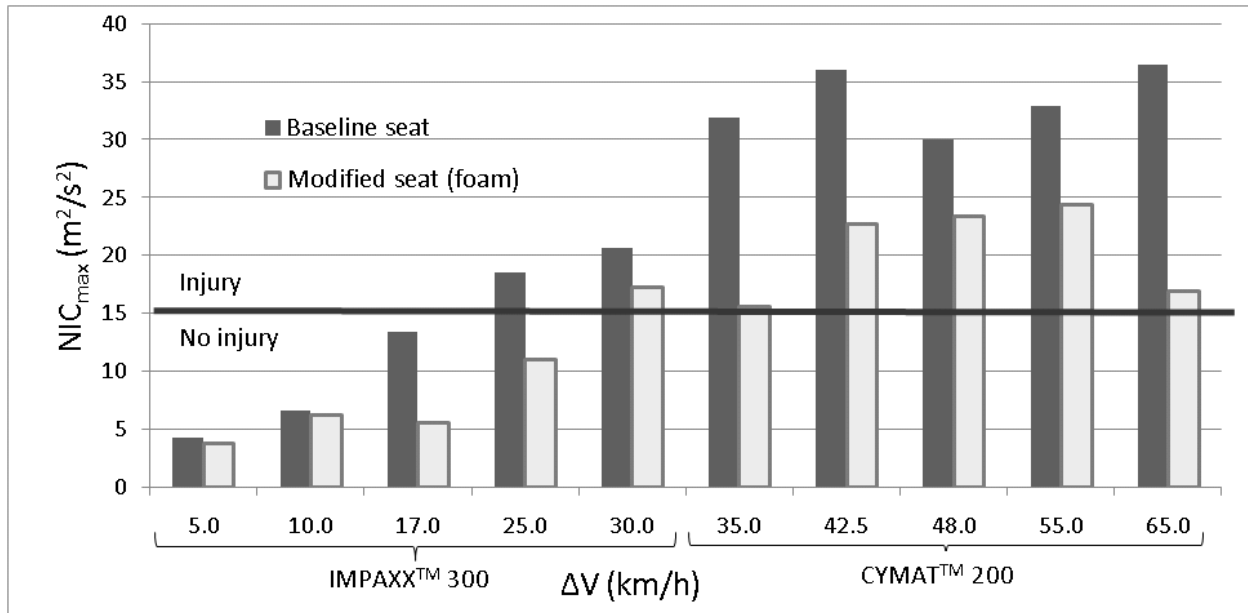
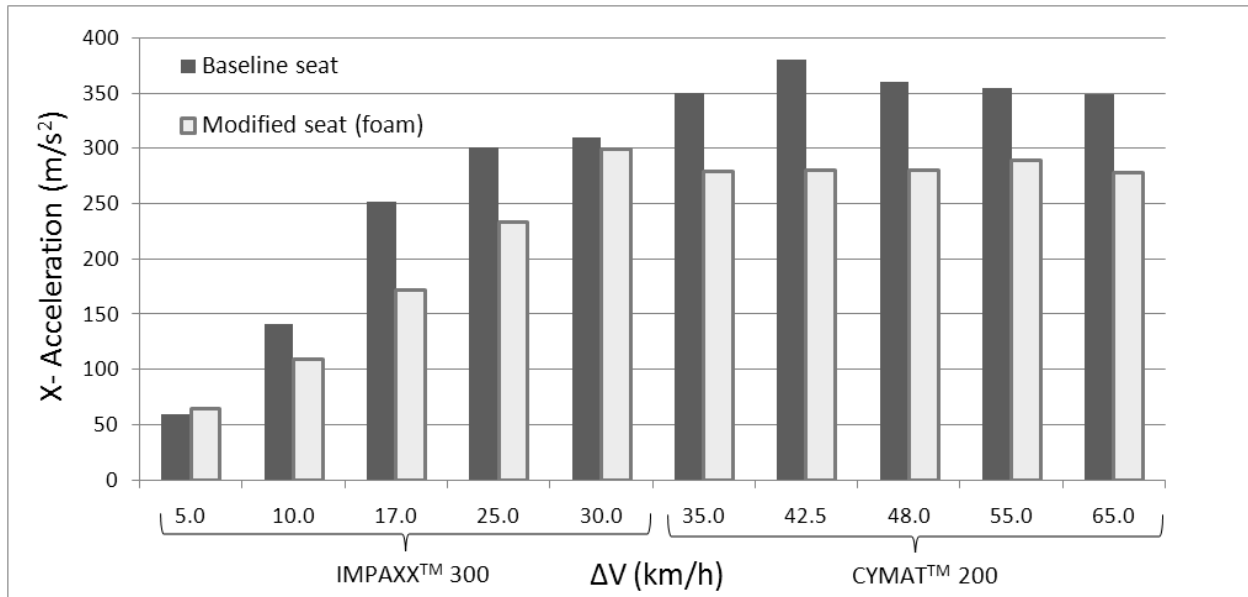


Figure 5-22: Predicted NIC_{max} for selected collision speeds (modified collision ranges)

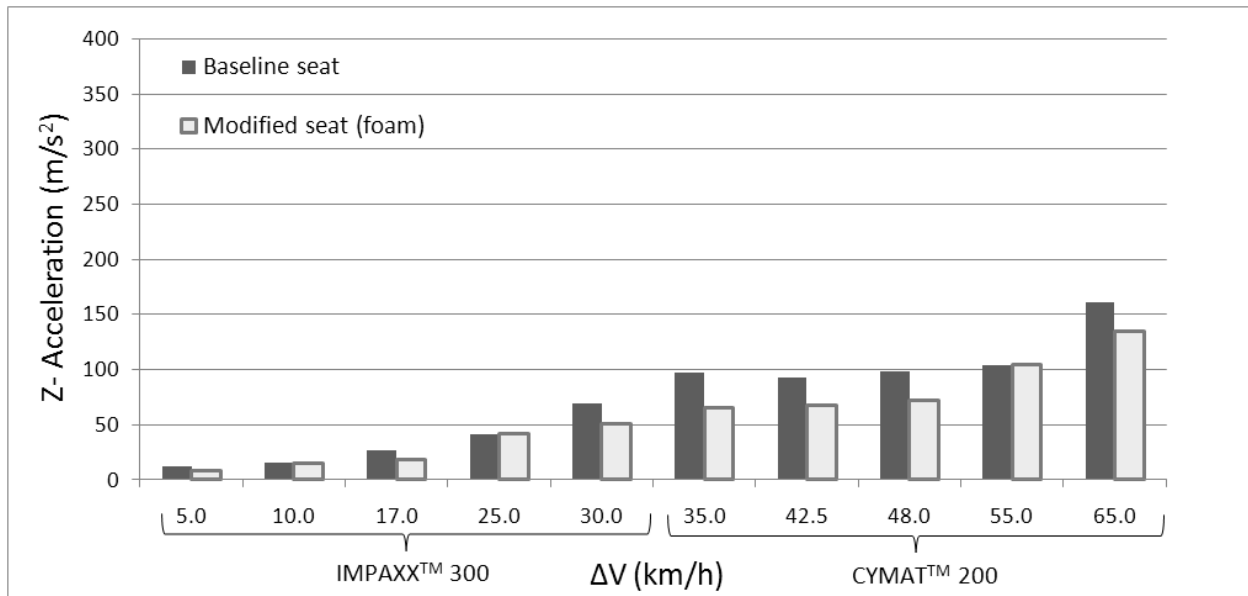
Adjusting the collision speed limits has allowed for the supplemental safety device to be effective for the entire range of collision severities (i.e. from 6% to 58% reduction in NIC_{max}). It is noted that at 5 and 10 km/h the device shows little improvement to occupant injury. This may indicate that the dynamic forces involved with these collision speeds are not capable of crushing the IMPAXX™ 300 foam. However, this is of little concern due to the fact that injury does not take place for NIC_{max} values that are significantly less than 15 m²/s².

5.5 Peak Head Acceleration

While NIC is determined by comparing relative velocities and accelerations between the T1 and C1 vertebra, head accelerations may also act to give an indication of whether the supplemental safety device is capable of reducing dynamic loading on the head of the occupant. The peak head accelerations in both the x- and z- directions are summarized in Figure 5-23a and b. These plots compare predicted head accelerations for the baseline seat and the modified seat with the supplemental safety system employing energy-absorbing foam for a range of simulated rear-end collision speeds.



a)



b)

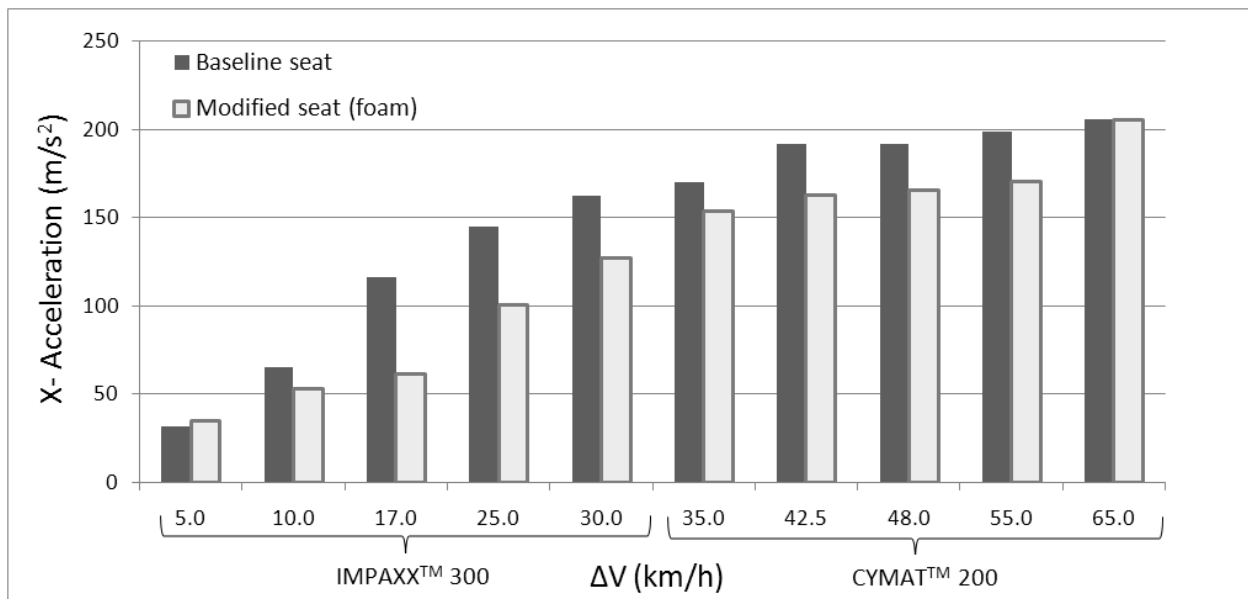
Figure 5-23: Peak Head accelerations for baseline vs. foam seat for: a) x-direction, b) z-direction

The addition of the supplemental safety system acts to reduce the x-direction head acceleration at every speed with the exception of 5 km/h. The decrease in peak x-acceleration may be indicative of an improved injury response by the occupant. The peak head accelerations in the z-direction also indicate a general trend of reduction for most of the collision speeds. These

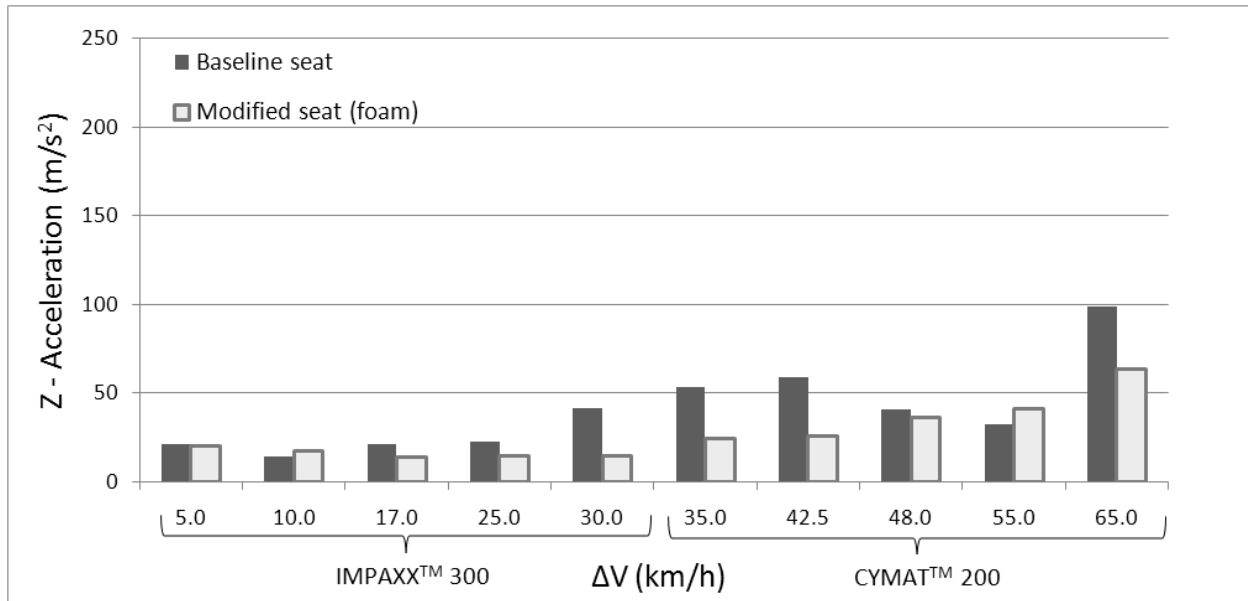
trends also demonstrate that peak head accelerations in the x-direction are significantly larger in magnitude when compared to z-direction accelerations.

5.6 Peak Torso Acceleration

While the likelihood of bodily injury to the torso is less likely in a rear-end collision, it is still a possibility. Thus the amount of acceleration experienced by the torso is provided in order to determine whether the supplemental safety device is capable of reducing the dynamic loading of the occupants torso during a rear-end collision. The torso accelerations in both the x- and z- directions are shown in Figure 5-24a and b. These figures, similar to Figure 5-23, show the peak torso accelerations for the baseline seat for a range of collision speeds and the accelerations for the seat with the foam added for the same range of collision speeds.



a)



b)

Figure 5-24: Torso accelerations for baseline vs. foam seat for a) x-direction b) z-direction

Similar to the head accelerations, all of the x-directional torso accelerations have been shown to decrease with the implementation of the supplemental safety system. The trend is similar for z-directional torso accelerations with the exception of the 10 km/h and 55 km/h collision speeds. While these results indicate that the presence of the supplemental safety system has caused an increase in torso acceleration, this is negligible due to the increase being minimal given the lower magnitude of z-directional accelerations when compared to accelerations experienced in the x-direction.

5.7 Head Restraint Contact Forces

Having a properly positioned head restraint is beneficial in preventing the relative motion between the head and torso; however, at very high collision speeds contact forces to the head could prove to be injurious to the occupant. For this reason the effect of adding the supplemental safety system on contact forces between the head and the head restraint was examined. Predicted peak forces were determined which represent the force on the head occurring from direct contact with the head restraint. The collision simulation results for the resultant forces on the head are shown in Figure 5-25.

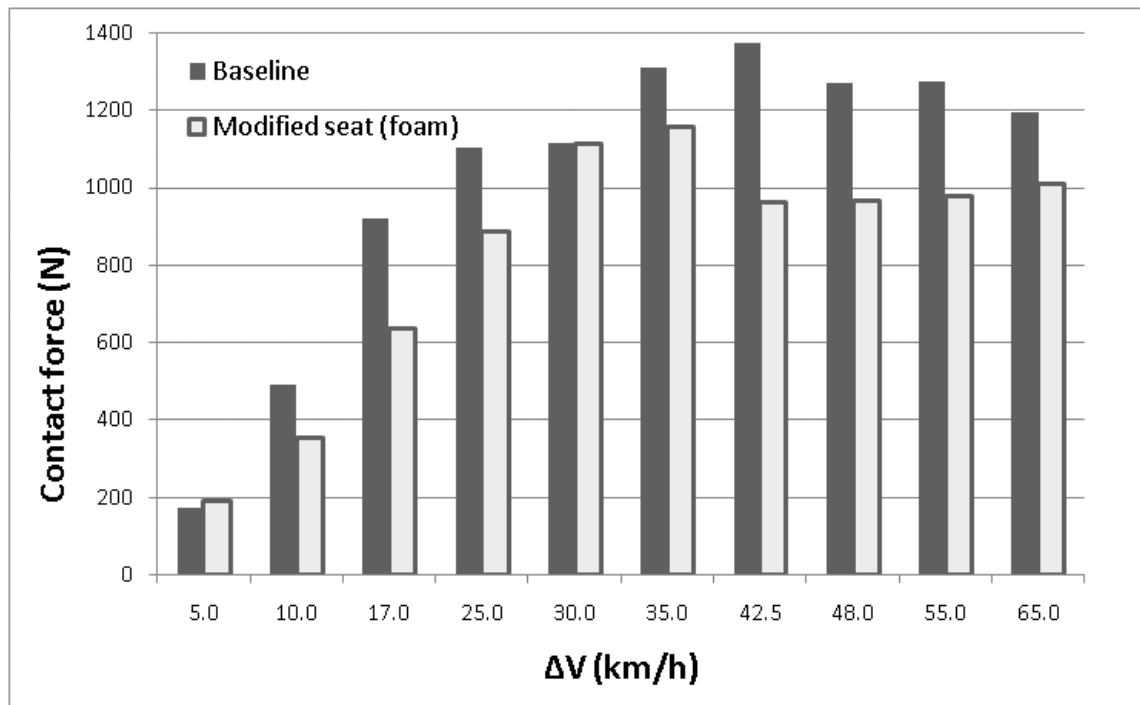


Figure 5-25: Peak resultant head restraint contact force

The results summarized in Figure 5-25 illustrate that the addition of the supplemental safety system has been beneficial to the reduction of head restraint contact force. However, there is shown to be a slight increase in contact force in the 5 km/h collision. Since head trauma injury is unlikely experienced during a 5 km/h rear-end collision, it is still possible to state that the addition of the supplemental safety system is beneficial in reducing head contact force during a rear-end collision.

5.8 Seat Back Deflection

A major concern for occupant safety in rear-end collisions is that occupant ejection can occur at higher collision speeds (see Chapter 1). Ideally, any safety system that is implemented into the vehicle would allow for a similar or reduced injury response with less deflection in the seat back when compared to the unmodified baseline seat. This could potentially mean that the seat back could be designed to be less stiff (i.e. lighter and perhaps less costly) or that simply the risk of occupant ejection is reduced. Therefore, the effect of adding the supplemental safety system on the extent of seat back deflection experienced during a rear-end collision was examined over the entire collision severity range considered. Figure 5-26 compares the amount of

deflection (measured in degrees from the initial seating angle) for both the baseline seat and the modified seats with energy-absorbing foam added.

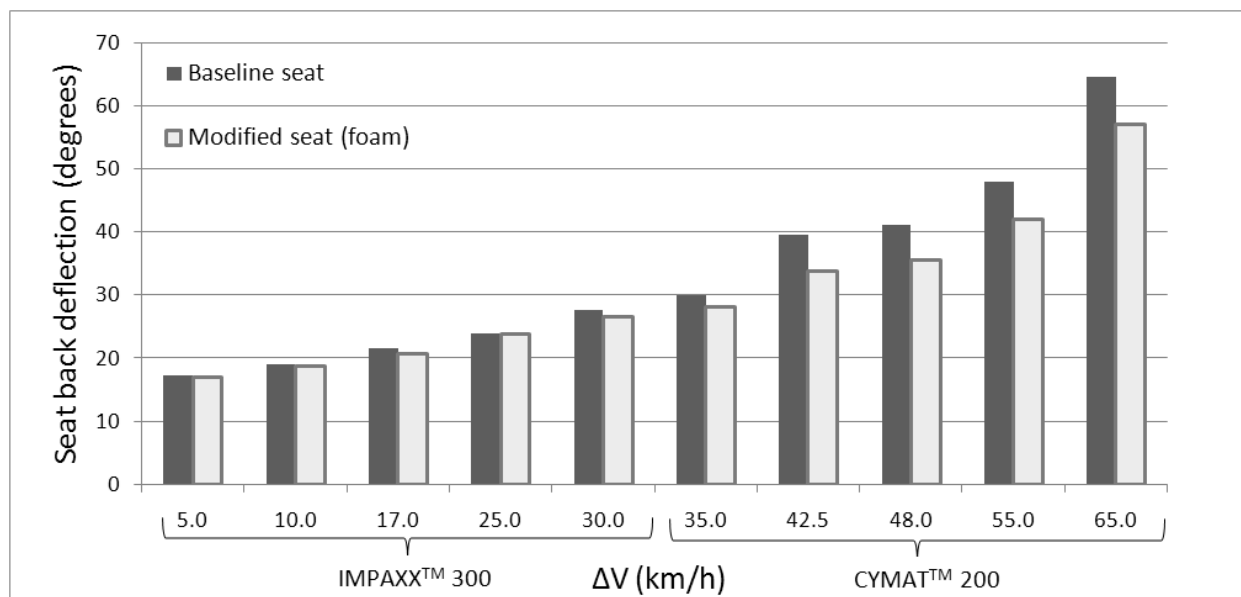


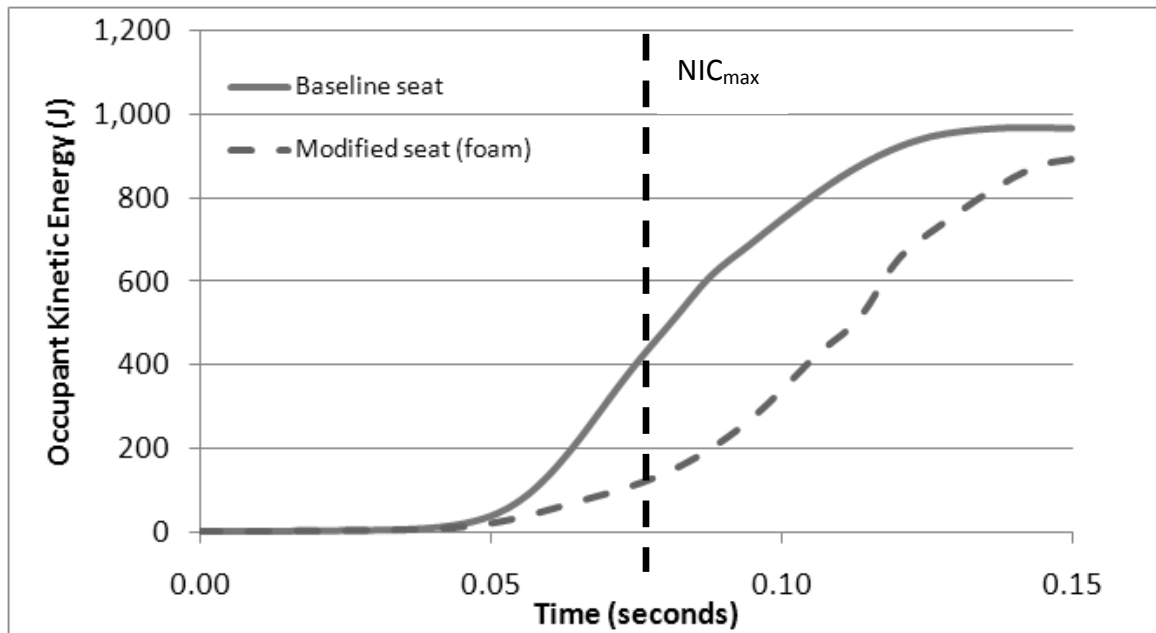
Figure 5-26: Peak seat back deflection of the baseline seat vs. seat with foam added

Figure 5-26 indicates that at lower collision speeds, the addition of the supplemental safety system has little to no effect on seat back deflection, which is acceptable given that occupant ejection is not a problem at low collision speeds. However, at higher collision speeds where occupant ejection is more likely, the amount of seat back deflection is reduced between 12-15% over the 42.5-65% km/h collision speed range. This indicates that the implementation of this supplemental safety system does not only act to reduce the risk of whiplash injury as defined by NIC_{max} , but may also act to reduce the risk of more severe occupant injury or fatality due to potential excessive seat back deflection leading to ejection. This is an important feature to the device as one of the primary goals of this research was to design a system that was capable of mitigating injury at both low and high rear-end collision severities.

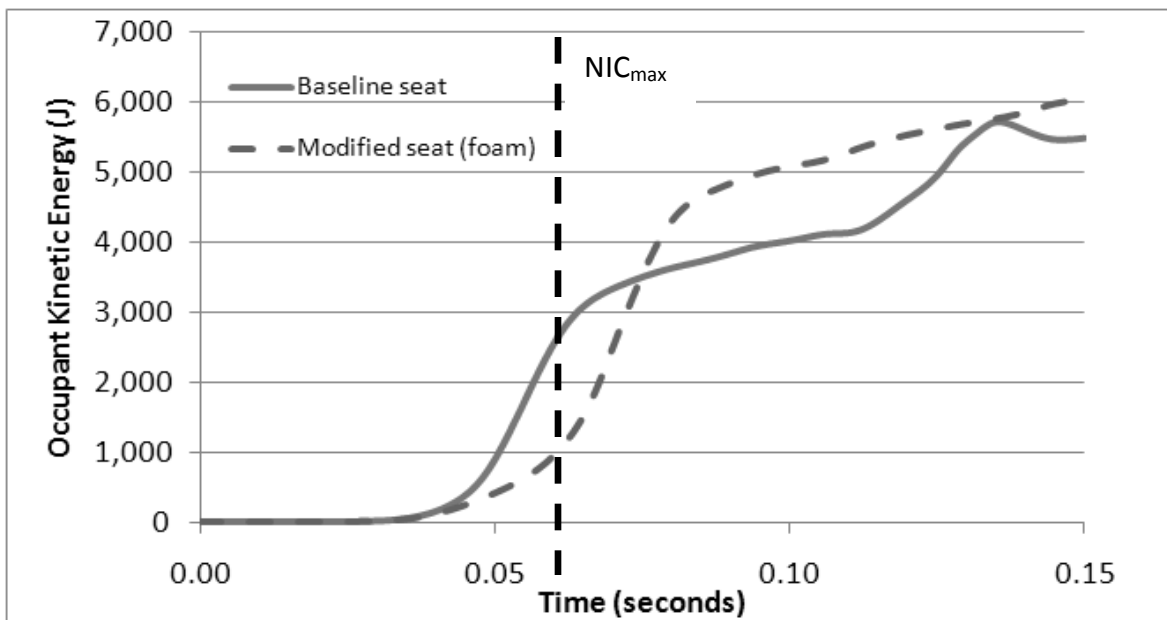
5.9 Occupant Kinetic Energy

Originally, it was theorized that the addition of foam to the seat base would act to reduce the amount of kinetic energy experienced by the occupant during the collision. This in turn would

play a role in reducing the overall injury outcome of the occupant. The plots for kinetic energy vs. time for the 17 km/h and 65 km/h collision severities are shown in Figure 5-27.



a)



b)

Figure 5-27: Occupant kinetic energy vs. time for a) 17 km/h b) 65 km/h

As can be seen in Figure 5-27a and b, the implementation of an energy-absorbing foam-based supplemental safety system reduces the initial kinetic energy gradient thus delaying the build-up of kinetic energy by approximately 0.01 – 0.02 seconds. The magnitudes of peak occupant kinetic energy are nearly identical for both seats (with and without foam). However, at the time where NIC_{max} is observed (0.0755 seconds for the 17 km/h collision, and 0.063 seconds for the 65 km/h collision) the corresponding level of kinetic energy is lower in the modified seat. This may indicate that the peak level of kinetic energy experienced by the occupant is actually delayed until after the peak NIC level is reached- and thus contributes less significantly to the onset of injury. The occupant kinetic energy plots for the other collision speeds being examined in this study can be found in Appendix B and illustrates that the supplemental safety device is more effective at delaying the ramp up of occupant kinetic energy for collision speeds greater than 10 km/h.

5.10 Limitations

The results from this study were acquired based on two computer based simulations. While these models may provide a proper indication of the injury trends seen during a rear-end collision, the exact displacement, velocity, and acceleration magnitudes experienced by the 50th percentile Hybrid III dummy representing a human vehicle occupant remains in question until physical validation can be conducted.

The performance of the simulated Hybrid III dummy may also differ from a physical Hybrid III dummy. Differences in neck response may act to change the injury response. This variability between not only the simulated dummy and the real dummy, but also the real dummy and the response seen in a human vehicle occupant may act to change the injury responses significantly. A dummy cannot account for muscle response, age effects, previous neck injuries, etc. This is an inherent issue related to this type of research that can only be accounted for by doing human testing

The GM High Retention seat simulation created by Skipper and Romilly [31] was produced using physical test data obtained from key structural components within the seat. These tests were

performed quasi-statically, and therefore may not account for strain rate effects that certain seat components may experience at high to severe crash scenarios. Therefore, there is a need to physically validate the seat model, especially at higher collision speeds where the response of the seat is not as predictable.

NIC as an injury criterion capable of predicting injury was designed to be used predominantly at low collision speeds. This study has shown that while NIC rises steadily with increasing collision speed, as the collision speed increases in magnitude (i.e. >42.5 km/h), the response from NIC begins to differ from the predictable trend seen at low collision speeds. This indicates that while NIC values have been generated for high to severe collision speeds, NIC may need to be reviewed in terms of its accuracy in properly predicting injury at these higher collision speeds.

This research has investigated potential injury risk for a relatively severe crash scenario (i.e. a large truck striking a small passenger vehicle head on) and thus, the results from this study may only be applicable to this specific test scenario and should not be assumed to translate to other collision scenarios. The trends predicted for other rear-end collision scenarios may not be the same if changes are made to collision angle, occupant size, occupant seating position, etc.

This work was conducted with the use of the GM High Retention seat as well as a properly positioned head restraint. It is expected that these conditions may act to reduce the values of NIC when compared to results that would have been attained had the tests been conducted with a different seat or an improperly placed head restraint. The result being that the actual potential benefits of the proposed supplemental safety system may actually be greater than predicted if these relatively ideal conditions were not present.

5.11 Summary

The objective of the current research was to first, determine whether the addition of a supplemental seat base safety system (comprised of energy-absorbing foam) could act to mitigate injury during low and high speed rear-end collisions. Secondly, upon verification of the first objective, to determine relationships between the characteristics of the foam and the predicted level of injury risk. In order to accomplish these objectives a study examining the

effect of changing foam radius and length on occupant injury was conducted at the upper limits of two predetermined collision severity ranges. The most optimal foams were then selected (based on foam type and geometry) and implemented into the supplemental safety system. In order to verify the overall efficacy of the supplemental safety system, the foams were tested at intermediate collision speeds in order to determine whether or not they would act to mitigate injury for the wide range of collision severities considered within the study. As such, the major findings of this research have been outlined and discussed in order to gain an understanding of how the addition of this supplemental safety system can affect occupant dynamics. These results indicate that the addition of energy-absorbing foam to the seat base can, in-fact, reduce the values of NIC_{max} , peak head and torso accelerations, head restraint contact force, seat back deflection, and the amount of kinetic energy experienced by the occupant (at the time of injury only). These trends will be summarized in the following chapter.

6 Conclusions

The seat base supplemental safety system that was developed within this work employs an energy-absorbing foam as a means of altering the acceleration pulse transmitted to the seat, thus altering the occupant dynamics as a means of reducing injury during a rear-end collision. By utilizing two computer-based simulations, the relationships between collision severity and occupant dynamic response were determined by comparing easily measureable quantities such as displacement, velocity, and acceleration. These quantities were then used to quantify occupant risk through NIC_{max} , which is a well established neck injury criterion commonly used by researchers in this field.

After determining the baseline values of occupant injury risk for a variety of impact speeds for the selected unmodified seat, several energy-absorbing foams commonly found in industry were employed as key elements of a supplemental safety system and incorporated into the computer-based seat and dummy simulation to determine whether the safety system would prove to be beneficial. Based on an injury risk assessment over a wide range of collision speeds, the identified foams and corresponding foam geometries that were found to maximize injury risk reduction were selected for use in the seat base supplemental system. The results and conclusions of this research are summarized below:

NIC_{max} and Foam Geometry

The primary indicator of occupant injury used in this research is NIC_{max} . The study provided in Chapter 5 attempted to determine whether a relationship existed between the radius and length of the energy-absorbing foam and the level of NIC_{max} achieved, for a specific foam type. It was shown that the level of NIC_{max} was sensitive to the radius of foam when compared to the length of the foam. While these relationships offered some insight into how NIC_{max} was affected by foam geometry, it was necessary to examine another parameter defined as the relative crush time (Δt) (defined in Chapter 5). Utilizing this parameter, which was based on the relative times of foam crush and acceleration pulse completion, it was possible to establish stronger relationships between NIC_{max} and this relative crush time parameter. While the foams have

been shown to be strain rate insensitive in terms of the shape of the stress vs. volumetric strain curve, it was found that the relative crush time (Δt) decreases, resulting in an increase in NIC_{max} as: 1) the collisions become more severe, 2) the foam becomes too stiff (as a result of increasing foam cross-sectional area), and 3) the foam becomes too compliant (as a result of decreasing foam cross-sectional area). Based on these findings, several observations from this study are shown below.

- Based on the limited range of foam lengths examined in this study, foam length does not significantly impact NIC_{max} .
- A reasonably strong relationship exists between NIC_{max} and the relative crush time (Δt). This is indicated by a second degree polynomial fit with R^2 values of 0.9265 and 0.9227 for IMPAXXTM 300 and IMPAXXTM 500 foams respectively (17 km/h), and a linear fit with an R^2 value of 0.7873 for the CymatTM 200 foam (65 km/h). The FraunhoferTM foam showed a poor correlation (i.e. a linear fit with an R^2 value of 0.2485) likely due to the foam failing to achieve crush at higher foam radii.
- A relationship exists between the relative crush time (Δt) and foam radius. This is indicated by a linear fit with R^2 values of 0.7966 and 0.6409 for IMPAXXTM 300 and IMPAXXTM 500 foams respectively (17 km/h), and a second order polynomial fit with R^2 values of 0.8533 and 0.6916 for the CymatTM 200 and Fraunhofer foams respectively (65 km/h). These relationships, combined with the relationships established between NIC_{max} and relative crush time (Δt) allow for the designer of the supplemental safety system to relate foam geometry to occupant injury risk as defined by NIC_{max} , for a specific foam type.
- Based on the results of this work the supplemental safety system prototype will employ the use of two foams: 1) IMPAXXTM 300 foam for collision speeds that range from 5 km/h to 30 km/h, and 2) CymatTM 200 foam for collision speeds that range from 35 km/h to 65 km/h. The addition of energy-absorbing foam to the vehicle seat base has indicated an overall trend of NIC_{max} reduction when compared to the unmodified baseline seat, with up to 58% reduction predicted at collision speeds of around 17 km/h.

The results indicate that two foams are sufficiently capable of mitigating injury over the entire range of collision speeds examined in this study.

While these trends provide insight into how the foam should be selected, this study has shown that NIC_{max} is sensitive to collision speed, foam radius, and foam type. This introduces a difficulty in design as two foams are expected to provide an improved injury response over a large range of collision speeds. However, this study has shown that it is in fact possible to reduce NIC_{max} using only two foams.

Peak Head and Torso Acceleration

NIC_{max} is an acceleration-based injury criterion. However, it may be less predictable at higher collision speeds. Therefore, there was a need to examine the effect of adding the supplemental safety system on other measurable quantities that may give an indication of occupant injury risk, in order to ensure the efficacy of the device. The implementation of the supplemental safety system has been predicted to reduce head and torso accelerations when compared to the unmodified baseline seat. A reduction in occupant head and torso accelerations would likely result in a decrease in the dynamic forces on the occupant and, therefore, an improved injury response. Peak head and torso accelerations were recorded in both the x- and z- directions in order to capture the effect of a rotating torso during the collision. Several trends were identified based on this study.

- The peak head and torso x-accelerations were significantly higher than those of the z-accelerations for both the head and torso (up to 9.5 times larger at lower collision speeds (i.e. 5-30km/h) and up to 4.5 times larger for higher collision speeds (< 35 km/h)).
- Peak head and torso x-accelerations were shown to increase as collision speed increases up to 35 km/h where they became relatively constant. The addition of energy-absorbing foam to the seat base acted to reduce the amount of x-acceleration in both the head and torso for nearly every simulated collision speed.

- The peak head and torso z-accelerations do not follow any identifiable trend with the addition of energy-absorbing foam.

These trends indicate that a reduction in all x-directional accelerations and most z-directional accelerations occurs with the implementation of the supplemental seat base safety system.

Peak Resultant Head Restraint Contact Force

Head trauma can occur in a rear-end collision, especially at very high collision speeds. The peak head restraint contact forces were found in order to determine whether the addition of the supplemental safety system acted to reduce the amount of force in which the occupant's head is striking the head restraint. At higher collision speeds the head restraint contact force was shown to increase substantially when compared to lower speed collisions. This increase in contact force is seen up until for collision speeds up until 42.5 km/h where the head restraint contact force was shown to remain constant or even decrease slightly for higher collision speeds. The trends seen in this study are summarized below.

- Peak head restraint contact force has been predicted to remain constant or decrease in high to severe collision speeds (>42.5 km/h). This may be attributed to a large amount of seat back deflection which may act to extend the duration of the collision reducing accelerations experienced by the head and thus dynamic loads to the head.
- The addition of the supplemental safety system was predicted to reduce the amount of head restraint contact force for nearly all collision speeds with the exception of the 5 km/h case. Since head trauma is not typically associated with such a low collision speed, the slight increase in head restraint contact force at 5 km/h is negligible.
- A reduction of peak head restraint contact force was predicted for the remaining collision speeds (i.e. > 5 km/h). NIC_{max} was reduced by up to 30.8% (17 km/h) indicating that the risk of head trauma is likely reduced with the implementation the supplemental safety system.

Seat Back Deflection

At higher collision speeds, whiplash is still a possibility; however the risk of occupant ejection increases substantially. Due to this fact, the amount of seat back deflection was assessed (see Chapter 5) in order to determine whether the addition of foam will act to reduce the risk of occupant ejection. It was found that:

- Seat back deflection increased with increasing crash severity
- The implementation of the supplemental safety system acted to reduce seat back deflection for all collision speeds, however, the results showed the greatest reduction at higher speeds (between 12-15% angle reduction for collision speeds ranging from 42.5 to 65 km/h).

The reduction in seat back deflection with the implementation of the supplemental safety system indicates that this device may not only be capable of reducing the amount of whiplash experienced by the occupant, but may also act to increase the likelihood that the occupant will remain in their seat during a high speed rear-end collision, thus, reducing the risk of ejection.

Occupant Kinetic Energy

It was theorized that by crushing foam between the vehicle floor and the seat the amount of impact energy transferred to the occupant would be decreased. The trends provided in Chapter 5 indicate that energy-absorbing foam acts to reduce the initial kinetic energy gradient of the occupant. The occupant kinetic energy vs. time plots for all the collision speeds investigated in this study can be found in Appendix B. The trends found in this study indicate that:

- The addition of the supplemental safety system acted to delay the rise in kinetic energy to the occupant by 0.01 to 0.02 seconds.
- NIC_{max} occurs between 0.06 and 0.08 seconds for all collision speeds, coinciding with the period of time in which the kinetic energy gradient is reduced (i.e. occurring after 0.04 seconds) due to the implementation of the supplemental safety system.

It is theorized that due to the fact that NIC_{max} occurs in the early stages of the collision, delaying the ramp up of energy to the occupant during this critical time, results in a decreased risk of

occupant injury as defined by NIC_{max} . These results also indicate that, based on the injury predictions in this study, removing kinetic energy from the system does not necessarily mean that injury risk will be reduced. These results indicate that it is possible to reduce occupant injury by simply delaying the increase of kinetic energy, reducing the amount of energy experienced by the occupant during the critical injury time. This result may be beneficial to researchers in the future who are attempting to recreate this work, or perhaps utilize another energy absorptive device in the seat base.

Summary

The first research task was to obtain the means to assess the dynamics experienced by a seated occupant in a rear-end collision over a range of collision severities. This was made possible through the use of two simulations created in LS-DYNA. The vehicle crash model was capable of determining the acceleration pulse at the driver seat based on a specific impact velocity. The second model used the acceleration pulse generated from the vehicle model as an input, and determined the displacements, velocities, and accelerations of the occupant and the seat.

The second research task was to use these tools to predict the extent of injury risk experienced by the occupant for a range of collision speeds with and without the use of the supplemental safety system. This was done utilizing both simulations to produce occupant dynamics data and then using this data to determine an established injury criterion (NIC). The values of NIC_{max} for a seat with and without the supplemental safety device, for a wide range of collision speeds, were summarized in Chapter 5.

The third research task was to develop relationships between the safety system design parameters and the reduced risk of occupant injury. These relationships are summarized below. Based on these findings the designer of the supplementary seat base safety system should select a foam that can achieve full crush (as this will cause the NIC plot to remain constant as well as delay the ramp up of occupant kinetic energy) however, ensuring that the foam is not too compliant (as this will increase the relative crush time), or that the foam is not too rigid (as little to no foam crush will also act to increase the relative crush time).

The last research task was to determine the optimal characteristics of the safety system for a range of collision severities based on the trends seen in injury mitigation. Two foams were selected (one for low speed and one for high speed collision ranges) based on their ability to mitigate injury at the upper limits of these speed ranges (17 km/h and 65 km/h). These two foams were IMPAXXTM 300 (low speed) and CymatTM 200 (High speed). These foams were then tested at several intermediate collision speeds in order to determine whether they were capable of reducing injury over a large range of collision speeds. The results of this study indicated that the lower speed foam should be extended to facilitate 25 km/h and 30 km/h collisions.

Based on the findings of this study, it is concluded that the addition of the proposed supplemental safety system to a vehicle seat base will be effective at reducing the risk of injury to the occupant after a rear-end collision for both low and high speed rear-end collisions. The effectiveness of such a device can be illustrated by comparing the NIC_{max} values for collision scenarios with and without the device installed. For example, one could make the statement that based on the simulations from this work, the occupant injury level sustained for a 65 km/h collision with the device installed would be equivalent to the occupant injury level sustained for a 30 km/h collision without the supplemental system active. Such an effective reduction in collision severity due to such a system should make a significant contribution to reducing the societal cost of injury from rear-end collisions.

Clearly there are more steps required to validate these findings, more specifically future prototype testing prior to installation into passenger vehicles. However the successful implementation of this research into a commercial device could significantly reduce occupant injury during rear-end collisions.

7 Safety System Design and Future Work

This work has indicated that the addition of a supplemental seat base safety system utilizing energy-absorbing foam can be beneficial in reducing occupant injury risk for a range of low to relatively severe (light-truck vs. small car), rear-end scenarios. While this has been shown for a wide range of collision speeds (5-65 km/h ΔV), there remain several studies that must be conducted before implementation of the seat base safety system can occur. These studies are summarized below:

Occupant Variation Study

While this study has been conducted for the 50th percentile male, it has still yet to be seen as to whether these injury trends would be similar for smaller or larger individuals. A future study should include replicating the process described in this thesis with the 5th and 95th percentile occupant. While this may give a better indication between the relationship between the supplemental seat base safety system and occupant size, other factors such as age, existing neck conditions, and different occupant seating positions may influence the trends predicted in this work.

Vehicle Collision Scenario

This study aimed to model a severe rear-end collision by simulating a large bullet vehicle (C2500 Pickup truck) striking a small target vehicle (Geo Metro) in a direct rear-end collision. While this may address the severe rear-end collisions scenario, it has yet to be determined what the influence of altering vehicle impact angle may be on the trends observed in this study. Changing vehicle size (bullet or target) may affect the crush performance of the crush zones present in both vehicles, potentially altering the shape of the acceleration pulse at the vehicle seat. In the future it will prove beneficial to examine the effect of changing the external impact scenario to determine how this will affect the crash pulse and subsequently, the performance of the supplemental seat safety system.

Physical Validation of the Baseline and Modified Seat

There is a need to validate the baseline seat and dummy simulation. The validity of the simulated seat is one of the key factors in determining whether or not the results acquired from this study are accurate. The seat was developed with data that was developed quasi-statically, therefore, the response of the real seat at high speeds may differ from that seen in the simulation. In order to ensure that the results seen in this study are accurate, the seat should be tested with the use of a physical Hybrid III dummy at a crash testing facility. The seat strength standards (FMVSS#207) that were defined in Chapter 2 of this thesis must also be taken into consideration. Future implementation of the seat supplemental safety system must see that the seat with the supplemental safety device is capable fulfilling the same compliance testing requirements that are defined in FMVSS#207. There is also a need to verify that the foam properties obtained from the aforementioned foam studies and data sheets are in fact accurate. It is apparent that the stress vs. volumetric strain response of both the IMPAXXTM and the CymatTM 200 foam are very similar. However, these foams are different in material and relative density indicating that there may be another factor contributing to the response of the foam other than just the stress vs. volumetric strain response. This must be investigated further.

Prototype Conception and Fabrication

Currently the supplemental safety device is modeled as four rods crushed between two rigid plates. This is a simplified model that does not account for a number of design considerations. Some of these design considerations are outlined below:

Foam actuation – This study determined that the supplemental safety system must utilize two foams (i.e. IMPAXXTM 300 and CymatTM 200) in order to facilitate safety over the entire range of collision speeds (i.e. 5-65 km/h). As a result, the supplemental safety system must be able to determine how fast an incoming vehicle is approaching so that it can activate the correct foam. In order to do this it may be necessary to implement a sensor into the rear bumper of the target vehicle. This is possible using a Millimeter-wave radar sensor (Figure 7-1).

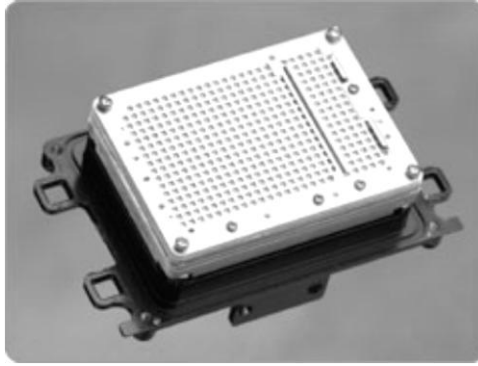


Figure 7-1: Millimeter-wave radar sensor [76]

This sensor emits a wave towards a proceeding vehicle. The wave is reflected off of an object, in this case the incoming vehicle, and is interpreted by the sensor. The velocity, distance, and direction of that object can be determined. This sensor is capable of detecting relative velocities of up to 200 km/h and can detect objects from distances up to 150 m. The addition of this sensor in the bumper could act as an input for the seat base safety system.

Safety

The seat base supplemental safety system must only be activated in the event of a collision. If the system is triggered during normal day to day activity it may allow for a slight lateral displacement of the seat which may act to distract the occupant and could lead to the occupant losing control of the vehicle. It is for this reason that any locking mechanism that is put in place to prevent the safety system from activating must be sufficiently durable.

The seat base is only allowed to displace a distance of no greater than four inches. This displacement limit was established in order to prevent any injury to rear passengers seated behind the occupant. The mechanism itself must adhere to this constraint; therefore, the mechanical components within the supplemental safety system should be sufficiently strong such that lateral displacement of the seat must stop immediately once the four inch limit is reached.

Foam Replacement

After a collision has taken place, the foam within the device must be replaced. This introduces a need for the foam within the device to be easily accessible. This must be taken into consideration when designing the mechanism itself as the device is designed for multiple uses. The device itself must also be able to be reset easily without damage to non-foam components. Therefore, careful structural analysis on the device components including the locking mechanism, actuation system, outer casing, etc. must be conducted so that the components are shown to be durable under repeated loading.

Cost and Weight

Automobile manufacturers aim to produce components that are not only inexpensive to produce, but are also lightweight. Expensive components translate into an increase in vehicle cost which may directly influence vehicle sales. The weight of the vehicle will reduce the fuel economy which is also a major selling point for manufacturers. Therefore, while functionality is the largest concern, cost and weight must also be minimized. This may be achieved through material selection of the seat safety system components, intelligent design, and by reducing the number of components within the safety system.

Prototype Design

This research has focused primarily on showing that a device utilizing energy-absorbing foam is capable of mitigating injury as opposed to the design and construction of the mechanism itself. However, a preliminary design was created in order to visualize how such a system may be implemented. The functions that this device must perform in order to operate properly are outlined in Figure 7-2.

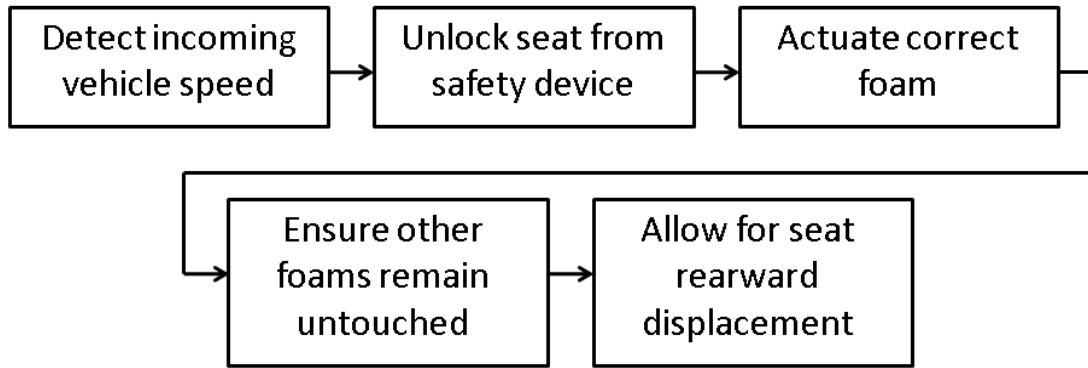


Figure 7-2: Device functionality

In order to simplify the design of the mechanism it was felt that only one actuation mechanism should be deployed in order to select the appropriate foam as opposed to two separate crush systems.

The supplemental safety system designs discussed in this chapter are designed to illustrate how energy-absorbing foam may be implemented into the seat base in a way that does not interfere with the seat itself or other critical components within the vehicle. Future work will see the validation of the vehicle seat, verification of the trends seen in this study for the 5th and 95th percentile occupant and for different collision scenarios (i.e. indirect rear-end collision), and a more detailed design that will lead to prototype design followed by physical testing.

Bibliography

- [1] NHTSA, "Traffic safety facts 2008," National Highway Traffic Safety Administration, U.S. Department of Transportation, 2008.
- [2] D. C. Viano, *Role of the Seat in Rear Crash Safety*. Warrendale, PA: Society of Automotive Engineers, Inc., 2002.
- [3] M. Kleinberger, E. Sun, J. Saunders and Z. Zhou, "Effects of head restraint position on neck injury in rear impact," in Vancouver, Canada, 1999, .
- [4] M. K. Shin, G. J. Park and G. J. Park, "Occupant Analysis and Seat Design to Reduce Neck Injury from Rear End Impact," *International Journal of Crashworthiness*, pp. 573-581, 2003.
- [5] O. Bostrom, Y. Haland, R. Fredriksson, H. Mellander and M. Y. Svensson, "A sled tests procedure proposal to evaluate the risk of neck injury in low speed rear impacts using a new neck injury criterion (NIC)," in Windsor, Canada, 1998, .
- [6] S. M. Foreman and A. C. Croft, *Whiplash Injuries: The Cervical Acceleration/Deceleration Syndrome*. Baltimore, MD: Lippincott Williams & Wilkins, 2002.
- [7] B. Lundell, L. Jakobsson, M. Lindstrom and L. Simonsson, "The whips seat - A car seat for improved protection against neck injuries in rear end impacts," in Windsor, 1998, pp. 1586-1596.
- [8] K. Wiklund and H. Larsson, "Saab Active Head Restraint (SAHR) - Seat Design to Reduce the Risk of Neck Injuries in Rear Impacts," *SAE Technical Paper Series*, 1998.
- [9] G. Chappuis and B. Soltermann, "Number and cost of claims linked to minor cervical trauma in Europe: results from the comparative study by CEA, AREDOC and CEREDOC," *Eur Spine J.*, vol. 17(10), pp. 1350-1357, 2008.
- [10] M. Edwards, S. Smith, D. S. Zuby and A. K. Lund, "Improved Seat and Head Restraint Evaluations," *SAE Technical Paper Series*, 2005.
- [11] ICBC, "Traffic collision statistics," Insurance Corporation of British Columbia, British Columbia, Canada, 1007.
- [12] G. T. Deans, J. N. Magalliard, M. Kerr and W. H. Rutherford, "Neck Sprain - A Major Cause of Disability Following Car Accidents," *Journal of Injury*, vol. 18(1), pp. 2-10, 1897.
- [13] N. Kaneko, M. Wakamatsu, M. Fukushima and S. Ogawa, "Study of BioRID II Sled Testing and MADYMO Simulation to Seek the Optimized Seat Characteristics to Reduce Whiplash Injury," *SAE Technical Paper Series*, 2004.

- [14] K. P. Quinlan, J. L. Annest, B. Myers, G. Ryan and H. Hill, "Neck Strains and Sprains Among Motor Vehicle Occupants - United States, 2000," *Accident Analysis and Prevention*, vol. 36, pp. 21-27, 2002.
- [15] J. O'Day and R. E. Scott, "Safety Belt Use, Ejection and Entrapment," *Health Education Quarterly*, vol. 11(2), pp. 141-146, 1984.
- [16] D. F. Huelke, J. O'Day and R. A. Mendelsohn, "Cervical Injuries Suffered in Automobile Crashes," *J Neurosurg.*, vol. 53(3), pp. 316-22, 1981.
- [17] British Columbia Pharmacy Association Department of Professional Services, "Clinical Update: Whiplash " vol. 2009, 2000.
- [18] S. H. Norris and I. Watt, "The Prognosis of Neck Injuries Resulting from Rear-End Vehicle Collisions," *British Editorial Society of Bone and Joint Surgery*, 1983.
- [19] Y. Sterner and B. Gerdle, "Acute and Chronic Whiplash Disorders - A Review," *J Rehabil Med*, vol. 36, pp. 193-210, 2004.
- [20] K. Hagan, S. Naqui and M. Lovell, "Relationship Between Occupation, Social Class and Time taken off Work Following a Whiplash Injury," *Ann R Coll Surg Engl.*, vol. 89(6), pp. 624-626, 2007.
- [21] G. P. Seigmund, B. A. Winkelstein, P. C. Ivancic, M. Y. Svensson and A. Vasavada, "The Anatomy and Biomechanics of Acute and Chronic Whiplash Injury," *Traffic Injury Prevention*, vol. 10, pp. 101-112, 2009.
- [22] D. Ferrante, "Whiplash Injuries," vol. 2009, .
- [23] D. C. Rizzo, *Fundamentals of Anatomy and Physiology*. Clifton Park, NY: Cengage Learning, 2010.
- [24] Mercedes-Benz, "2010 ML350 BlueTEC," vol. 2010, 2010.
- [25] D. C. Viano, "Seat Design Principles to Reduce Neck Injuries in Rear Impacts," *Traffic Injury Prevention*, vol. 9, pp. 552-560, 2008.
- [26] Canadian Motor Vehicle Safety Standard #207, "Seat Anchorage," 2010.
- [27] SAE J 879, "Motor vehicle seating systems," Society of Automotive Engineers, Inc., Warrendale, PA, 1963.

- [28] C. Y. Warner, C. E. Strother, M. B. James and R. L. Decker, "Occupant Protection in Rear Collisions II: The role of Seat Back Deformations in Injury Reduction," *35th Stapp Car Crash Conference*, 1991.
- [29] K. J. Saczalski, "Petition to national highway traffic safety administration," Tech. Rep. Docket 89-20-NO1-001, 1989.
- [30] M. M. Panjabi, J. Cholewicki, K. Nibu, J. N. Grauer, L. B. Babat and J. Dvorak, "Mechanism of Whiplash Injury," *Journal of Clinical Biomechanics*, vol. 13, pp. 239-249, 1998.
- [31] C. S. Skipper, "Seat Structural Design Choices and the Effect on Occupant Injury Potential in Rear End Collisions," 2005.
- [32] J. R. Schultz, "Cervical Facet Joint," vol. 2009, 2010.
- [33] J. M. Cavanaugh, Y. Lu, C. Chen and S. Kallakuri, "Pain Generation in Lumbar and Cervical Facet Joints," *J Bone Joint Surg Am.*, vol. 88-A, pp. 63-67, 2006.
- [34] B. D. Stemper, N. Yoganandan, T. A. Gennarelli and F. A. Pintar, "Localized Cervical Facet Joint Kinematics under Physiological and Whiplash Loading," *J Neurosurg Spine*, vol. 3, pp. 471-476, 2005.
- [35] Vertical health, "Spinal Ligaments and Tendons," vol. 2009, 2010.
- [36] H. Gray, *Anatomy of the Human Body*. New York, NY: Lea & Febiger, 1918.
- [37] Y. Tominga, A. B. Ndu, M. P. Coe, A. J. Valenson, P. C. Ivancic, S. Ito, W. Rubin and M. M. Panjabi, "Neck Ligament Strength is Decreased Following Whiplash Trauma," *BME Musculoskelet Disord.*, vol. 7, pp. 103, 2006.
- [38] Encyclopaedia Britannica, "vertebral artery," vol. 2010, 2010.
- [39] P. B. Dobrin, "Mechanical Properties of Arteries," *Physiological Reviews*, vol. 58, pp. 397-460, 1978.
- [40] K. Nibu, J. Cholewicki, M. M. Panjabi, L. B. Babat, J. N. Grauer, R. Kothe and J. Dvorak, "Dynamic elongation of the vertebral artery during an in vitro whiplash simulation," *Eur Spine J.*, vol. 6, pp. 286-289, 1997.
- [41] Demos Medical Publishing, "Gross Anatomy," vol. 2010, 2003.
- [42] M. Y. Svensson, O. Bostrom, J. Davidsson, H. A. Hansson, Y. Haland, P. Lovsund, A. Suneson and A. Saljo, "Neck injuries in car collisions--a review covering a possible injury mechanism and the development of a new rear-impact dummy." *Accid Anal Prev.*, vol. 32, pp. 167-175, 2000.

- [43] L. Eriksson and A. Kullgren, "Influence of Seat Geometry and Seating Posture on NICmax Long-Term AIS 1 Neck Injury Predictability," *Traffic Injury Prevention*, vol. 7, pp. 61-69, 2006.
- [44] K. Schmitt, M. H. Muser, F. H. Walz and P. F. Niederer, "N km - A Proposal for a Neck Protection Criterion for Low-Speed Rear-End Impacts," *Traffic Injury Prevention*, vol. 3, pp. 117-126, 2002.
- [45] R. Eppinger, E. Sun and S. Kuppa, "Development of improved injury criteria for the assessment of advanced automotive restraint systems - II," National Highway Traffic Safety Administration, Vehicle Research and Test Center, 2000.
- [46] IIHS, "Frontal offset crashworthiness evaluation: Guidelines for rating injury measures," Insurance Institute for Highway Safety, Arlington, VA, 2009.
- [47] M. H. Muser, F. H. Walz and K. Schmitt, "Injury Criteria Applied to Seat Comparison Tests," *Traffic Inj Prev.*, vol. 3, pp. 224-232, 2002.
- [48] M. M. Panjabi, S. Ito, P. C. Ivancic and W. Rubin, "Evaluation of the intervertebral neck injury criterion using simulated rear impacts," *J Biomech.*, vol. 38, pp. 1694-1701, 2005.
- [49] M. K. Shin, K. J. Park and G. J. Park, "Occupant analysis and seat design to reduce neck injury from rear end impact," *IJ Crash*, vol. 8, pp. 573-581, 2003.
- [50] D. P. Romilly and C. S. Skipper, "Seat Structural Design Choices and the Effect on Occupant Injury Potential in Rear End Collisions," *SAE Technical Paper Series*, 2005.
- [51] M. Y. Svensson, P. Lofsund, Y. Haland and S. Larsson, "The influence of seat-back and head-restraint properties on the head-neck motion during rear-impact," *Accid Anal Prev.*, vol. 28, pp. 221-227, 1996.
- [52] S. Himmetoglu, M. Acar, K. Bouazza-Marouf and A. J. Taylor, "Energy-absorbing car seat designs for reducing whiplash," *Traffic Inj Prev.*, vol. 9, pp. 583-591, 2008.
- [53] G. P. Seigmund, B. E. Heinrichs, D. D. Chimich, A. L. DeMarco and J. R. Brault, "The effect of collision pulse properties on seven whiplash injury criteria," *Accid Anal Prev.*, vol. 37, pp. 275-285, 2005.
- [54] M. Krafft, A. Kullgren, A. Ydenius and C. Tingvall, "Influence of Crash Pulse Characteristics on Whiplash Associated Disorders in Rear Impacts - Crash Recording in Real Life Crashes," *Traffic Inj Prev.*, vol. 3, pp. 141-149, 2002.
- [55] P. Sendur, R. Thibodeau, J. Burge and A. Tencer, "Parametric Analysis of Vehicle Design Influence on the Four Phases of Whiplash Motion," *Traffic Inj Prev.*, vol. 6, pp. 258-266, 2005.

- [56] M. Krafft, A. Kullgren, A. Lie and C. Tingvall, "The Risk of Whiplash Injury in the Rear Seat Compared to the Front Seat in Rear Impacts," *Traffic Inj Prev.*, vol. 4, pp. 136-140, 2003.
- [57] J. Mordaka and C. R. Gentle, "Biomechanical analysis of whiplash injuries; women are not scaled down men," in *4th European LS-DYNA Users Conference*, 2003, .
- [58] NCAC, "National Crash Analysis Center," vol. 2009, 2010.
- [59] Motortrend, "2000 Chevrolet C2500 Specs," vol. 2010, 2010.
- [60] Motortrend, "1997 Geo Metro Specs," vol. 2010, 2010.
- [61] IIHS, "How should my head restraint be positioned?" vol. 2010, 2010.
- [62] A. Kim, K. F. Anderson, J. Berliner, J. Hassan, J. Jenson, J. Kleinert, H. J. Mertz, H. Pietsch, R. Rouhana, R. Scherer and A. Sutterfield, "A comparison of the BioRID II, hybrid III, and RID2 in low severity rear impacts," in *19th ESV*, 2005, .
- [63] S. Kuppa, J. Saunders, J. Stammen and A. Mallory, "Kinematically based whiplash injury criterion," National Highway Traffic Safety Administration, Transportation Research Center Inc., US, Tech. Rep. 05-0211, 2005.
- [64] K. Schmitt, M. H. Muser and P. F. Niederer, "A new neck injury criterion candidate for rear-end collisions taking into account shear forces and bending moments," in *Proceedings of the 17th International Conference on the Enhanced Safety of Vehicles*, Amsterdam, 2001, .
- [65] L. J. Gibson, "Mechanical behavior of metallic foams," *Annual Review of Materials Science*, vol. 30, pp. 191-227, 2000.
- [66] F. Simancik, "Reproducibility of aluminium foam properties," in Bremen, 1999, .
- [67] A. Paul and U. Ramamurty, "Strain rate sensitivity of a closed-cell aluminum foam," *Materials Science and Engineering*, 2000.
- [68] B. Croop and H. Lobo, "Selecting material models for the simulation of foams in LS-DYNA," in *7th European LS-DYNA Conference*, Salzburg, Austria, 2009, .
- [69] R. W. Bielenberg and J. D. Reid, "Modeling crushable foam for the SAFER racetrack barrier," in Dearborn, Michigan, 2004, .
- [70] J. C. Nichols III, M. E. Cohen and R. A. Johnson, "Benchmarking of LS-DYNA for use with impact limiters," in Tuscon, AZ, 2001, .

[71] DOW, "Tech data sheet IMPAXX energy absorbing foam," The Dow Chemical Company, Sarnia, ON, Tech. Rep. 299, 2006.

[72] Cymat Technologies Ltd., "CYMAT technical manual," Cymat Corp., 2000.

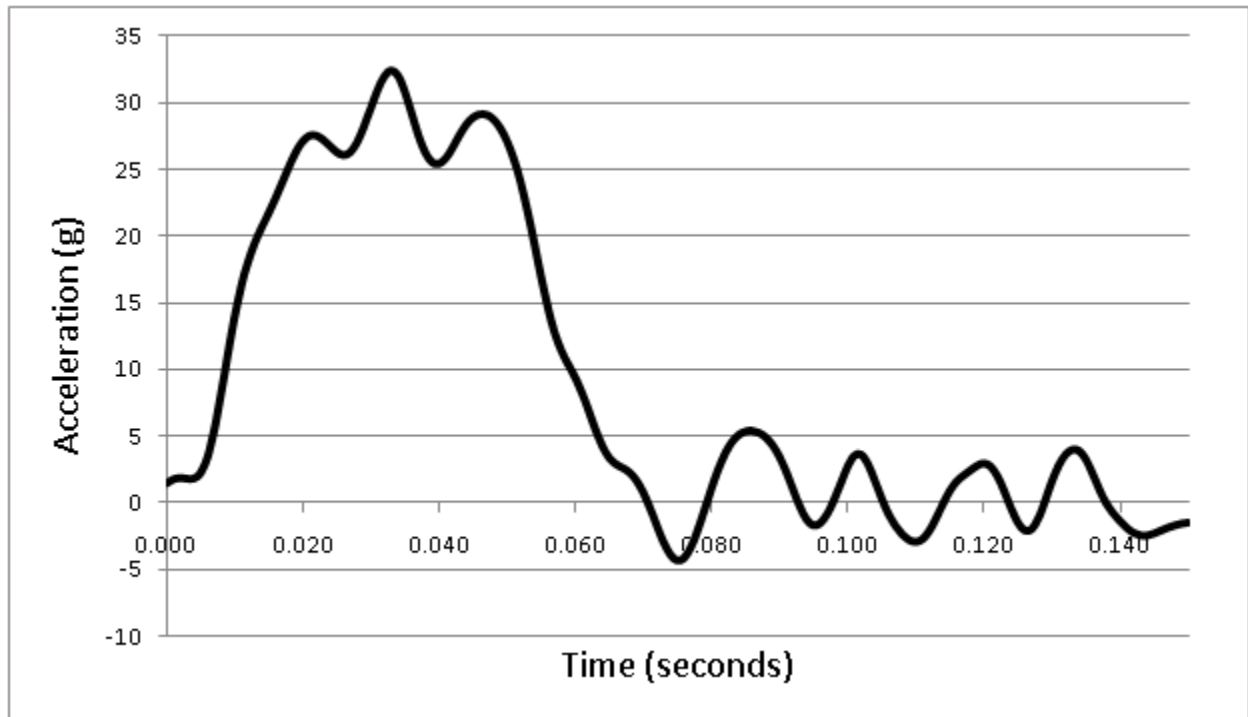
[73] I. W. Hall, M. Guden and C. J. Yu, "Crushing of Aluminum Closed Cell Foams: Density and Strain Rate Effects," *Scripta Mater*, vol. 43, pp. 515-521, 2000.

[74] G. Slik and G. Vogel, "Use of high efficient energy absorption foam in side impact padding," Dow Automotive, 2007.

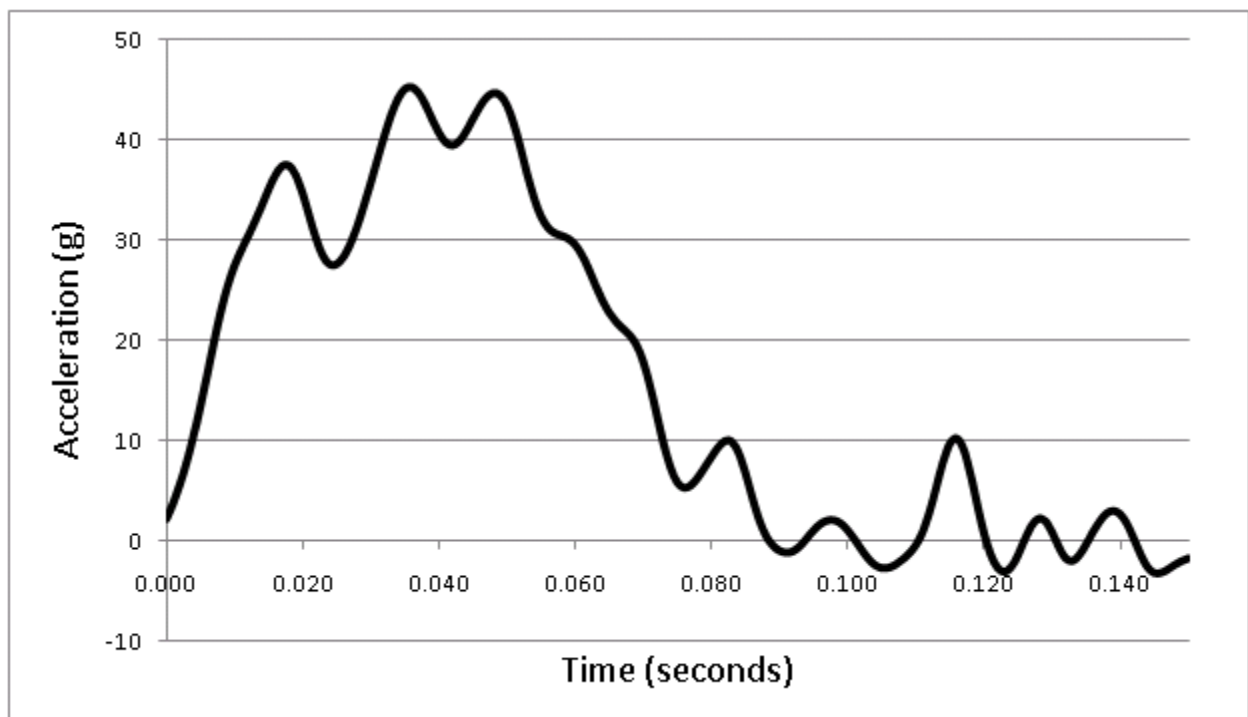
[75] D. Ruan, G. Lu, F. L. Chen and E. Siores, "Compressive behaviour of aluminium foams at low and medium strain rates," *Composite Structures*, vol. 47, pp. 331-336, 2002.

[76] Denso, "Millimeter-Wave Radar," vol. 2010, 2010.

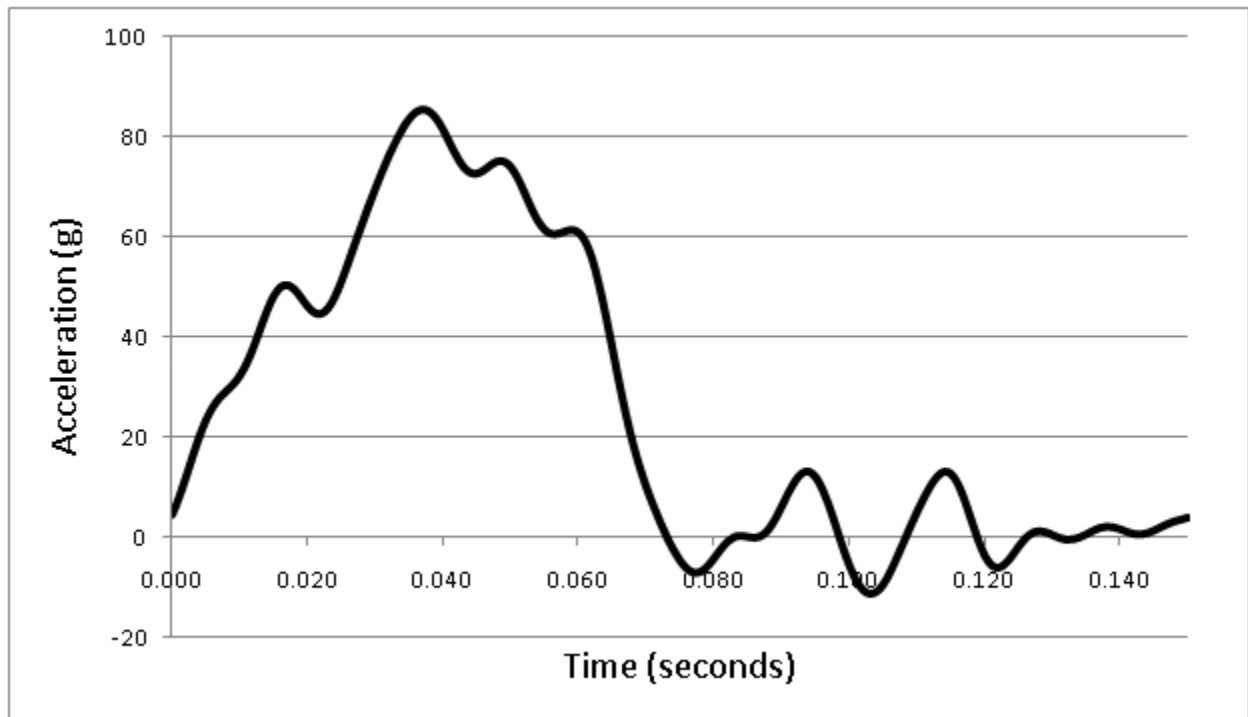
Appendix A: Acceleration Pulses



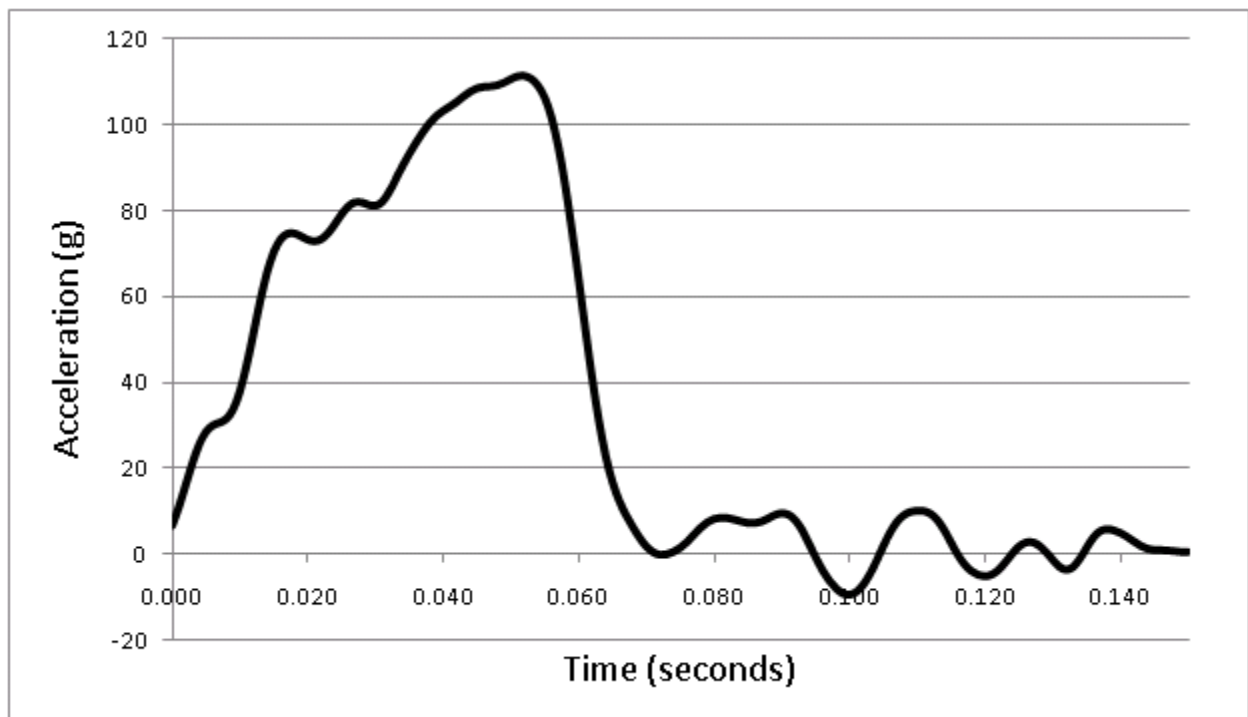
5 km/h Acceleration Pulse



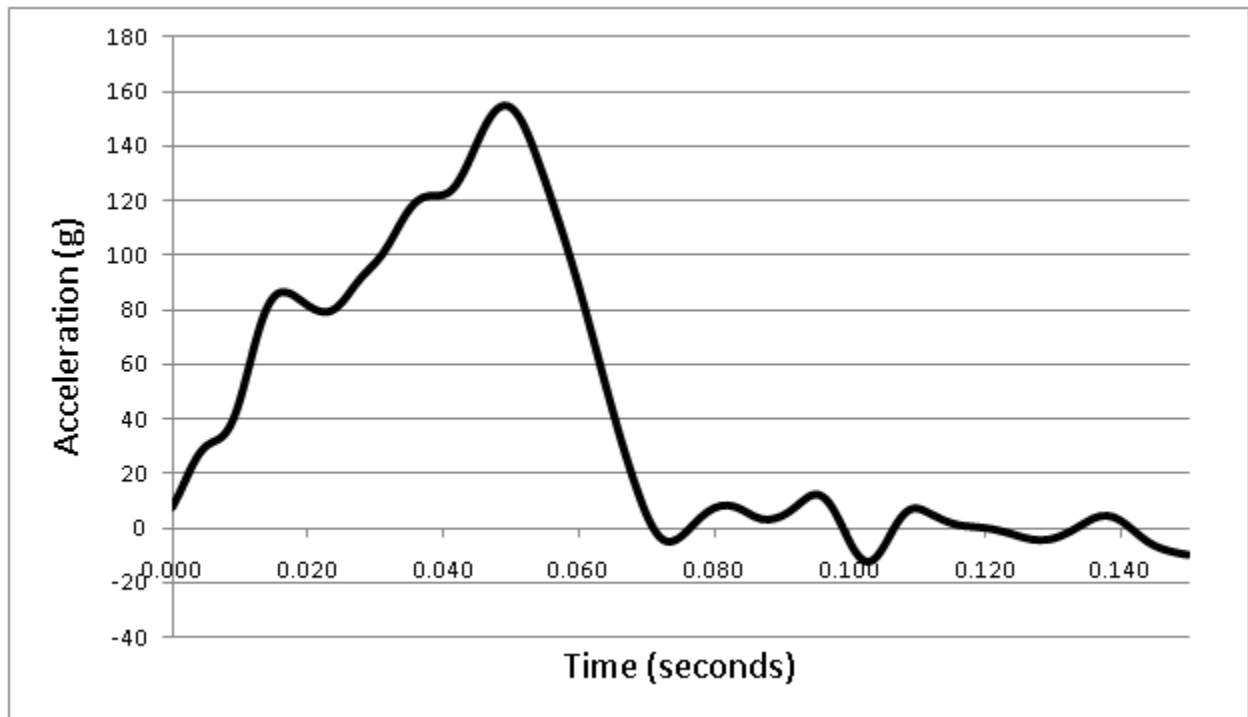
10 km/h Acceleration Pulse



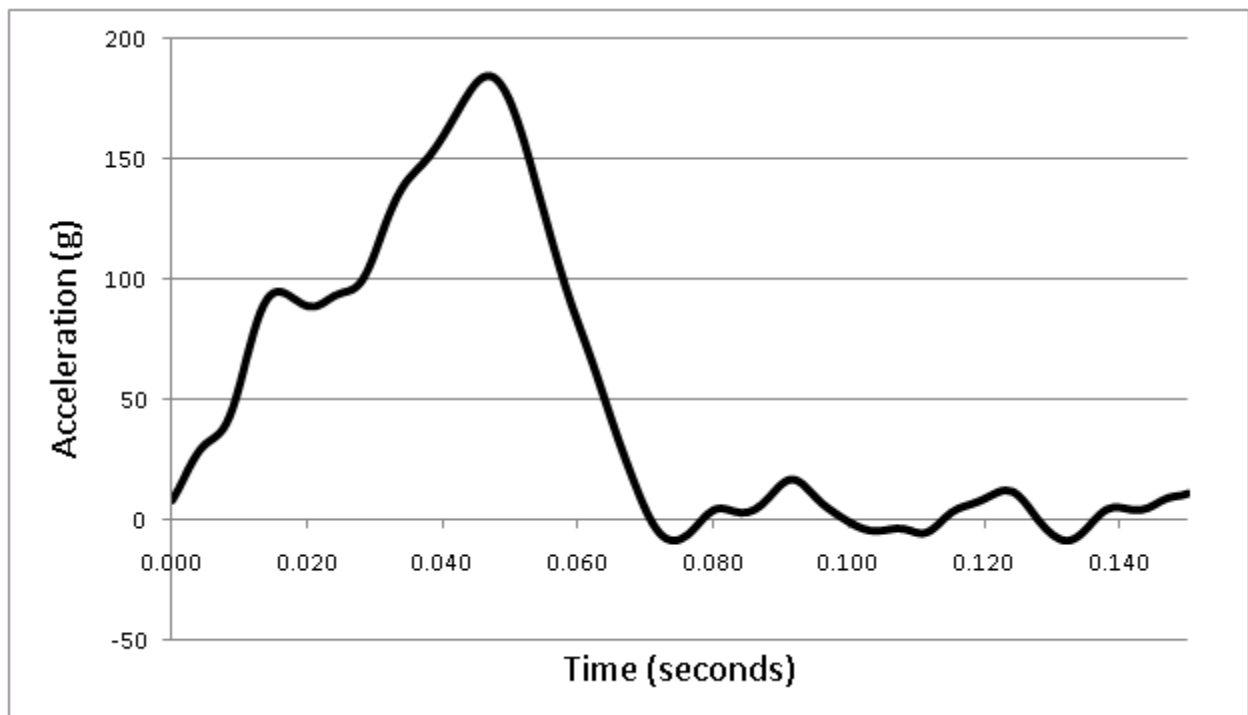
17 km/h Acceleration Pulse



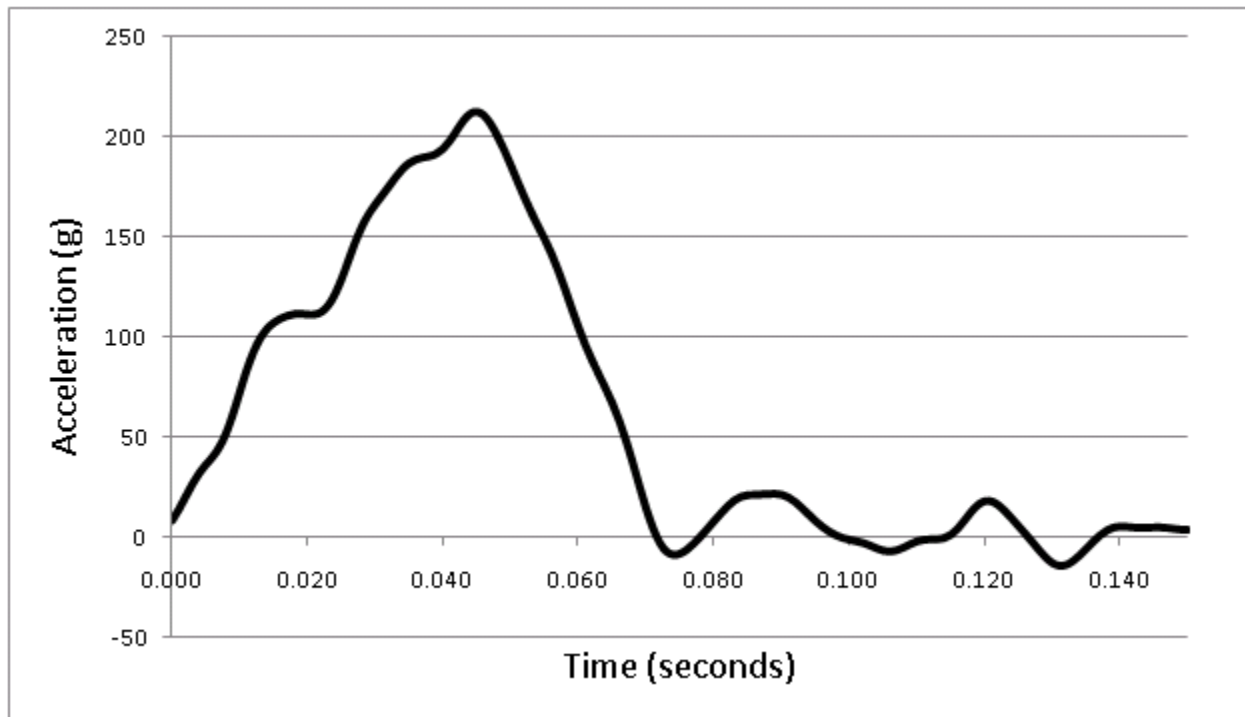
25 km/h Acceleration Pulse



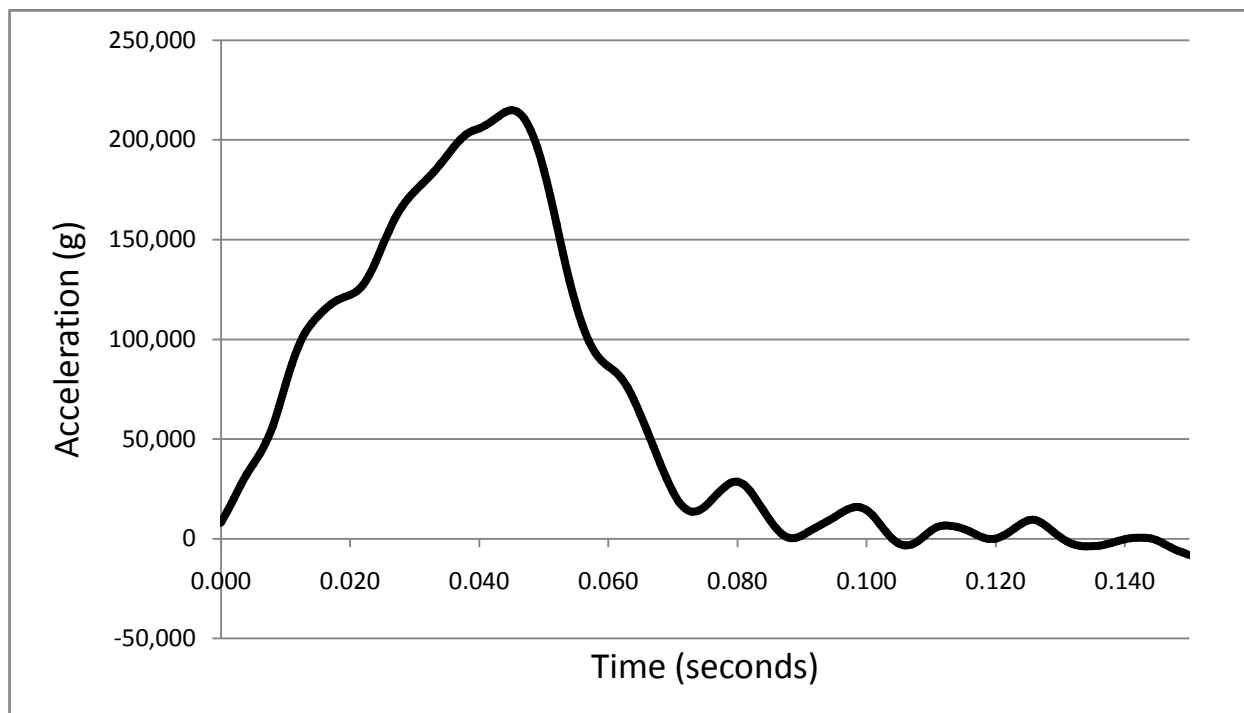
30 km/h Acceleration Pulse



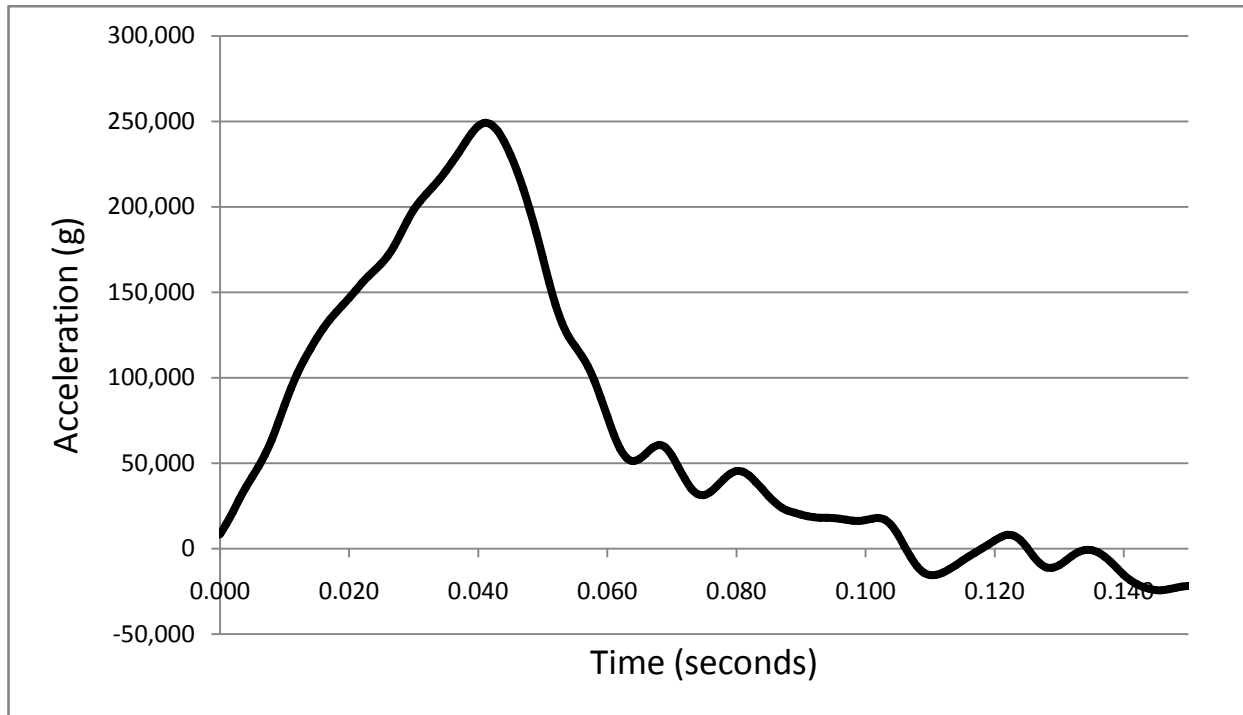
35 km/h Acceleration Pulse



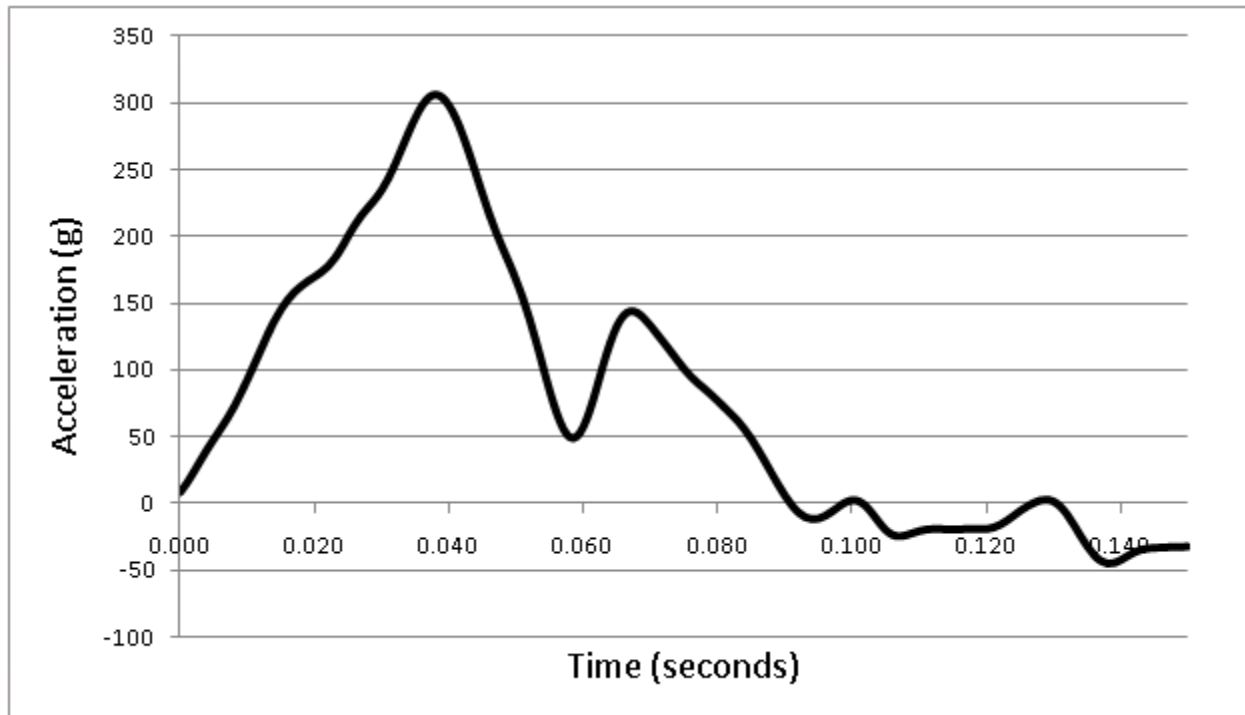
42.5 km/h Acceleration Pulse



48 km/h Acceleration Pulse

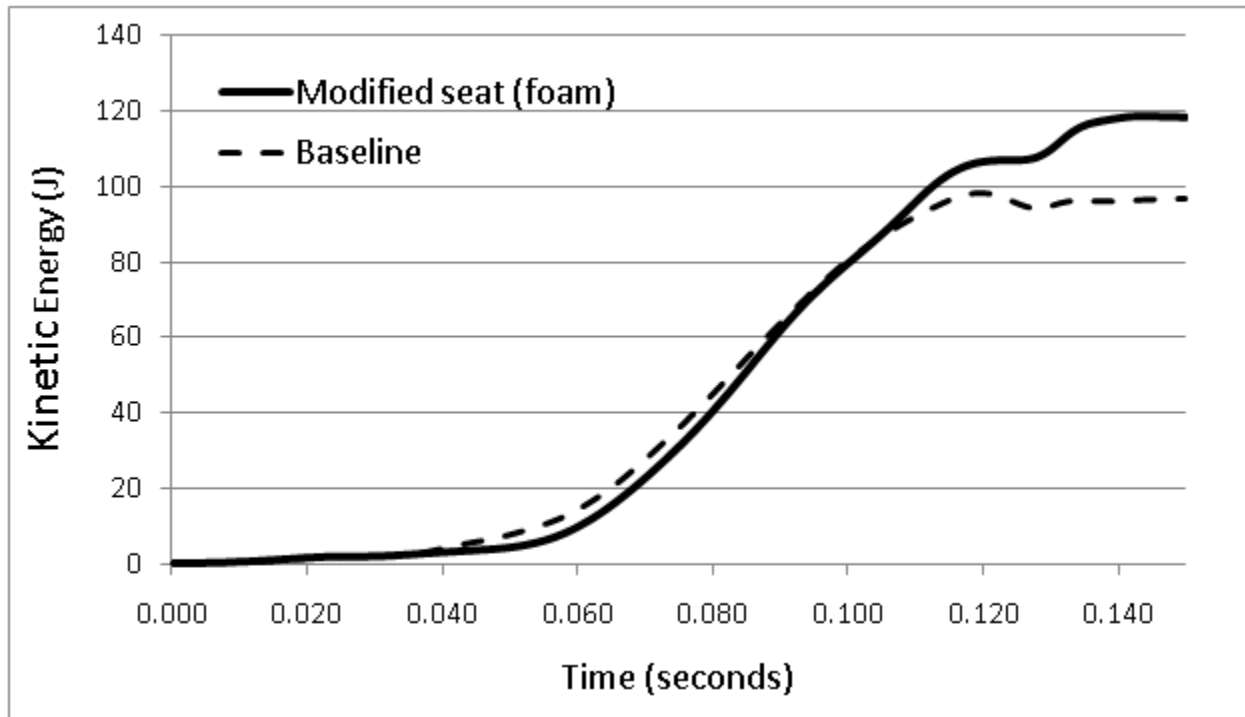


55 km/h Acceleration Pulse

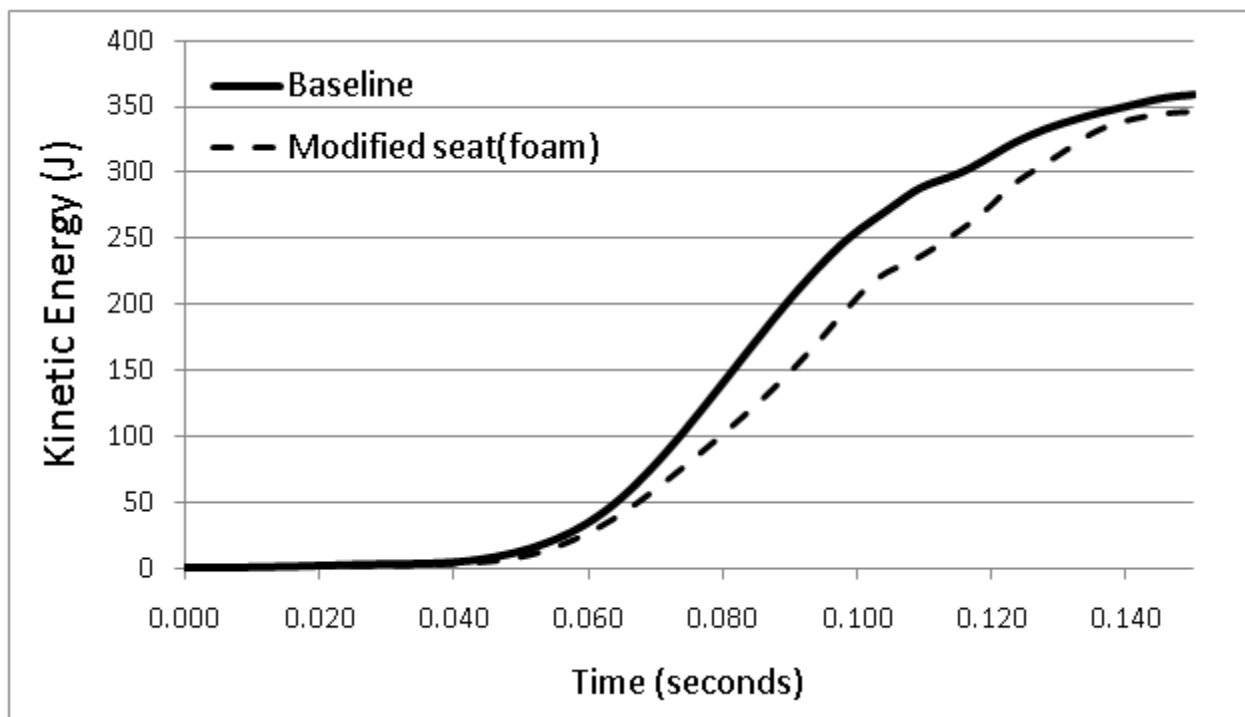


65 km/h Acceleration Pulse

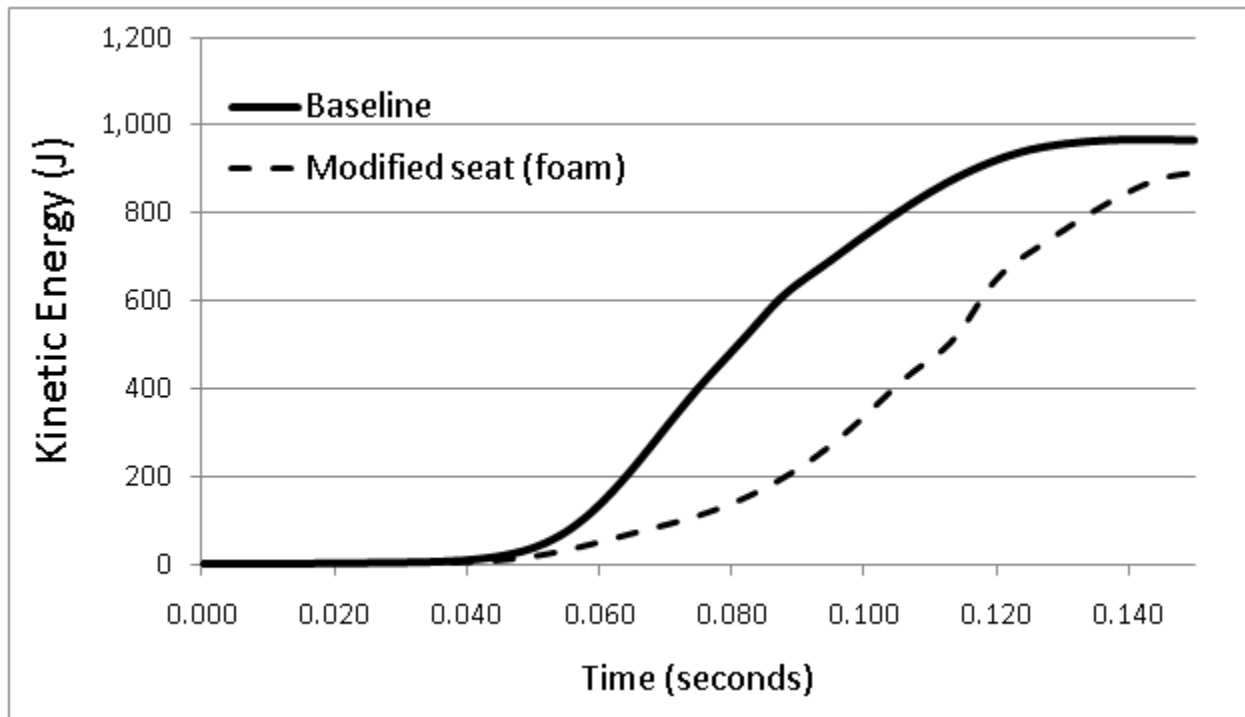
Appendix B: Occupant Kinetic Energy



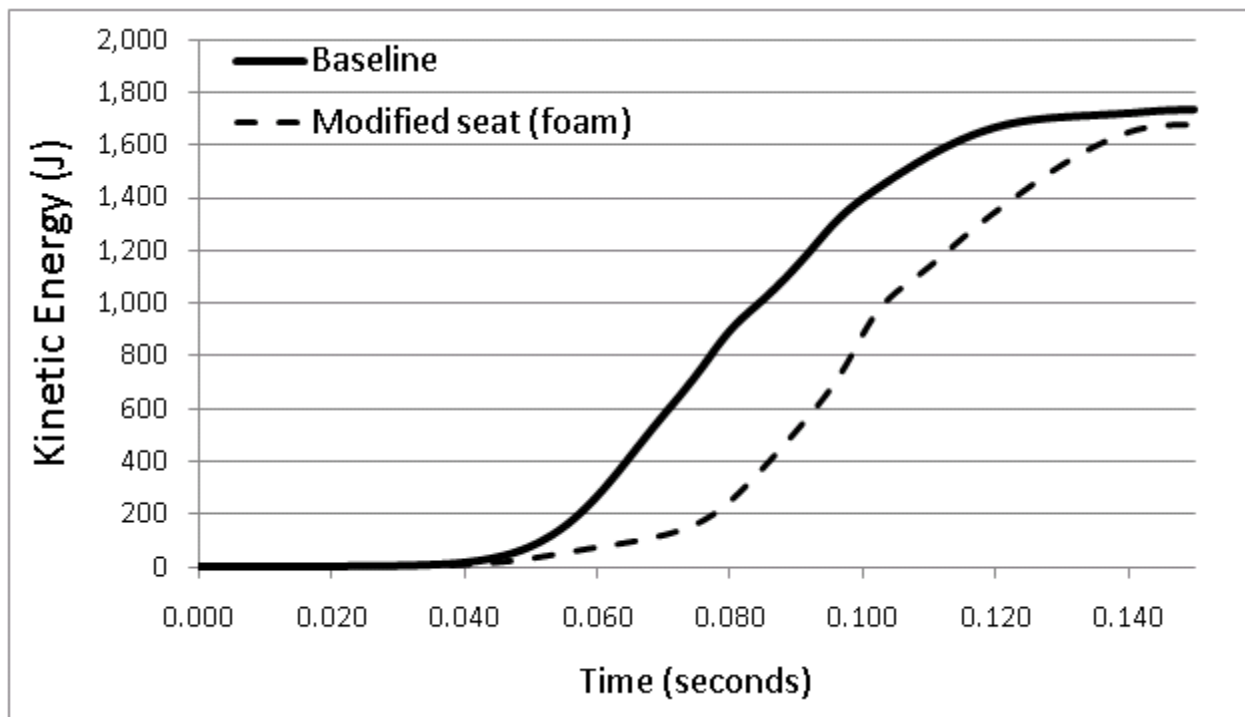
Occupant kinetic energy with and without foam (5 km/h)



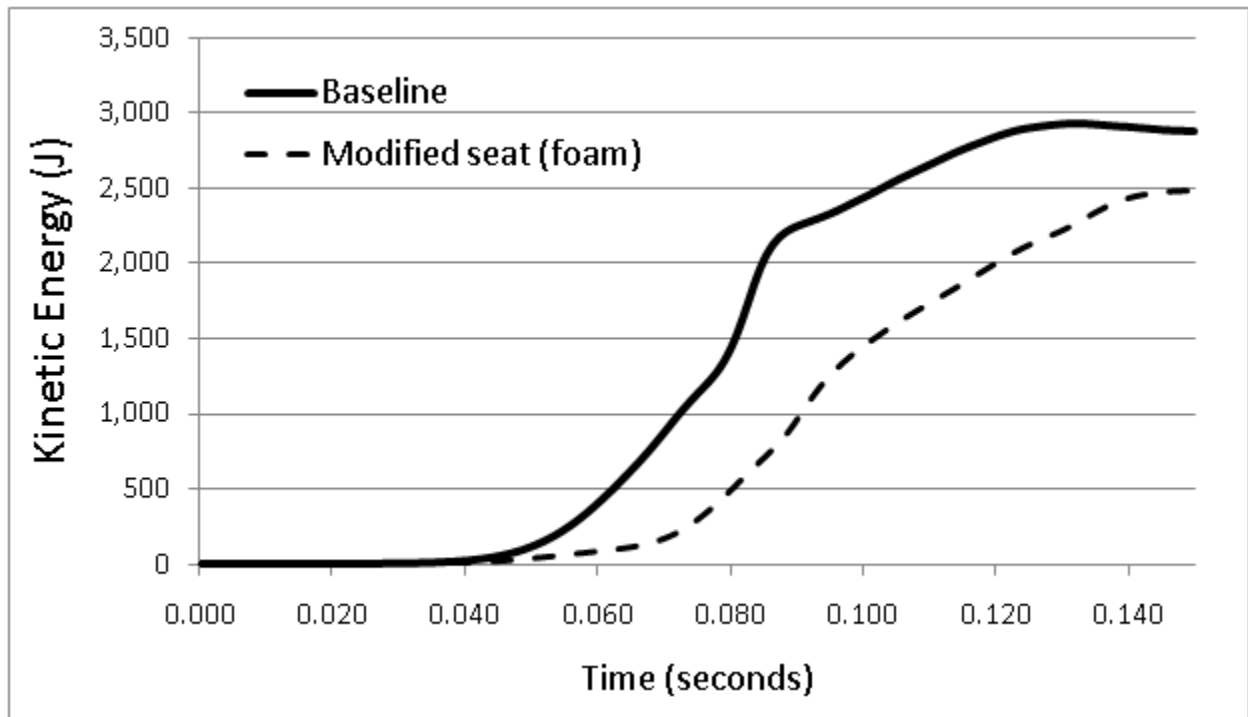
Occupant kinetic energy with and without foam (10 km/h)



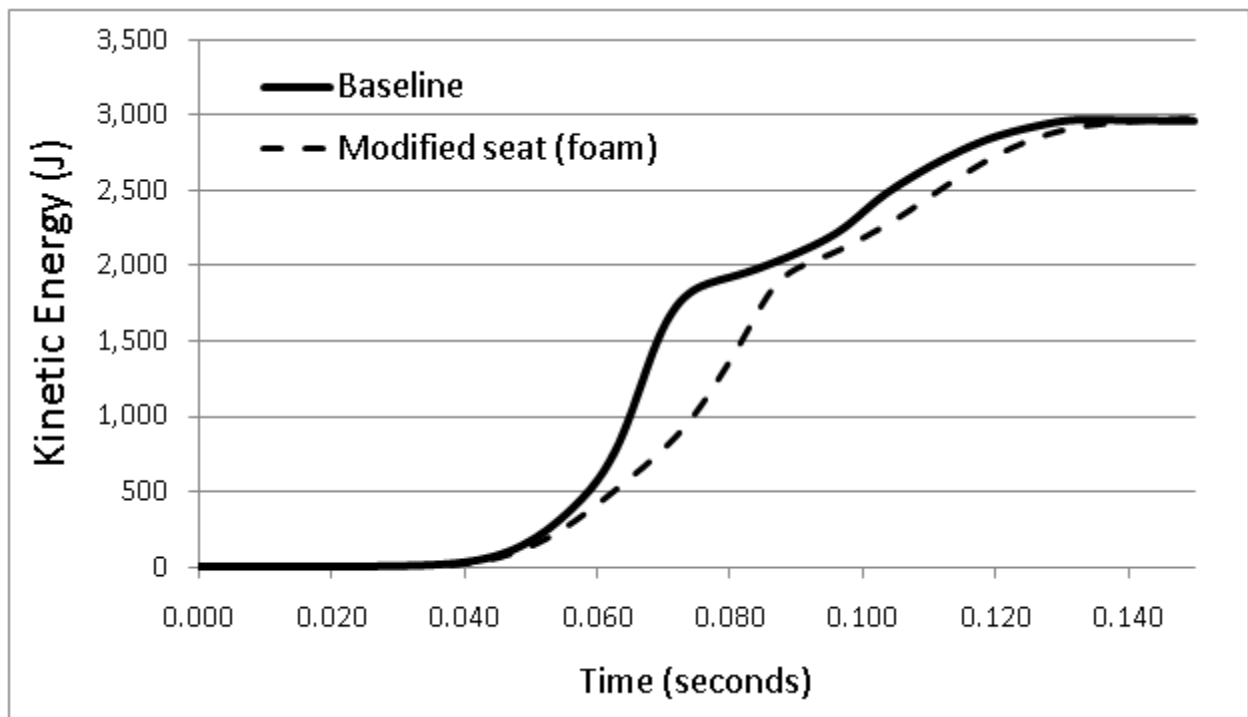
Occupant kinetic energy with and without foam (17 km/h)



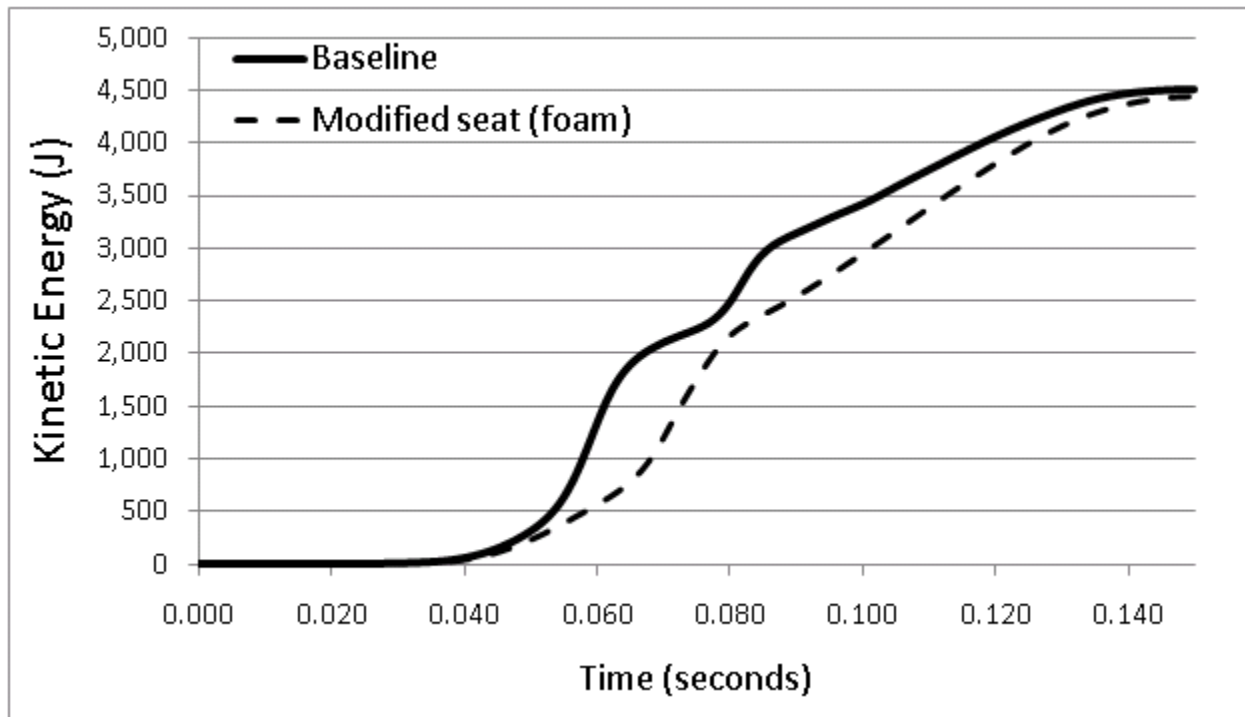
Occupant kinetic energy with and without foam (25 km/h)



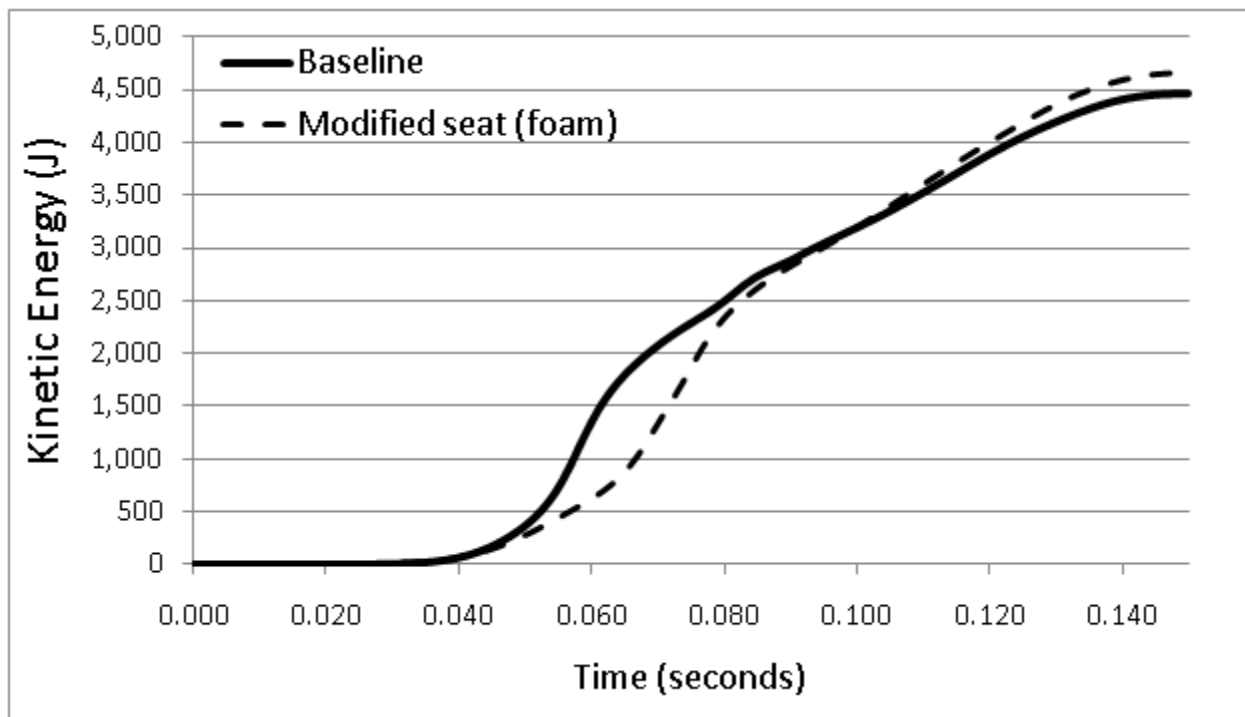
Occupant kinetic energy with and without foam (30 km/h)



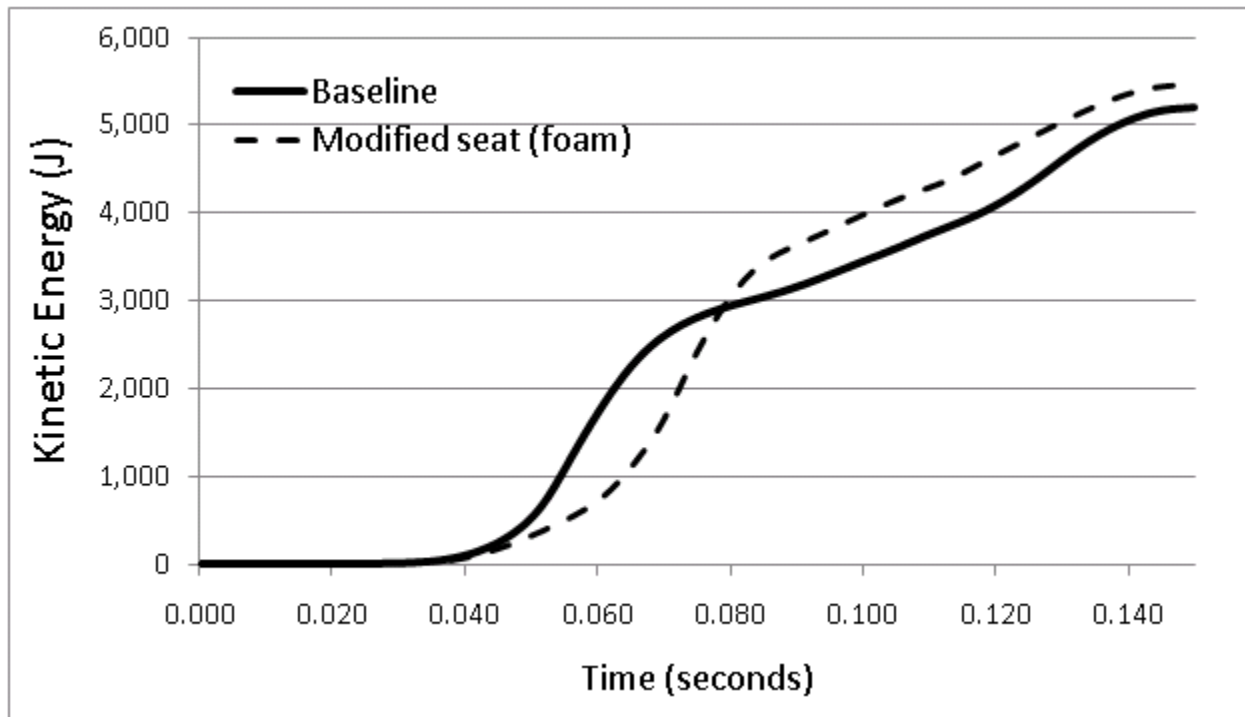
Occupant kinetic energy with and without foam (35 km/h)



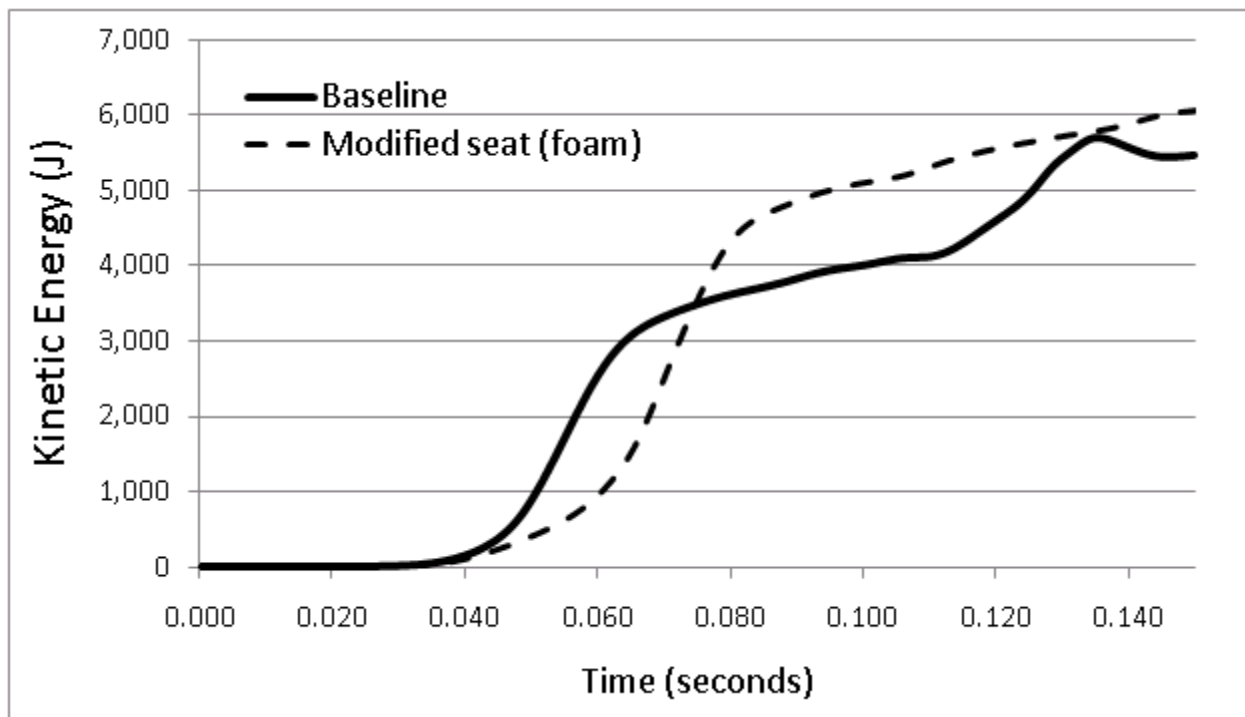
Occupant kinetic energy with and without foam (42.5 km/h)



Occupant kinetic energy with and without foam (48 km/h)



Occupant kinetic energy with and without foam (55 km/h)



Occupant kinetic energy with and without foam (65 km/h)